Cape Peninsula University of Technology

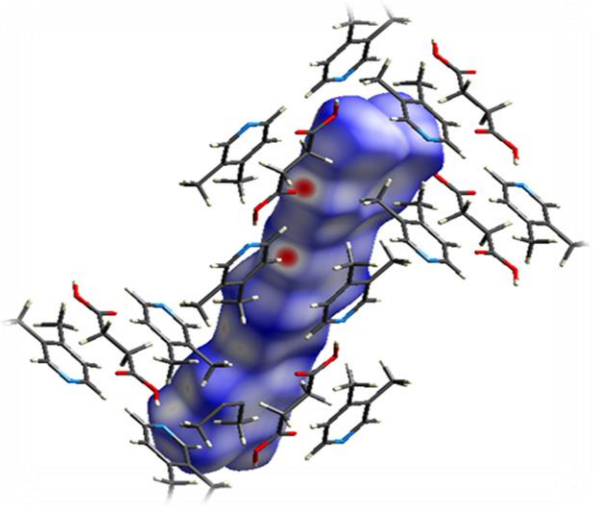

Melting point-structure relationships of multicomponent crystals

by

ALBAN AYAMINE

Thesis submitted in fulfilment of the requirements for the degree

Magister Technologiae: Chemistry

in the Faculty of Applied Sciences at the

CAPE PENINSULA UNIVERSITY OF TECHNOLOGY

Supervisor: Dr N.B. Báthori

Cape Town

November 2015

The financial assistance of the National Research Foundation (NRF) towards this research is hereby acknowledged. Opinions expressed and conclusions arrived at, are those of the author and are not necessarily to be attributed to the NRF.

DECLARATION

I, ALBAN AYAMINE, declare that the contents of this thesis represent my own unaided work, and that the thesis has not previously been submitted for academic examination towards any qualification. Furthermore, it represents my own opinions and not necessarily those of the Cape Peninsula University of Technology.

Signed **Date**

ABSTRACT

Twelve multicomponent crystals of dicarboxylic acids (succinic, adipic and suberic acid) with derivatives of picoline (4-picoline, 2,4-lutidine, 3,4-lutidine and 3,5-lutidine) were analyzed with the aim of finding correlation between their melting points and crystalline structural features. The solvates of SUC•2,4LUT, SUC•3,4LUT, SUC•3,5LUT and ADP•4PIC are already known structures but were remade for completeness and to obtain their accurate melting temperatures. The acids were selected because of their systematically increasing chain lengths and the selection of the picoline derivatives were based on the systematic variation of the positions of the methyl groups around the pyridine moiety.

All the formed multicomponent crystals were analyzed with single crystal X-ray diffraction and parallel to the solution crystallizations, grinding experiments were carried out to prepare the aimed inclusion compounds by using much less of the solvent of crystallization.

Thermogravimetry was used to confirm the solvent content of the bulk material and differential scanning calorimetry was applied to obtain information about the melting process, such as the onset and the peak temperature of the melting and the concomitant enthalpy change. The melting temperatures revealed that the inclusion formation significantly decreased the melting points of the staring materials and the melting points of the inclusion compounds for the same acid varied significantly.

Hirshfeld surfaces of the base-acid-base moieties and the related fingerprint plots were compared both qualitatively and quantitatively. The melting points of the compounds were plotted against the percentage contribution of the various intermolecular interactions.

ACKNOWLEDGEMENTS

I wish to thank:

- My family, friends and colleagues for their support and encouragement
- My supervisor, Dr N.B. Báthori for her help, advice and support
- The Staff of the Department of Chemistry, Cape Peninsula University of Technology

DEDICATION

I dedicate this thesis to my family.

TABLE OF CONTENTS

LIST OF FIGURES

LIST OF TABLES

LIST OF APPENDICES

GLOSSARY

Term/Acronyms/Abbreviations	Definition/Explanation
pKa	**-log(acid ionization constant)**
API	**Active Pharmaceutical ingredient**
TG	**Thermogravimetry**
DSC	**Differential Scanning Calorimetry**
PXRD	**Powder X-ray Diffraction**
a, b, c	**Unit cell axes**
α	**Angle between b and c unit cell axes**
β	**Angle between a and c unit cell axes**
γ	**Angle between a and b unit cell axes**
V	**Unit cell volume**
Z	**Number of formula unit per cell**
ρ	**Density**
SUC	**Succinic acid**
ADP	**Adipic acid**
SUB	**Suberic acid**
4PIC	**4-picoline**
3,4LUT	**3,4-Lutidine**
2,4LUT	**2,4-Lutidine**
3,5LUT	**3,5-Lutidine**

Chapter 1

Introduction

Chapter 1: Introduction

1.1 Structure-property relationships

The molecular structure of a compound inherently carries factors which defines its physical or chemical properties. For this reason, the prediction of certain features, such as protonation, partitioning or dipole moment, is possible by knowing the molecular structure exclusively. One of the widely used computational method for prediction of a series of physicochemical properties for a given, single component compound is UPPER[1] (Unified Physicochemical Property Estimation Relationships). When molecules cluster together into a highly ordered microscopic structure and form a crystal, intermolecular interactions form between them. Thus the properties exhibited by this many-body system are different from the individual units and therefore the prediction of the properties presented by the crystalline material is extremely challenging. In itself, the prediction of the structure of this new crystalline material is not fully understood and developed but great effort is presented by many research groups in the chemical community. From 1999, five of the so called blind tests[2] have been conducted by the Cambridge Crystallographic Data Centre of organic crystal-structure prediction methods. The blind tests have shown substantial development in crystal structure prediction for smaller molecules and look promising for the prediction of larger, more "drug-like" molecules. The latest, sixth blind test started in September 2014, has five target systems, including a rigid molecule, a salt hydrate, a co-crystal and a molecule with five known but unpublished polymorphs, one of which has Z'>1. The first three test were focused on the prediction of single component structures mainly. The first attempt to predict structures for a co-crystal built from two simple molecules (2-amino-4-methylpyrimidine: 2-methylbenzoic acid) was successfully carried out in the 4th blind test. Based on this achievement, slightly more complex molecular pairs were targeted in the fifth blind test (1,8-naphthyridinium fumarate and gallic acid monohydrate), however with less success. These compounds are much less complex than an average drug molecule, which has generally great torsional flexibility and multiple hydrogen bond donor and acceptor sites. For these reasons, the crystal structure prediction of drugs remains a challenging problem.

Once the crystal structure of a given compound is available, the next challenging step is to predict the property of the bulk material. Polymorphism,[3] when a compound exist in more than one form or crystal structure, is an interesting phenomenon but clearly complicates the prediction of structure-property relations because different polymorphs will present different physicochemical properties. Desiraju et al[4] analyzed the polymorphic behavior of curcumin, a spice component, and sulfathiazole, an antibacterial drug and the solubilities of the different polymorphs were explained with structural features of the crystal forms. Also an inverse correlation was found between solubility and hardness for both the polymorphs which may suggests that hardness could be utilized as a parameter to predict the solubility order in such close energy-related polymorphic systems.

In the pharmaceutical industry a central problem is that after identifying a handful of drug candidates, some of them (occasionally the best performing ones) present poor bioavailability, dissolution or solubility. A possible way to bypass this problem is to alter the unwanted property without changing the molecular structure of the active pharmaceutical ingredient (API). This can reached via formulation or the formation of multicomponent systems, such as hydrates, solvates, salts or co-crystals. In the case of the latter, the *ab initio* prediction of the new multicomponent material is extremely challenging for the reasons discussed previously. Currently the typical way to gain information about structure-property relationships of multicomponent crystals is to (1) synthesize them, (2) measure the targeted property and (3) search for factors to link the two together. Changes to the physical properties may be achieved by varying the co-crystallizing component in a systematic manner, for example increasing/decreasing the alkyl chain of an aliphatic dicarboxylic acid.[5] Aakeröy and coworkers[6] synthesized a series of co-crystals from hexamethylenebisacetamide, an anticancer drug, with aliphatic saturated dicarboxylic acids (succinic, adipic, suberic, sebacic and dodecanedioic acids) and found that the highest-melting co-crystal contains the dicarboxylic acid with the highest melting point, and the lowest-melting acid produces the lowest melting co-crystal. Thus they have demonstrated that the melting behavior of the co-crystals formed can be modulated in a predictable manner. A similar series of crystallization between *trans*-1,2-bis(4-pyridyl) ethylene and aliphatic saturated (glutaric acid, 2,2'-thiodiacetic acid, 2,2-selenodiacetic acid) or unsaturated dicarboxylic acids (fumaric acid, glutaconic acid, *trans*,*trans*-muconic acid and 1,4-phenylenediacrylic acid) was carried out.[7] The melting point of the co-crystals and their coformers were compared and it was noted that in

the case of the isostructural co-crystals (formed with glutaric acid, 2,2'-thiodiacetic acid or 2,2-selenodiacetic acid) there is a significant elevation of the melting point compared to both starting materials and the higher the melting point of the acid the higher will be the melting point of the corresponding co-crystal. The hygroscopic stability of S-oxiracetam, a nootropic chiral drug, has also been studied by the formation of its co-crystals with gallic acid and 3,4-dihydroxybenzoic acid.[8] The result showed that the hygroscopic stability of S-oxiracetam has been enhanced only with the formation of its co-crystal with gallic acid.

Clarke and coworkers investigated the structure-stability relationships in co-crystal hydrates.[9] The eleven organic hydrates were divided in four groups according to the temperature of the loss of water. Group one contained the organic hydrates that lost the water of crystallization under 100ºC; crystals in the second group lost the water between 100 and 120ºC; the third group lost the water at higher temperature than 120ºC and the last group contained co-crystal hydrates whose dehydration process is combined with the melt. It was conclude that there are numerous structural features that may influence the thermal stability and the way as the water may bond in the structure is unpredictable, thus the structure-thermal stability relationship remains largely unpredictable. The only partial conclusion that may be drawn is if the water molecules are arranged in channels, these crystals present low melting points.

To summarize, the structure-property relations of monocomponent crystals are still not fully understood, however there is significant improvement in predicting their possible crystal forms. The crystal structure prediction of multicomponent crystals is at the center of interest but currently not in a state of application.

1.2 Crystal Engineering

Crystal engineering is defined as the design and synthesis of molecular or ionic crystalline solids with desired properties by using intermolecular interactions instead of forming or breaking covalent bonds. The two main strategies currently in use for the formation of solid crystalline structures are based on hydrogen bonding and coordination complexation.[10] In 1962 Von Hippel introduced the term 'molecular engineering'[11] and not much later, Schmidt initiated its use when working on the correlation of solid-state reactivity in photodimerizable compounds.[12] Crystal

engineering became 'fashionable' in the late 1980s when many modern crystallography techniques and aspects such as solid-sate modification of compounds and structure prediction were developed quickly.

1.3 Intermolecular Interactions

Intermolecular interactions which are also known as non-covalent interactions represent the crystal structure in the free energy minimum. This free energy is due from a balance of attractive and repulsive forces. Intermolecular interactions are weaker than covalent interaction and can be divided in two groups: (i) long-range hydrogen bonds or anisotropic interactions and (ii) short-range van der Waals interactions or isotropic interactions.[13]

1.3.1 Hydrogen bond

Hydrogen bond is a type of interaction when a hydrogen atom from a molecule or fragment (X-H where X must be more electronegative than H) forms a non-covalent interaction with an atom or group of atoms in the same molecule or different molecule.[11] The hydrogen bond in crystal engineering is considered as 'the master-key' of molecular recognition because its interactions are relatively strong (4-120 kJ mol^{-1}) and directional. Jeffery defined the hydrogen bond as "the most important intermolecular interaction in term of designing a new solid-state material, due to the strong and directional properties which result from a special dipole-dipole interaction".[14] A hydrogen bond forms between a proton donor (D) and a proton acceptor (A) generally and described as D-H···A. In the recent years it was recognized that (D) can be atoms like C, O, P or S and (A) must be an electronegative non-metal atom or functional group, such as O, F, N, Cl, Br, alkenes or alkynes. The last important features of hydrogen bond is the D-H···A angle which is typically close to 180º. Generally hydrogen bonds can be classified based on their strength into three groups, namely (i) very strong, (ii) strong and (iii) weak hydrogen bonds.

- Very strong hydrogen bonds are usually laid on a D···A range of 2.2-2.5 Å, with linear angle, (175-180º). They are important because their formation is relatively well predictable thus have an important role in crystal engineering and the prediction of the crystalline structure. Typically they may be found to form between acids and bases.

- Strong hydrogen bonds lie in the D···A range of 2.5-3.2Å, with angles between linear and bent arrangement (130-180º). These interactions are mainly electrostatic and usually found them in acids, alcohols and organic compounds.
- Weak hydrogen bonds lie on a D···A range of 3.2-4.0Å, they are less linear and more bent. Their angles can be between 90 and 150º; they are usually be found as C-H···π and O-H···π bonds.

Figure 1.3 presents different geometries of hydrogen bonding that are usually seen in the crystal structure intermolecular interaction and **table 1.3** summarize the parameters of hydrogen bonds.

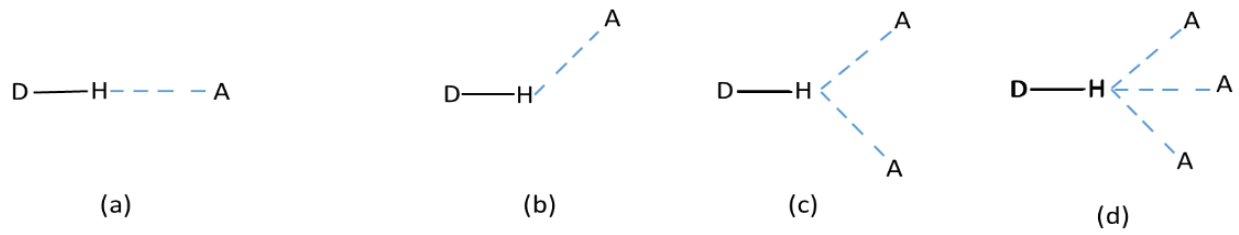

Figure 1.3 Different types of hydrogen bonding geometries, (a) linear, (b) bent, (c) bifurcated and (d) trifurcated

Table 1.3 Typical parameters of hydrogen bonds.[13]

strength	D-H···A	d(D···A)(Å)	d(H···A)(Å)	D-H···A(°)
very strong	$[F\text{-}H\text{-}F]^-$	2.2-2.5	1.2-1.5	175-180
strong	O-H…O-H	2.6-3.0	1.6-2.2	145-180
	O-H…N-H	2.6-3.0	1.7-2.3	140-180
	N-H…O=C	2.8-3.0	1.8-2.3	150-180
	N-H…O-H	2.7-3.1	1.9-2.3	150-180
	N-H…N-H	2.8-3.1	2.0-2.5	135-180
weak	C-H…O	3.0-4.0	2.0-3.0	110-180

1.3.2 Weak interactions

- Van der Waals interactions are one of the weak intermolecular interactions and occur when the electron cloud is polarized by the nearest adjacent nucleus and this results in a weak electrostatic attraction.[15] In crystal engineering, van der Waals interactions can be

defined as the sum of all stabilizing and destabilizing interactions in which hydrogen bonding and other anisotropic interactions are excluded. They can influence many physical properties such as solubility, density and melting point in organic compounds. In addition, van der Waals interactions are most important in supramolecular chemistry in term of formation of inclusion compounds.

- Dipole-dipole interactions result when two dipolar molecules interact with each other and the partially negative portion of one of the polar molecules is attracted to the partially positive portion of the other polar molecule. This type of interaction between molecules accounts for many physically and biologically significant phenomena such as the binding of individual amino acids to secondary structures to tertiary structures and even the formation of quaternary structures of proteins.

1.4 Supramolecular synthons and synthons engineering

Supramolecular synthons are structural units within a molecule which are related to a possible synthetic operation or make predictable interaction between two molecules. In crystal engineering, synthons can provide or establish important interactions between two groups of molecules with reliable properties.[16] Supramolecular synthons are fundamental in crystal structures because they can give a full description of the entire structure.[17] They may be classified as homo- or heterosynthons. While homosynthons built from the same functional groups, heterosynthons contain different moieties. Perhaps the most common example for the homosynthon is the formation of carboxylic acid dimers (Fig. 1.4 A) while the same carboxylic acid is likely will form a heterosynthon with a pyridine derivative if is available (Fig. 1.4 B).[18] A survey of the literature revealed that heterosynthons are more common than homosynthons in the acid-amide co-crystals.[19] More recent studies by Wilson et al and Zaworotko et al lead to the same observation in alcohols[20], amines and alcohol-pyridine[21] multicomponent crystals.

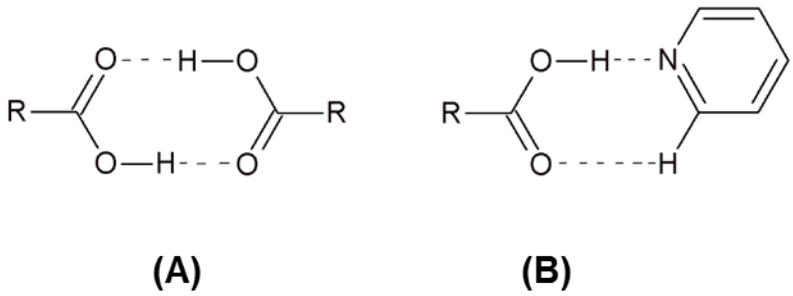

Figure 1.4 Representation of a supramolecular homosynthons (A) and heterosynthons (B).

1.5 Multicomponent crystals

Multicomponent crystals have at least two different chemical constituents and may be classified as co-crystals, salts, solvates or hydrates. The first multicomponent crystal reported by Wöhler was quinhydrone which is constituted by benzoquinone and hydroquinone in 1:1 ratio.[22,23] The definition of a co-crystal is at the center of interest of supramolecular chemistry from many years ago.[24] Historically co-crystals were called organic molecular compounds,[25] mixed binary molecular crystals,[26] molecular complexes[27] and heteromolecular compounds.[28] Aakeröy's definition gives a more detailed explanation "Co-crystals are made from reactants that are solids at ambient temperature".[29] Co-crystals may be defined as multicomponent crystals formed from two neutral compounds while in salts the building components may be organic or inorganic ionic species. However, the universal definition of what constitutes a co-crystal is still uncertain.[30,31] The latest and perhaps the more detailed definition states that "*"cocrystals are solids that are crystalline single phase materials composed of two or more different molecular and/or ionic compounds generally in a stoichiometric ratio which are neither solvates nor simple salts".*[32] The main difference between co-crystals and salts is that salts must have stoichiometric compositions because of their charged nature while co-crystals do not necessary exhibit fixed stoichiometries.

1.6 Pharmaceutical co-crystals

The formation of pharmaceutical co-crystals focus on the prospect of optimizing physicochemical properties. When drugs are taken by humans, they take a certain amount of time

to dissolve in the blood. Some of the important drugs cannot dissolve fast enough or do not dissolve at all. Co-crystals have an important part in developing groups of new solid forms of pharmaceutical substances. Melting point is one of the physical properties that characterize a compound and is simple to determine. It is defined by the temperature at which the solid phase is at equilibrium with the liquid phase at a fixed pressure (usually 1 atmosphere). Solubility is important in the preformulation of drug substances. Solubility measurement of solid materials is a time consuming process. Formulating co-crystals of known drug substances is a possible way to alter their physical-chemical properties without modifying their chemical structure.[33,34] Pharmaceutical co-crystals are generally formed by an active pharmaceutical ingredient (API) and a co-crystal former or excipient.[35,36] The APIs are generally chemically robust and present the ability to form strong non-bonded interaction with the coformers which typically have low molecular mass and good hydrogen bonding properties.[37] Pharmaceutical co-crystals can be prepared with a variety of methods, such as solution crystallization, dry grinding, solvent-drop grinding, or co-melting the ingredients.[38,18,39,40]

1.7 Multicomponent model-crystals

Multicomponent model-crystals can be defined as a simplified versions of the pharmaceutical co-crystals or salt. In the model co-crystals the API is replaced by a simple molecular unit with restricted conformational freedom and hydrogen bonding properties. Thus a model co-crystal has the ability to present the same type of supramolecular behavior as a pharmaceutical co-crystal but the interpretation of the structure is simpler and easier to understand the structure-property relations of these crystals. Solvates may be treated as a subset of multicomponent model-crystals because typically one of the building unit is a solvent molecule which is generally a small chemically simple compound with one hydrogen bonding site.

1.8 Melting point- structure relationships in multicomponent crystals

Melting point is one of the physical properties that characterize a compound and it simple to determine. It is defined by the temperature at which the solid phase is at equilibrium with liquid phase. To find a suitable solid form of a drug substance which can have superior properties is one of the big challenges in pharmaceutical development. In recent years interest increased

toward novel solid forms of active pharmaceutical ingredients which have improved physical-chemical properties.[41]

Aakeröy and co-workers[42] combined three ditopic compounds, namely 2-aminopyrazine, 2-amino-5-bromopyrazine and 2-amino-3,5-dibromopyrazine with thirty carboxylic acids with the aim of (i) obtaining binding preferences and (ii) to investigate the yield of the supramolecular reaction. By using semi-empirical calculations, each compound was mapped with their electrostatic surface. This experiment established that the electrostatic charge on the N-heterocyclic base influences the ability of the compound to form intermolecular hydrogen bonds in the solid state. Similarly to the previous study, Aakeröy and co-workers[43] also analyzed five co-crystals of azopyridine with the aim to understand how intermolecular interactions can influence the supramolecular assembly. The result showed a correlation between the melting point of the co-crystals and the homomeric molecular solids of the corresponding carboxylic acids. They concluded that the melting point of the azopyridine co-crystals showed non-linear correlation with the carbon chain length in the corresponding diacids. In and other study, Aakeröy and co-workers[44] synthesized five co-crystals of dicarboxylic acids and hexamethylenebisacetamide, a drug used against the proliferation of lung cancer cells. The result showed a clear linear correlation between the melting points of the used carboxylic acids and related co-crystals; the co-crystal with the highest melting point was formed with the highest melting dicarboxylic acid. Melting point alternation was also investigated by Vishweshwar and co-workers[45] when five co-crystals of dicorboxylicacids and isonicotinamide were synthesized. They found that the melting point of the five co-crystals were higher than the pure diacids and this observation was described by stronger hydrogen bond formation and more efficient packing.

One of the problems in pharmaceutical drug development is poor bioavailability which is influenced by the melting point of the drug substance; the important question to ask is how the melting point can be related to molecular structures. To provide more explanations, certain studies like to link the API and the given compound (which is solid in ambient conditions) via intermolecular forces to provide more information. Katritzky and co-workers[46] studied the relationship between melting point and chemical structure. It was concluded that the melting point is a difficult property to correlate because the available molecular descriptors do not describe accurately the many-body crystal packing effects.[47] Dearden pointed out that the

melting point of a compound is determined by three factors of the crystal structure, namely (i) the intermolecular forces, (ii) the molecular symmetry, and (iii) the conformational degrees of freedom of the molecule.[48] To gain more insight about how the crystal structure and the intermolecular interactions effect the melting point in multicomponent crystals some of the three factors should be held constant. Applying model crystals we may simplify the nature of the intermolecular forces and restrict the degrees of freedom and this may lead us to understand how a certain interaction influences the melting point of the crystalline material.

1.9 Aspect of this research

This project was designed to find correlation between the melting point and structural features of multicomponent crystals.

In our previous work four multicomponent model co-crystals and two salts of the hosts adipic acid (ADI) and fumaric acid (FUM) were prepared with the guests 1,4-diazabicyclooctane (DABCO), 3-picoline (3PIC) and 4-picoline (4PIC).[49] The melting points of the multicomponent crystals were recorded and solubility measurements were carried out by using the gravimetric method with ethanol and water as solvents. The result of the melting point measurements showed that the pure acids (ADI and FUM) have the highest melting points. The salts (ADIDABCO and FUMDABCO) have lower melting points than the related pure acids but higher melting points than the inclusion compounds (ADI3PIC, ADI4PIC, FUM3PIC and FUM4PIC). The solubility results obtained from ethanol did not correlate with the melting points of the compounds at all. The aqueous solubility values showed partial correlation: as the melting point increases the solubility decreases with the exception of the value related to ADI3PIC and FUM3PIC. The structures are very similar in that the molecules formed by the acid-base pairs are connected primarily via strong O–H•••N hydrogen bonds. Secondary interactions such as H•••H, CH•••O, π•••π and CH•••π are utilised in the packing. The melting point showed partial correlation with water solubility but no correlation with ethanol solubility. Analysis of the crystal structures using Crystal Explorer[50] provided a breakdown of the intermolecular interactions and it was found that the O•••H interactions correlate with the melting point; a decrease in melting point corresponds to a decrease in O•••H interactions while the C•••H interactions show an inverse relationship to the aqueous solubility.

Haynes and co-workers[51] conducted a systematic study on fumaric acid and succinic acid solvates of lutidine isomers. Six co-crystals of the host succinic acid, two co-crystals and five salts of the host fumaric acid were prepared by adding six isomers of lutidines and it was concluded that fumaric acid has a predominance to form salts with lutidines while succinic acid is likely to form co-crystals. All structures contained the expected base-acid-base unit (the dicarboxylic acid hydrogen bonded to two aromatic amines) but the overall packing of the crystals was very sensitive to the small changes of molecular shape in the disposition of the methyl groups in the lutidines but no further correlation of structure to any physical properties, such as melting point or solubility was investigated.

Based on Haynes's findings on the roboustness of the base-acid-base unit, we designed and synthesized a series of multicomponent model crystals of dicarboxylic acids and systematically varied co-crystallizing agents. In this project twelve solvates were crystallized via combining succinic acid (SUC), adipic acid (ADP) and suberic acid (SUB) with the 4-picoline, 2,4-lutidine, 3,4-lutidine and 3,5-lutidine. The solvates of SUC•2,4LUT (CSD refcode: RESGAY), SUC•3,4LUT (RESHAZ), SUC•3,5LUT (RESHIS), and ADP•4PIC structure were previously published[49] but were resynthesized to obtain their melting points. The acids were selected because of their systematically increasing chain lengths and the selection of the picoline derivatives were based on the systematic variation of the methyl groups around the pyridine. (**Figure 1.9)** The crystals were analyzed and structural features, such as type of percentage interactions were related to the melting points.

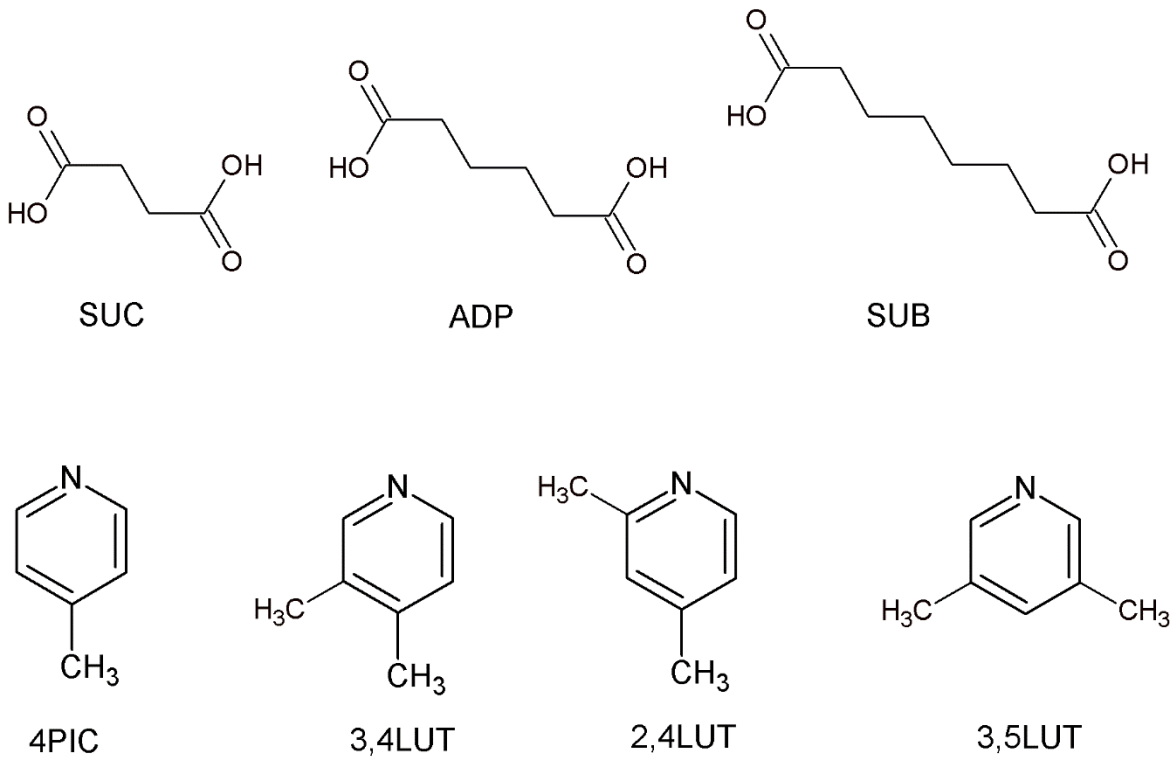

Figure 1.9 Structural line diagrams of used dicarboxylic acids (succinic acid (SUC), adipic acid (ADP) and suberic acid (SUB)) and aromatic amines (4-picoline (4PIC), 3,4-lutidine (3,4LUT), 2,4-lutidine (2,4LUT) and 3,5-lutidine (3,5LUT)).

References

[1] Lian, B; Yalkowsky, S.H. *J. Pharm. Sci,* 2014, **103**, 2710-2723.

[2] (a) Lommerse, J.P.M; Motherwell, W.D.S; Ammon, H.L; Dunitz, J.D; Gavezzotti, A; Hofmann, D.W.M; Leusen, F.J.J; Mooij, W.T.M; Price, S.L; Scheweizer B; Schmidt, M.U; Van Eijck, B.P; Verwer, P; Williams, D.E. *Acta Crystallogr.,Sect.B:Struct.Sci.,* 2000, **B56**, 697-714; (b) Motherwell, W.D.S; Ammon, H.L; Dunitz, J.D; Dzyabchenko, A; Erk, P; Gavezzotti, A; Hofmann, D.W.M; Leusen, F.J.J; Lommerse, J.P.M; Mooij, W.T.M; Price, D.L; Scheraga, H; Schweizer, B; Schmidt, M.U; Van Eijck, B.P; Vewer, P; Williams, D.E. *Acta Crystallogr.*, *Sect.B:Struct.Sci.,* 2002, **B58**, 647-661; (c) Day, G.M; Motherwell, W.D.S; Ammon, H.L; Boerrigter, S.X.M; Della Valle, R.G; Venuti, E; Dzyabchenko, A; Dunitz, J.D; Scheweizer B; Van Eijck, B.P; Erk, P; Facelli, J.C; Bazterra, V.E; Ferraro, M.B; Hofmann, D.W.M; Leusen, F.J.J; Liang, C; Pantelides, C.C; Karamertzanis, P.G; Price, S.L; Lewis, T.C; Nowell, H; Torrisi, A; Scheraga; H.A; Arnautova, Y.A; Schmidt, M.U; Verwer, P. *Acta Crystallogr.*, *Sect.B:Struct.Sci.,* 2005, **B61**, 511-527; (d) Day, G.M; Cooper, T.G; Cruz-Cabeza, A.J; Hejczyk, K.E; Ammon, H.L; Boerrigter, S.X.M; Tan, J.S; Della Valle, R.G; Venuti, E; Jose, J; Gadre, S.R; Desiraju, G.R; Thakur, T.S; Van Eijck, B.P; Facelli, J.C; Bazterra, V.E; Ferraro, M.B; Hofmann, D.W.M; Neumann, A; Leusen, F.J.J; Kendrick, J; Price, S.L; Misquita, A.J; Karamertzanis, P.G; Welch, G.W.A; Scheraga; H.A; Arnautova, Y.A; Schmidt, M.U; van de Streek, J; Wolf, A.K; Scheweizer B. *Acta Crystallogr*, *Sect.B:Struct.Sci.,* 2009, **B65**, 107-125; (e) Bardwell, D.A; Adjiman, C.S; Arnautova, Y.A; Bartashevich, E; Berrigter, S.X.M; Braun, D.E, Cruz-Cabeza, A.J; Della Valle, R.G; Desiraju, G.R; Van Eijck, B.P; Facelli, J.C; Ferraro, M.B; Grillo, D; Habgood, M; Hofmann, D.W.M; Jovan Jose, K.V; Karamertzanis, P.G; Kazantsev, A.V; Kendrick, J; Kuleshova, L.N; Leusen, F.J.J; Maleev, A.V; Misquita, A.J; Mohamed, S; Needs, R.J; Neuman, M.A; Nikylov, D; Orendt, A.M; Pal, R; Pantelides, C.C; Pickard, C.J; Price, S.L; Scheraga; H.A; van de Streek, J; Thakur, T.S; Tiwari, S; Venuti, E; Zhitkov, L.K. *Acta Crystallogr., Sect.B:Struct.Sci.,* 2011, **B67**, 535-551.

[3] Bernstein, J. 2002. *Polymorphism in molecular crystals*. Oxford University Press, Oxford, UK.

[4] Mishra, M.K; Palash Sanphui, Ramamurty, U; Desiraju, G.R. *Cryst. Growth Des*. 2014, **14**, 3054−3061.

[5] (a) Thalladi, V. R; Nüsse, M; Boese, R. *J. Am. Chem. Soc*, 2000, **122**, 9227. (b) Vishweshwar, P; Nangia, A; Lynch, V. M. *Cryst. Growth Des*, 2003, **3**, 783. (c) Morrison, J. D; Robertson, J. M. *J. Chem. Soc*, 1949, **2**, 980. (d) Verweel, H. J; MacGillavry, C. H. *Nature*, 1938, **142**, 161.

[6] Aakeröy, C.B; Forbes, S; Desper, J. *J. Am. Chem. Soc*, 2009, **131**, 17048-1709.

[7] Tsaggeos, K.V; Masiera, N; Niwicka, A; Dokorou, V; Siskos, G.M; Skoulika, S; Michaelides, A. *Cryst. Growth Des.*, 2012, **12**, 2187-2194.

[8] Wang, Z.Z; Chen, J.M; Lu. T.B. *Cryst. Growth Des.*, 2012, **12**, 4562-4566.

[9] Clarke, H.D; Arora, K.K; Bass, H; Kavuru, P; Ong, T.T; Pujang, T; Wojtas, L; Zaworotko, M.J. *Cryst. Growth Des.*, 2010, **10**, 2152-2167.

[10] Derisaju, G.R. *J. Am. Chem. Soc*, 2013, **135**, 9952-9967.

[11] Von Hippel, A.R. *Science*, 1962, **138**: 91-108.

[12] Schmidt, G.M.J. *Pure Appl. Chem.* 1971*,* **27**:647-678.

[13] Desijaru, G.R; Vital, J.J; Ramanan, A. *Crystal engineering: a textbook*. World Scientific, Singapore.

[14] Jeffrey, G.A. 1997. *An Introduction to Hydrogen Bonding*, Oxford University Press, Oxford, UK.

[15] Schneider, H.-J, Steed, J.W & Atwood, J.L. 2004. (Eds), *Marcel Dekker*, New York, NY, USA, **2**, 1550-1556.

[16] Desiraju, G.R. *Angew. Chem*, *Int Ed. Engl.* 1995, **34**, 2311.

[17] Desiraju, G.R. *Angew. Chem*, *Int Ed. Engl.* 2007, **46**, 8342.

[18] Aakeröy, C.B; Beaty, A.M; Helfrich, B.A & Nieuwenhuyzen, M. *Cryst. Growth Des.*, 2003, **3**, 159.

[19] Allen, F.S; Motherwell, W.D.S; Raithby, P.R; shields, G.P; Taylor, S. *New J. Chem.*, 1999, **23**, 25-34.

[20] Vangala, V.R; Bhogala, B,R; Dey, A; Desiraju, G,R; Brodet, C.K; Smith, P.S; Mondal, R; Howard, J. A. K; Wilson, C. C. *J. Am. Chem. Soc.*, **125**, 14495-14509.

[21] Biradha, K; Zaworotko, M.J. *J. Am. Chem. Soc.*, 1998, **120**, 6431-6432.

[22] Wöhler, F.. *Untersuchungun über das chinon*. Annalen, 1844, **51**, 153.

[23] Ling, A.R; Baker, J.L. *J. Chem. Soc.*, 1893, **63**, 1317-1327.

[24] Kitaigorodskii, A.I. 1984. *Mixed crystals*. New York: Spinger-Verlag.
[25] Anderson, J.S. *Nature*, 1937, **140**, 583-584.
[26] Remyga, S.A; Myasnokiva, R. M; Kitaigorodski, A.I. *Z. Strukturnoi. Khimii*, 1969, **10**, 1131-1133.
[27] Van Niekerk, J.N; Saunder, D.H; *Acta Crystallogr*, 1948, **1**, 44.
[28] Peter, S; Kováts, É; Oszlányi, G; Bényei, G; Klupp, G; Bortel, G; Jalsovszky, I; Jakab, E; Borondiscs, F; Kamarás, K; Bokor, M; Kriga, G; Tompa, K; Faigel, G.. *Nature Mat*., 2005, **4**, 764-767.
[29] Aakeröy, C.B; Salomon, C.B. *CrystEngComm*, 2005, **7**, 439-448.
[30] Dunitz, J.D. *CrystEngComm*, 2003, **4**, 506.
[31] Desiraju, G.R. *CrystEngComm*, 2003, **5**, 466-467.
[32] Aitipamula, S., Banerjee, R., Bansal, A.K., Biradha, K., Cheney, M.L., Choudhury, A.R., Desiraju, G.R., Dikundwar, A.G., Dubey, R., Duggirala, N., Ghogale, P.P., Gosh, S., Goswami, K.P, Goud, N.R., Jetti, R.R.K., Karpinski, P., Kaushik, P., Kumar, D., Kumar, V., Moulton, B., Mukherjee, A., Mukherjee, G., Myerson, A.S., Puri, V., Ramanan, A., Rajamannar, T., Reddy, C.M., Rodriguez-Hornedo, N., Rogers, R.D., Row, T.N.G., Sanphui, P., Shan, N., Shete, G., Singh, A., Sun, C.C., Swirft, J.A., Thaimattam, R., Thakur, T.S., Thaper, R.K., Thomas, S.P., Tothadi, S., Vangala, V.R., Variankaval, N., Vishweshwar, P., Weyna, D.R. & Zaworotko, M.J. *Cryst. Growth Des*, 2012, 2147-2152.
[33] Sculthеiss, N; Newman, A. *Cryst. Growth Des.*, 2009, **9**, 2950-2967.
[34] Almarsson, Ö; Zaworotko, M. *J. Chem Com*, 2004, **17**, 1889-1896.
[35] Viehweshwar, P; McMahom, J.A; Bis, J.A; Zaworotko, M.J. *J Pharm Sci*, 2006, **95**, 499-516.
[36] Sekhons, B.S. *Ars. Pharm.*, 2009, **50**, 99-117.
[37] Etter, M. C. J. *Chem. Phys*. 1991, **95**, 4601–4610.
[38] Jones, W; Motherwell, W.D.S; Trask, A.V. *MRS Bull*, 2006, **31**, 875-879.
[39] Peterson, M.L; Hickey, M.B; Zaworotko, M.J; Almarsson, O. *J. Pharm. Sci.*, 2006, **9**(3), 317-326.
[40] McNamara, D.P; Kuduva, S.S; McMahom, J.A; Moulton, B; Walsh, R.B; Rodriguez-Hornedo, N; Zaworotko, M.J. *Cryst. Growth Des.*, 2003, **3**, 909-919.
[41] Blagden, N; Berry, D.J; Parkin, A. Javed, H; Ibrahimm A; Gavan, P.T; De Matos, L.L; Seaton, C.C. *New J. Chem.*, 2008, **32**, 1659.
[42] Aakeröy, C.B; Chopade, P.D; Ganser, C; Rajbanshi, A; Desper, J. *CrystEngComm*, 2012, **14**, 5845-5853.
[43] Aakeröy, C.B; Panikkatu, S; Dehaven, B; Desper, J. *CrystEngComm*, 2013, **15**, 463-470.
[44] Aakeröy, C.B; Forbes, S; Desper, *J. Am. Chem. Soc*, 2009, **131**, 17048-17049.
[45] Vishweshwar, P; Nangia, A; Lynch, V.M *Cryst. Growth Des.*, 2003, **3**(5), 783-790.
[46] Katritzky, A.R; Jain, R; Lomaka, A; Petrukhin, R; Maran, U; Karlson, M. *Cryst. Growth Des.*, 2011, **1**(4), 261-265.
[47] Katritzky, A. R.; Lobanov, V. S.; Karelson, M. *Chem. Soc*. *Rev.* 1995, 279.
[48] Dearden, J. C. *Sci. Total Environ*. 1991, **109**/110, 59.
[49] Batisai, E.; Ayamine, A.; Kilinkissa, O. E. Y.; Báthori, N. B. *CrystEngComm*, 2014, **16**, 9992-9998.
[50] Wolff, S.K, Grimwood, D.J, McKinnon, J.J, Spackman, M.A. 2007. *Crystal Explorer 2.1. University of Western Australia*, Perth.
[51] Haynes, D.A; Jones, W; Motherwell, W.D.S. *CrystEngComm*, 2006, **8**, 830-840.

Chapter 2

Experimental methods and materials

Chapter 2: Experimental methods and materials

The following methods were used in this project:

- Design of new supramolecular systems with the aid of the Cambridge Structural Database
- Crystallization
- Thermoanalysis (thermogravimetry and differential scanning calorimetry)
- Structure determination (powder-X-ray diffraction and single crystal X-ray diffraction)
- Structure analysis was conducted with a series of suitable programs

2.1. Crystallization

The process of formation of crystals precipitating from a solution is called crystallization. Crystallization is also solid-liquid separation technique in which mass transfer from liquid solution to a pure solid crystalline phase occurs. The main processes of crystallization are nucleation and crystal growth. Nucleation is the step where the solute molecule starts to gather into clusters. These molecular aggregates must be stable; in case of unstable aggregates they will redissolve. In crystal growth, nucleation and growth continue to occur simultaneously while supersaturation exists. Supersaturation is the driving force of the crystallization.

Many methods can be used for crystallization:

- Cooling
- Addition of a second solvent to reduce the solubility of the solute
- Slow evaporation: This is the method that will be used in this project

100 mg of the solid hosts: ADP, SUC, SUB were introduced into 4 ml of the liquid guests: 4PIC; 2,4lUT; 3,4LUT and 3,5LUT. The mixture was stirred for about 15 min, after the solution became clear, it was left to evaporate at room temperature. Block, colourless crystals appeared after 2-3 weeks, their melting point was taken to characterize them.

2.2. Compounds used for crystallization

Inclusion compounds of selected carboxylic acids and amines were used to prepare multicomponent crystals.

2.2.1. Dicarboxylic acids

Dicarboxylic acids have the same chemical behaviour as monocarboxylic acids. The ionisation of the second carboxylic group occurs less readily than the first.

They are useful materials for the preparation of fragrances, polyamides, adhesives, lubricants and polyesters.

Safety precautions:

Carboxylic acids are generally weak acids. But they cannot be corrosive or pose other hazards. Always use proper personal protective equipment (PPE) such as goggles and gloves when working with carboxylic acids. Take care to avoid storage or use with incompatible chemicals such as bases. Avoid storing containers in metal cabinets, which can corrode. Carboxylic acids may also be flammable or combustible.[1]

The selection criteria of the applied carboxylic acids were based on small structural modification of succinic acid, by increasing the length with a $–CH_2$ group or adding an aromatic functional group, the systematic change may fine tune the crystal structure and its properties. The structural line diagrams of the selected dicarboxylic acids are shown on Figure 2.1 and their physical properties are listed in Table 2.1.

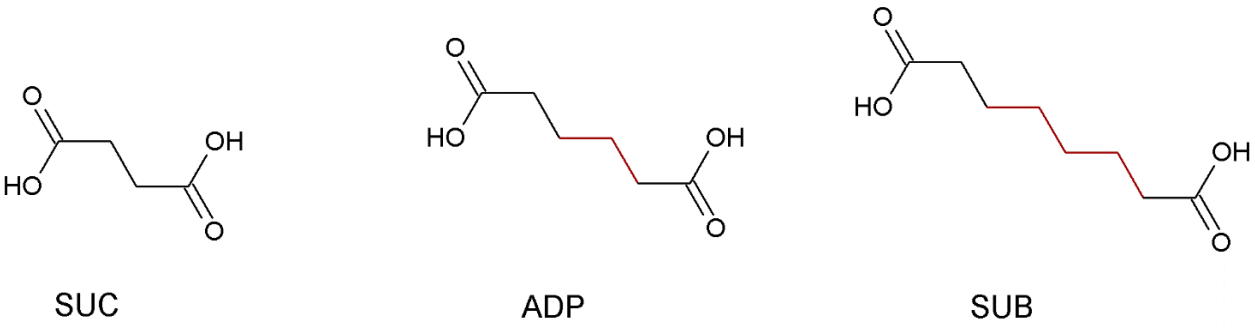

Figure 2.1 Host compounds ADP (adipic acid), SUB (suberic acid) and SUC (succinic acid) the systematic modification is highlighted with red.

.

Table 2.1 Physical properties of dicarboxylic acids[2]

Name	formula	Melting point (ºC)	*pKa* at 25 ºC	
			pKa_1	pKa_2
Succinic acid (SUC)	$C_4H_6O_4$	173-176	4.2	5.6
Adipic acid (ADP)	$C_6H_{10}O_4$	152.1	4.4	5.4
Suberic acid (SUB)	$C_8H_{14}O_{14}$	174.2	4.5	5.4

2.2.2. Aromatic amines

The pyridine derivatives were used in this project are presented in Figure 2.2.

Safety precautions:

Alkyl-pyridines can irritate the skin and cause corrosive burns. If inhaled, they can cause symptoms which may include ataxia, narcosis and depressed respiration. Alkyl-pyridines can also cause corrosive to the gastrointestinal system and people with liver and skin problems may be more vulnerable when working with these chemicals.[3]

The selection criteria of the applied amines were bond on small structural modification of 4PIC, by adding on extra $–CH_3$ functional group. This systematic change may fine tune the crystal structure and its properties eventually.

As a safety precaution, during the crystallization, safety glass and safety gloves were worn and the experiments were carried out in a fume cupboard. The physical properties of the used amines compounds are listed in table 2.2.

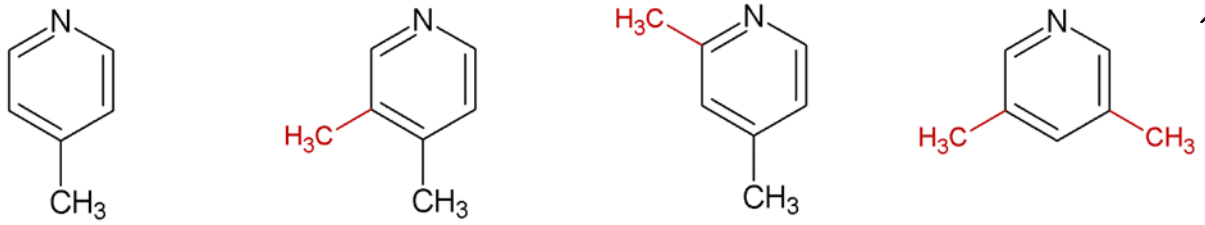

4PIC **3,4LUT** **2,4LUT** **3,5LUT**

Figure 2.2 Guest compounds 4PIC (4-picoline), 3,4LUT (3,4-lutidine), 2,4LUT (2,4-lutidine), 3,5LUT (3,5-lutidine) and the systematic modification of molecular structure is highlighted with red.

Table 2.2 Physical properties of pyridine derivatives[2]

Name	Formula	Molar mass g.mol^{-1}	Boiling point ^{o}C	*pKa* at 25 ^{o}C *pKa**
4-picoline (4PIC) *(4-methylpyridine)*	C_6H_7N	93.13	145	5.85
3,4-lutidine (3,4LUT) *(3,4-dimethylpyridine)*	C_7H_9N	107.15	169-141	6.33
2,4-lutidine (2,4LUT) *(2,4-dimethylpyridine)*	C_7H_9N	107.15	159	6.58
3,5-lutidine (3,5LUT) *(3,5-dimethylpyridine)*	C_7H_9N	107.15	169-170	6.14

** pKa values of the protonated base*

2.3. Thermogravimetry (TG)

Thermogravimetry is a technique in which the change of the weight of the sample is measured while it is heated or cooled in a furnace. Thermogravimetry is an essential laboratory tool and it used for material characterization in environmental, pharmaceutical, food, and petrochemical studies.

A Perkin-Elmer Pyris 6 series thermogravimeter was used as the equipment; the temperature is subject to a temperature programme. The components of the TG instrument are a thermobalance which is an analytical microbalance, furnace, temperature programmer, and sample holder, an enclosure for establishing the required atmosphere, and a recorder to display the data. A typical operating range for the furnace is from room temperature to 1000^{o}C, heating rate around 30 ^{o}C/min. A thermocouple is placed close to the sample to indicate the sample temperature.

Thermogravimetric curves are referred to as mass loss curves. Thermogravimetric curves can be used to evaluate the temperatures ranges, decomposition stages and fractional weight loss of each stage.[4]

This technique is effective for quantitative analysis of thermal reaction that is accompanied by mass changes, such as evaporation, decomposition, gas absorption and desolvation.

2.4. Differential Scanning Calorimetry

Differential scanning calorimetry (DSC) is used to measure changes of various physical quantities with changing temperature. It measures the difference in heat flow rate between sample and reference as a function of time and temperature. The main applications of DSC include determining phase transitions, melting points, glass transitions, crystallinity and kinetic studies.[14]

The equipment which was used in this study was a Perkin-Elmer Pyris 6 series. DSC was employed to estimate the onset temperature and enthalpy change during the departure of volatile guest system. These changes can be due to desolvation, phase transformation, melting and others thermal events. Two identical, crimped and vented aluminium pans with lids are used; one for the sample and the empty is the reference. The temperature of both pans is increased at a constant rate.[5]

Melting point of ADP•4PIC; ADP•3,4LUT; ADP•2,4LUT ADP•3,5LUT; SUB•4PIC; SUB•3,4LUT; SUB•2,4LUT; SUC•4PIC; SUC•3,4LUT; SUC•2,4LUT SUC•3,5LUT melting point was measured by using Perkin-Elmer Pyris 6 series and melting point of SUB•3,5LUT was measured by using by using a Q2000 TA instrument.

2.5. Powder X-ray Diffraction (PXRD)

X-ray diffraction is a technique where X-rays are used for structural characterization of materials. The phenomenon is based on interference between X-ray radiation and the crystalline material.

The diffraction is described by Bragg's law: $\mathbf{n\lambda = 2d\sin\Theta}$

Θ = is glancing angle between the X-ray beam and the plane of the crystal under irradiation.

d = is the distance between atomic layers in a crystal

λ = is the wavelength of the incident X-ray beam

n = is an integer

The diffraction occurs only when the Bragg's law is satisfied.

Inclusion compounds of carboxylic acids and amines were used in this work to make the model crystals. PXRD is a fundamental tool for the identification of compounds. It is used to monitor the phase changes or reaction kinetics for certain inclusion compounds. Samples were ground until they became a fine powder. Diffraction data for all compounds were collected on a Bruker D2 diffractometer.

2.6. Single crystal X-ray diffraction

X-rays are electromagnetic radiation with a very short wavelength ($\lambda = 10^{-10}$m = 1Å).[6] X-ray diffraction is generally a non-destructive analytical technique used to determine crystal structures and atomic spacing. Unit cell dimensions, bond-length, bond-angles, and details of site-ordering of crystalline materials can be obtained with the technique. Data obtained from X-ray analysis is refined and interpreted in order to solve crystal structures.[7] X-ray diffraction studies of crystalline materials have four major steps: crystallization, data collection, structure solution and refinement.

Diffraction data for all compounds were collected on a Bruker APEX II diffractometer with a graphite-monochromated MoKα = 0.71073 Å at 173 K using an oxford Cryostream 700.[8]

Structures were solved using SHELXS-97[9] which was run under a graphical user interface, X-seed.[10] The space group were determined by using the collected intensities and pre-determined cell parameters as inputs to program XPREP.[11] SHELXS-97[8] was used to solve all structures by direct methods and refinement was carried out with SHELXL-97[8] by employing full matrix least-squares against F^2 for unique reflection.

$$\Sigma w(F_o^2 - kF_c^2)^2$$

The agreement between the observed structure factors (F_O) and the calculated structure factors (F_c) were monitored by assessing the residual index R. The residual index R_1 is the agreement between the observed and calculated structure factors based on F, while the residual index, R_2, is the agreement based on F^2.

$$R_1=\frac{\Sigma||F_o|-|F_c||}{\sum|F_o|} \qquad R_2=\left[\frac{\sum w(F_o^2-F_c^2)^2}{\sum w(F_o^2)^2}\right]^{\frac{1}{2}}$$

The weighing scheme w was used to yield a constant distribution in terms of *a* and *b*, and further refined in the final cycles of structure refinement.

$$w=\frac{1}{\sigma^2(F_o^2)+(aP)^2+bP}$$

where

$$P=\frac{\max(o,F_o^2)+2F_c^2}{3}$$

Shelxl-97[8] refines against F^2, which leads to grater deviation of the Goodness of fit (S) from unity than the refinement against F. The Goodness of fit expression is:

$$S=\left[\frac{\sum w(|F_o|^2-|F_c|^2)^2}{(N-n_p)}\right]^{\frac{1}{2}}$$

The hydrogen atoms bound to carbon atoms were placed at idealized positions and refined as riding atoms with U_{iso} (H) = 1.2 U_{eq} (Ar-H, CH_2) or 1.5 U_{eq} (CH_3) of the atom to which the H is bound. H atoms bonded to carboxylic acid, amine or amide groups were located in the difference electron density map and their coordinates refined freely but their isotropic displacement parameters were fixed (U_{iso} (H) = 1.2 U_{eq}(O) or U_{eq} (N)) if it was necessary.

X-ray powder patterns were calculated using LAZY PULVERIX[12] and compared to experimental powder patterns for crystallization. All crystal packing diagrams were generated with POV-RAY.[13] The program LAYER[14] was utilized to test systematic absences and space group symmetry. For verification of types of voids occupied by guest molecule, the program SECTION[15] was used to slice through cross section of the unit cell. X-Seed were used as a graphical interface for the program SHELXS-97, SHELXL-97, LAZY PUVERIX, POV-RAY, LAYER and SECTION.

Other programs used in addition to X-Seed:

- Platon[16]

  A multipurpose analytical tool for crystal structure analysis; calculates all molecular parameters for the structures.

- ConQuest[17]

  Search engine using the Cambridge Structural Database (CSD) for informative and comparative structure details.

ADP•4PIC; ADP•3,4LUT; ADP•2,4LUT; ADP•3,5LUT, SUB•4PIC; SUB•3,5LUT; SUC•4PIC; SUC•3,4LUT; SUC•2,4LUT SUC•3,5LUT were collected on a Bruker APEX II diffractometer sand SUB•3,4LUT was collected on a Nonius Kappa CCD single crystal diffractometer.

2.7. Crystal Structure Analysis

Data reduction and unit cell refinement will be performed using SAINT-Plus[18] and the space groups were determined from systematic absences by XPREP[19] and further justified by the refinement results. The structures were solved with the aid of X-Seed[20] by direct methods using SHELXS-97[21] and refined using full-matrix least-squares/difference Fourier technique using SHELXL-97. Diagrams and publication material were generated using PLATON and X-Seed. All the crystal packing diagrams were generated with POV-Ray.

2.8. Computing components

ConQuest: The primary program for searching and retrieving from Cambridge Structural Database (CSD).[22]

SADABS (Siemens Area Detector Absorption Corrections)**:** an application in the APEX suite used to scale and correct data foe absorption collected on a Bruker AXS area detector.[23] The program is designed to exploit data redundancy, corrects for errors resulting from the variation in the volume of crystal, absorption by the crystal support and crystal decay during the measurement.

XPREP: This program determines the space group reads the raw data file (.raw) and the parameter file (.p4p) written by the diffractometer control program, also write the instruction file (.ins) and reflection data (hkl).

X-Seed: graphical user Interface for crystallography and graphical program.

Layer is a component of X-Seed. It display simulated precession photographs of the reciprocal lattice levels using the intensity data.

LAZY PULVERIX: software which calculates the theoretical powder X-ray diffraction pattern from single crystal X-ray diffraction data.

Pov-Ray: program which generates graphics.

Pov-Label: allows controlling the atom labels on an image rendered using Pov-Ray.

Mercury: Analysis software which provides options to aid the investigation and analysis of crystal structures. It can import chemical bond types, 2D connection tables and present them in 3D illustration generates packing diagrams defines and visualises Millers planes, and take a slice through a crystal in any direction also, it displays space group symmetry elements, calculates voids based either on contact surface or solvent accessible surface and intermolecular potentials, also it preforms basic gas phase calculation.[24]

2.9. Crystal Explorer[25]

Crystal Explorer is software, which serves to calculate Hirshfeld surfaces[26] of molecules within a crystal structure to map the intermolecular interactions between particular molecules. The Hirshfeld surface of a molecule is formulated by splitting the space in the crystal into sections where the electron distribution for the molecule dominates the corresponding sum over the crystal.[27] The isosurfaces generated from these calculations, with a specified weight function w (r) = 0.5, surrounds the molecule and partitioning the electron density of the molecular fragments.[28] Hirshfeld surfaces provide information about intermolecular interactions in the

crystal as the surface is calculated by splitting the electron density between the 'enclosed' molecule and its neighbours.[27] The analysis and comparison of the 3D Hirshfeld surfaces are difficult, thus typically its 2D interpretation, the so called 'fingerprint print plot' is generated.[29] The only prerequisite for quality data regarding intermolecular interactions to be extracted from Hirshfeld surfaces is that the crystal structures imported into the program are well-characterised with all hydrogen atoms located accurately.

The surfaces incorporated in this study are all calculated using the d_{norm} function so that the contact distance is normalized according to the formula.

$$d_{norm} = \frac{d_i - r_i^{vdW}}{r_i^{vdW}} + \frac{d_e - r_e^{vdW}}{r_e^{vdW}}$$

where d_i correspond the distance from the surface to the nearest atom interior to the surface; d_e correspond the distance from the surface to the nearest atom exterior to the surface. The sum of two distances would give an approximate contact distance.

References

[1] MSDS of dicarboxylic acids. http://www.sigmaaldrich.com/catalog/produc/aldrich/aldrich. Accessed on 28 of April 2015.

[2] The chemist's companion: A handbook of practical data, techniques, and references, ed. Gordon, A. J. and Ford, R. A. John Wiley and Sons, 1972.

[3] MSDS of alkyl-pyridine. http://www.sigmaaldrich.com/catalog/produc/aldrich/aldrich. Accessed on 28 of April 2015.

[4] Brown, M.E. 1998. Introduction to thermal Analysis. Chapman & Professional, London.

[5] Caira, M.R., Nassimbeni, L.R. 1996. *Phase transformations inclusion compounds, kinetics and thermodynamics of enclatharation. In Comprehensive Supramolecular chemistry,* MacNicol, D.D., Toda, F., Bishop, R., Eds; Pergamon: Oxford, Vol 6, Chapter 5.

[6] Rissanen, K. 2014. X-Ray Crystallography. Encyclopedia of Supramolecular Chemistry, 2:1586-1591.

[7] Brown, P.J, Forsyth, J.B. 1973. The crystal structure of solids. Edward Arnold Limited, London.

[8] Bruker 2005, APEX2.Version 1.0-27. Bruker AXS Inc., Madison, Wisconsin, USA.

[9] Sheldrick, G.M; Schneider, T.R. SHELXL: High resolution refinement. *Macromol. Crystallogr.,* 1997, **277**, 319-343.

[10] Barbour, L.J; X-Seed: Graphical interface for SHELX program. *J. Supramol. Chem,* 2003. **1**: 189-19.

[11] XPREP, Data Preparation and Reciprocal space Exploration, Version 5.1/NT ©1997, Bruker Analytical X-Ray systems.

[12] Yvon, K., Jeitschko, W. & Parthe, E.J. LAZY PULVERIX, a computer program, for calculating X-ray and neutron diffraction powder patterns. *J. Appl. Cryst.,* 1997 **10**: 73-74.

[13] Pov-Ray for Windows, version 3.1e. Watcom. Win32, The persistence of vision development team, ©1991-1999.

[14] Barbour, L.J. LAYER, A computer program for the graphic display of intensity data as simulated precession photographs. *J. Appl. Cryst.,* 1999. **32**: 351.

[15] Barbour, L.J. SECTION, A computer program for the graphic display of cross sections through a unit cell. *J. Appl. Cryst.* 1999. **32**: 351.

[16] Spek, A. L, PLATON, A multipurpose crystallographic tool, Version 10500, ©1980-2000.

[17] ConQuest, A program for the search of CSD, version 1.7, ©2001.

[18] Bruker 2004. SAINT-Plus (including XPREP). Version 7. 12. Bruker AXS Inc. Madison, Wisconsin, USA.

[19] XPREP-Data Preparation and Reciprocal Space Exploration. 1997. Version 5.1/NT, Bruker Analytical X-Ray System.

[20] Barbour, L.J; *J. Supramol. Chem.,* 2001, **1**, 189-191.

[21] Sheldrick, G.M; Schneider, T.R. *Macromol. Crystallorg.,* 1997 **B 277**: 319-343.

[22] Allen, F.H. *Acta Crystallogr., Sect. B: Struct. Sci.,* 2002, **58**, 380.

[23] Sheldrick, G.M. 2002. University of Göttingen, Germany.

[24] Macrae, C.F; Bruno, I.J; Chisholm, J.A; Edgington, P.R; McCabe, P; Pidcock, E; Rodriguez-Monge, L; Taylor, R; Van de Streek, J; Wood, P.A. *Mercury CSD 3.3.1 - New Features for the Visualization and Investigation of Crystal Structures*, *J. Appl. Crystallogr*., 2008, **41**, 466.

[25] Wolff, S.K, Grimwood, D.J, McKinnon, J.J, D., Spackman, M.A. 2007. Crystal Explorer 2.1. University of Western Australia, Perth.

[26] Hirshfeld, F.L. Bonded atom Fragments for Describing Molecular Charge Densities. *Theor. Chim Acta*, 1977. **44**:129-138.

[27] Spackman, M.A, Jayatilaka, D. Hirshfeld Surface Analysis, *CrystEngComm,* 2009, **11**: 19-22.

[28] The Crystal Explorer Manual. http://hirshfeldsurface.net/wiki/index.php/surface_properties. Accessed 15 February 2014.

[29] McKinnon, J,J; Jayatilaka, D; Spackman, M.A. *Chem.Commun,* 2007, **37**, 3814-3816.

Chapter 3

Single Crystal Structures

Chapter 3: Single Crystal Structures

3.1. Crystals of succinic acid (SUC) with substituted pyridines

In this chapter, single crystal structures of succinic acid (SUC) obtained from its solutions of substituted pyridines, such as 4-picoline (4PIC), 3,4-lutidine (3,4LUT), 2,4-lutidine (2,4LUT) and 3,5-lutidine (3,5LUT) will be discussed. All the crystal structure data of the succinic acid inclusions compounds (SUC•4PIC, SUC•3,4LUT, SUC-2,4LUT and SUC•3,5LUT) were collected on a Bruker APEX II diffractometer and summarized in **table 3.1** and their hydrogen bonding details are presented in **table 3.1.1**.

Table 3.1 Crystal data for SUC•4PIC, SUC•3,4LUT, SUC•2,4LUT and SUC•3,5LUT crystals.

Crystal data				
Compounds	**SUC•4PIC**	**SUC•3,4LUT**	**SUC•2,4LUT**	**SUC•3,5LUT**
Molecular formula	$C_{16}H_{20}N_2O_4$	$C_{18}H_{24}N_2O_4$	$C_{18}H_{24}N_2O_4$	$C_{18}H_{24}N_2O_4$
Formula weight (g.mol^{-1})	304.34	332.39	332.39	332.39
Crystal system	Triclinic	Monoclinic	Monoclinic	Monoclinic
Space group	$P\bar{1}$	$P2_1/c$	$P2_1/n$	$P2_1/c$
a (Å)	5.992(1)	9.783(2)	4.868(1)	10.443(2)
b (Å)	8.244(2)	6.034(1)	12.742(3)	4.964(1)
c (Å)	8.384(2)	15.574(3)	14.374(3)	17.057(3)
α (°)	84.30(3)	90.00	90.00	90.00
β (°)	80.65(3)	102.44(3)	96.27(3)	95.64(3)
γ (°)	70.02(3)	90.00	90.00	90.00
V (Å^3)	383.6(2)	897.8(3)	886.1(3)	879.9(1)
Z	1	2	2	2
ρ_{calc} (g.cm^{-3})	1.3172	1.2295	1.2456	1.2545
μ (MoKα) (mm^{-1})	0.095	0.087	0.088	0.089
F (000)	162	1.077	1.051	1.063
Crystal size (mm)	0.28 x 0.33 x 0.34	0.3 x 0.32 x 0.45	0.11 x 0.18 x 0.22	0.18 x 0.22 x 0.56
Temperature (K)	173(2)	173(2)	173(2)	173(2)
Radiation (Å)	MoKα, 0.71073	MoKα, 0.71073	MoKα, 0.71073	MoKα, 0.71073
Theta min-max (°)	2.46; 28.66	2.13; 28.08	3.20; 27.49	1.96; 28.43
Dataset	-8:7;10:11;-11:11	-12:12;-7:7;-20:20	-6:6;-16:16-18:18	-13:12; -6:6; -22:22
Final R indices [I>2.0(I)]	0.0455; 0.1222	0.0367; 0.0978	0.0538; 0.1507	0.0404; 0.1090
R indices [all data]	0.0524; 0.1276	0.0445; 0.1044	0.0818; 0.1738	0.0485; 0.1152
Tot., uniq. data, R (int)	4247; 1658; 0.0224	13732; 1810; 0.0265	3962; 1438; 0.0289	11138; 1858; 0.0278
N_{ref}, N_{par}	1945; 102	2170; 113	2027; 111	2214; 111
S	1.086	1.077	1.051	1.063
Max. and av. Shift/error	0.000/0.000	0.000/0.000	0.000/ 0.000	0.000/0.000
Min. and max. resd. dens. (Å^3)	-0.219; 0.333	-0.156; 0.263	-0.327; 0.410	-0.195; 0.265

Table 3.1.1 Hydrogen bonds in SUC•4PIC, SUC•2,4LUT, SUC•3,4LUT and SUC•3,5LUT

Crystals	D-H···A	d(D-H) (Å)	d(H··· A) (Å)	d(D··· A) (Å)	D-H···A (°)	Symmetry operator
SUC•4PIC	O7A-H7...N1	0.91	1.78	2.689(2)	179.7	
SUC•3,4LUT	C4-H4...O8B	0.95	2.43	3.353(2)	163.8	2-x, 1-y, 1-z
	O8A-H8...N1	0.88	1.76	2.627(1)	171.4	
	C5-H5…O8B	0.95	2.65	3.323(2)	128.0	
SUC•2,4LUT	C1-H1...O8B	0.95	2.73	3.370(2)	125.6	
	O8A-H8...N1	1.01	1.65	2.657(2)	170.6	
SUC•3,5LUT	C5-H5...O8B	0.95	2.54	3.236(2)	130.5	
	O8A-H8...N1	1.00	1.68	2.676(1)	176.4	

3.1.a Crystal structure of succinic acid with 4-picoline (SUC•4PIC)

Succinic acid (SUC) was introduced into a vial of 4 ml of 4-picoline (4PIC) and the mixture was stirred continuously. The acid dissolved easily in the 4PIC and the solution became clear after a few minutes. The solution was left to crystallize at room temperature and resulted in colorless block shaped crystals in two weeks (**figure 3.1**). A selected crystal with dimensions of 0.28 x 0.33 x 0.34 mm was subjected to single crystal X-ray structure analysis.

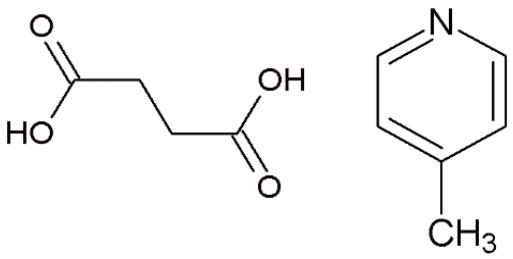

Figure 3.1 Structural line diagram of succinic acid (SUC) and 4-picoline (4PIC).

The SUC•4PIC solvate was solved in the triclinic centrosymmetric space group $P\ \bar{1}$ with the molecular formula $C_{16}H_{20}N_2O_4$ and was refined to R_1= 0.0455 and wR_2= 0.1276. The single crystal structure revealed that the diacid SUC captured two molecules of the 4PIC, and the asymmetric unit contains half of a SUC molecule (located at *Wyckoff position h*) and one 4PIC molecule. The main molecular unit consist of a SUC molecule hydrogen bonded to two 4PICs via the two carboxylic acid moieties through **O7A-H7···N1** hydrogen bonds (2.689(2) Å, 179.7°) (**figure 3.1.1**). The carboxylic acid group and the aromatic ring are not coplanar (11.44°) thus only one hydrogen bond forms between these moieties. These hydrogen bonded assemblies packed into layers in the crystal structure and no obvious hydrogen bonding can be observed between the units forming these layers (**figure 3.1.3**). The loosely packed layers arrange into the third dimension to form the crystal and these sheets of molecules are presented by different colours in **figure 3.1.4**.

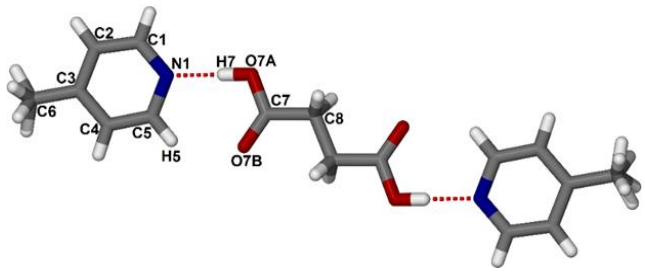

Figure 3.1.1 The structure of SUC•4PIC consists of hydrogen bonded molecular associates in the manner that one SUC bonds to two 4PICs. Only the asymmetric unit is labelled for clarity.

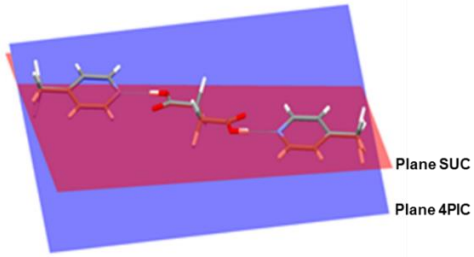

Figure 3.1.2 Molecular arrangement in the hydrogen bonded unit SUC•4PIC. The enclosed angle of the planes (red-COOH moieties of SUC, blue-aromatic ring of 4PIC).

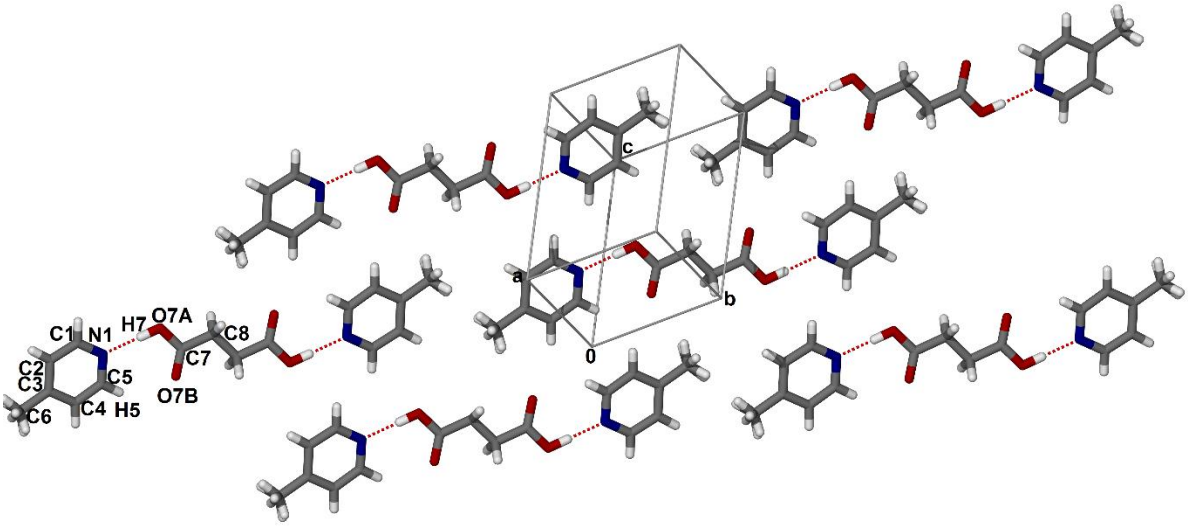

Figure 3.1.3 Packing diagram of SUC•4PIC showing the layers of molecular associates. Note the lack of hydrogen bonds between the acid-amine units forming the layered structure. Only the asymmetric unit is labelled for clarity.

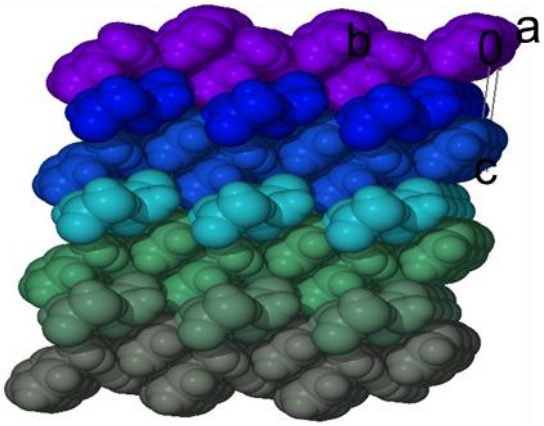

Figure 3.1.4 Packing diagram of SUC•4PIC presenting the sheets of molecules are forming the third dimension in the crystallographic direction of [001] and represented with different colors.

Powder X-ray analysis was conducted to show that the structure determined using one single crystal only (**figure 3.1.5**, SUC•4PIC single crystal, red) is representative of the bulk material (**figure 3.1.5**, SUC•4PIC bulk, green). Also PXRD analysis was used to show that the SUC•4PIC inclusion compound can be prepared with a more environmentally friendly method by using a minimal amount of solvent. Pure SUC was ground with a few drops of 4PIC and after 20 mins the PXRD pattern of the ground material (**figure 3.1.5**, SUC•4PIC grinding, blue) was compared to the starting pattern of SUC (**figure 3.1.5**, SUC, black). The patterns for the ground material and the single crystal is clearly different from the starting material, SUC. The pattern obtained from the single crystal structure shows some similarities with the bulk material but does not agree completely. It was noticed that the crystals were very unstable and decomposed (lost included solvent) easily. This can explain the observed difference between these patterns. The grinding experiment resulted a mixture of the starting material and another, unidentified phase. The solubility of the acid is very high in the 4PIC and after adding only several drops of solvent, the acid dissolved immediately. It is not sure if the required 1:2 H:G ratio was reached but it is more likely that a 1:1 or a non stoichiometric ratio of the materials were ground together.

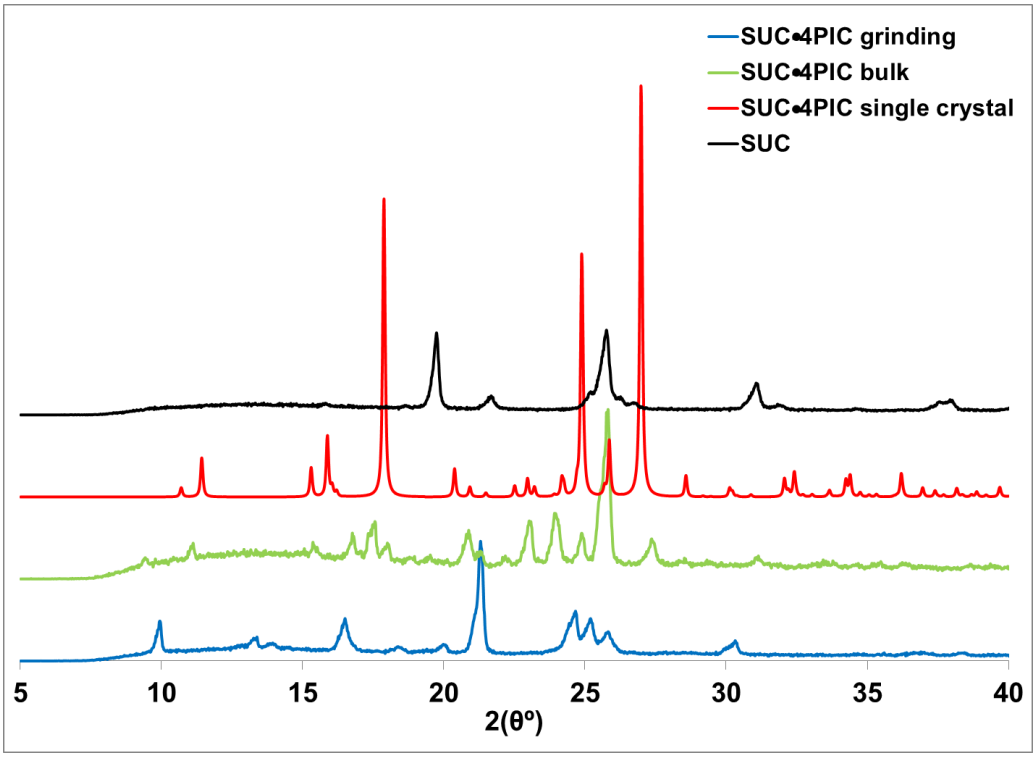

Figure 3.1.5 PXRD patterns for the pure acid (SUC, black), the single crystal structure (SUC•4PIC single crystal, red), the crystalline bulk material (SUC•4PIC bulk, green) and the result of the grinding experiment (SUC•4PIC grinding, blue).

3.1.b Crystal structure of succinic acid with 3,4-lutidine (SUC•3,4LUT)

The **SUC•3,4LUT** crystal structure was published earlier (CSD refcode: RESHAZ[1]). The compound was recrystallized for possible further analysis. Succinic acid (ca. 100 mg) was introduced into a vial of 4 ml of 3,4-lutidine and the mixture was stirred until the acid dissolved. The solution was left to crystalize at room temperature and after two weeks, well-shaped block crystals were obtained (**figure 3.1.6**). A selected crystal with dimensions 0.30 x 0.32 x 0.45 mm was subjected to single crystal X-ray structure analysis.

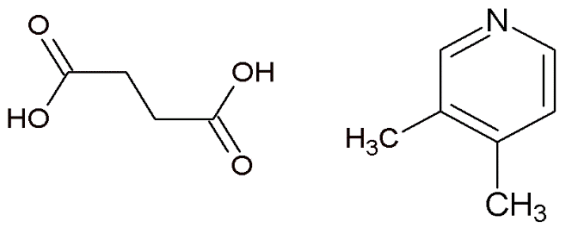

Figure 3.1.6 Structural line diagram of succinic acid (SUC) and 3,4-lutidine (3,4LUT).

The SUC•3,4LUT solvate was solved in the monoclinic achiral space group $P2_1/c$ with $C_{18}H_{24}N_2O_4$ molecular formula. The structure of SUC•3,4LUT was refined to R_1= 0.0367 and wR_2= 0.1044 and the structure analysis revealed that one SUC captured two molecules of the 3,4LUT. The carboxylic acid moieties hydrogen bond via **O8A-H7···N1** (2.627(1) Å, 171.4°) and **C5-H5···O8B** (3.323(2) Å, 128.0°) to two 3,4-lutidines (**figure 3.1.7**). The asymmetric unit contains a half SUC molecule (located at *Wyckoff position d*) and one 3,4LUT and this is, similarly to the previously discussed **SUC•4PIC** structure, the main molecular building block of the crystal. These hydrogen bonded assemblies arranged in tape-like motifs via **C4-H4···O8B** (3.353(2) Å, 163.8°) hydrogen bonds (**figure 3.1.8**) and the molecular tapes are forming an off-set zigzag pattern (**figure 3. 1.9)**.

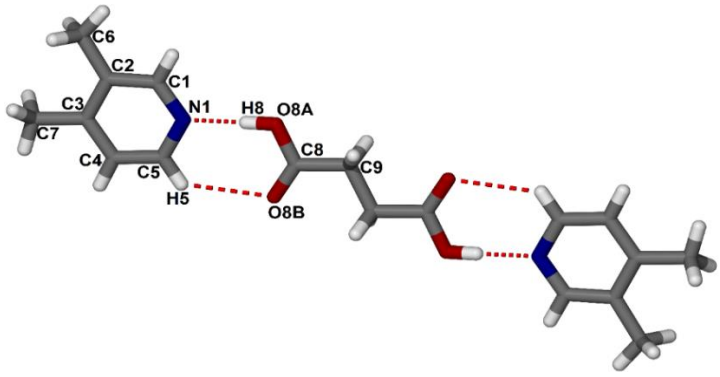

Figure 3.1.7 The structure of SUC•3,4LUT consists of hydrogen bonded molecular associates in the manner that one SUC bonds to two 3,4LUTs. Only the asymmetric unit is labelled for clarity.

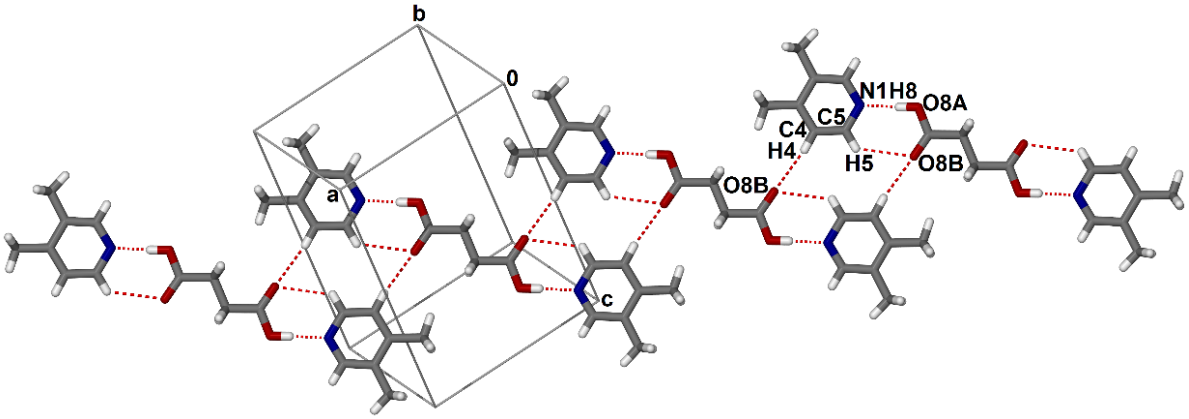

Figure 3.1.8 Packing diagram of SUC•3,4LUT showing the hydrogen bonded tapes formation from the acid-amine units. Only atoms involved in hydrogen bonds are labelled for clarity.

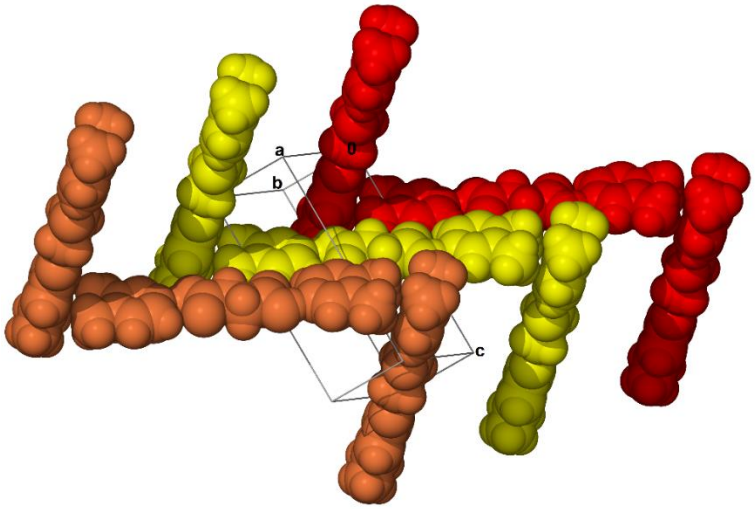

Figure 3.1.9 Packing diagram of SUC•3,4LUT showing the zigzag packing motif.

Similarly to the previous structure, powder X-ray analysis was used to prove that the single crystal structure is representative to the bulk material (**figure 3.1.10** SUC•3,4LUT single crystal, red and SUC•3,4LUT bulk, green). Grinding was used to reproduce this inclusion compound in a larger scale (**figure 3.1.10** SUC•3,4LUT grinding, blue). The pattern of the ground material (**figure 3.1.10** SUC•3,4LUT grinding, blue) was compared to the starting succinic acid (**figure 3.1.10** SUC, black) and it may be concluded that possibly the grinding resulted in a compound with different stoichiometry.

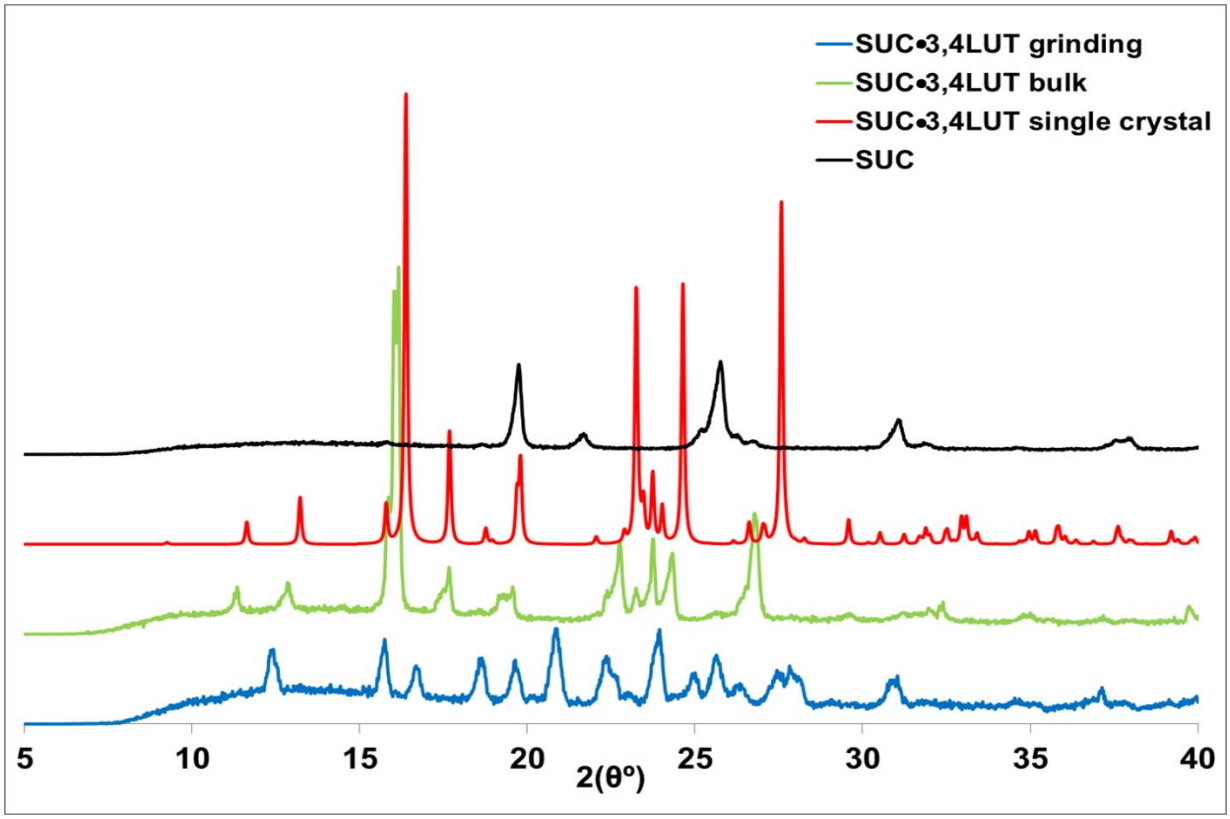

Figure 3.1.10 PXRD patterns for the pure acid (SUC, black), the single crystal structure (SUC•3.4LUT single crystal, red), the crystalline bulk material (SUC•3,4LUT bulk, green) and the result of the grinding experiment (SUC•3,4LUT grinding, blue).

3.1.c Crystal structure of succinic acid with 2,4-lutidine (SUC•2,4LUT)

This crystal structure also was published earlier (RESGAY[1]) but the compound was recrystallized for further analysis. The host, succinic acid (SUC) was introduced into 4 ml 2,4-lutidine (2,4LUT) and the mixture became clear after a few minutes of continuous stirring. The solution was left to crystallize at room temperature and resulted colorless block shape crystals in two weeks (**figure**

3.1.11). A selected crystal with dimensions 0.11 x 0.18 x 0.22 mm was subjected to single crystal X-ray structure analysis. The SUC•2,4LUT solvate was solved in the monoclinic achiral space group $P2_1/n$ with $C_{18}H_{24}N_2O_4$ molecular formula. The inclusion compound SUC•2,4LUT was refined to R_1= 0.0538 and wR_2= 0.1738. The asymmetric unit consist of half SUC molecule (located at *Wyckoff position d*) and one 2,4LUT molecule hydrogen bonded via **C1-H1···O8B** (3.370(2) Å, 125.6°) and **O8A-H8···N1** (2.657(2) Å, 170.6°) interactions (**figure 3.1.12**).

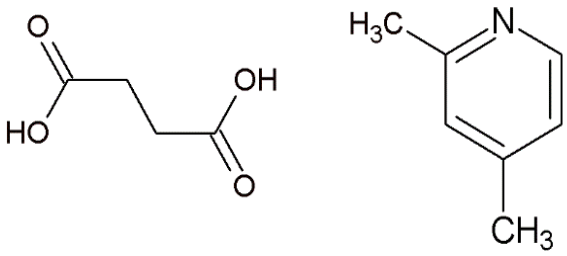

Figure 3.1.11 Structural line diagram of succinic acid (SUC) and 2,4-lutidine (2,4LUT)

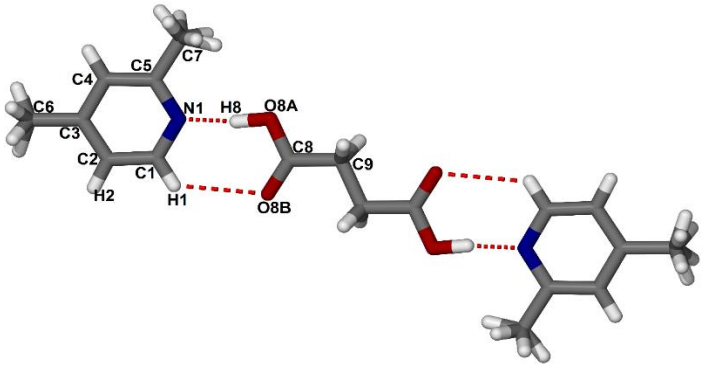

Figure 3.1.12 The structure of SUC•2,4LUT consists of hydrogen bonded molecular building blocks in the manner that one SUC bonds to two 2,4LUTs. Only the asymmetric unit is labelled for clarity.

It is also noticeable that the methyl groups of the lutidine molecules are disordered and were modelled in two positions with equal site occupancies. The hydrogen bonded assemblies are packed into columns down [100] crystallographic direction with no observable strong secondary interactions between them. This arrangement differs significantly from the previously observed packing motifs in SUC•4PIC (**figure 3.1.3**) and SUC•3,4LUT (**figure 3.1.8**). These molecular columns (**figure 3.1.13 (a))** forming zigzag motifs in the crystal (**figure 3.1.13 (b))**, view down the *a* axis).

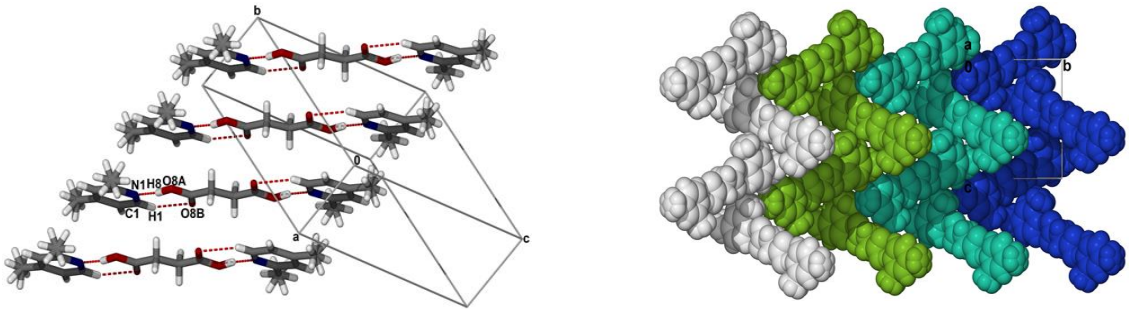

(a) **(b)**

Figure 3.1.13 (a) Packing diagram of SUC•2,4LUT showing the molecular columns with labels of the atoms involved in hydrogen bonding. (b) Packing diagram of SUC•2,4LUT presenting the zigzag motif.

PXRD analysis was used to prove that the structure of the single crystal (**figure 3.1.14** SUC•2,4LUT single crystal, red) is representative of the bulk (**figure 3.1.14** SUC•2,4LUT, green). The grinding method was used to produce SUC•2,4LUT solvate with small amount of 2,4LUT and its pattern was compared to the pattern of the pure acid (**figure 3.1.14** SUC•2,4LUT grinding, blue and **figure 3.1.14** SUC, black). The pattern of the single crystal agrees well with the with the bulk material, thus the collected single crystal structure is representative to the bulk material. The pattern of the ground material contains peaks related to the starting material and the inclusion compound too, as a result the experiment was a partial success.

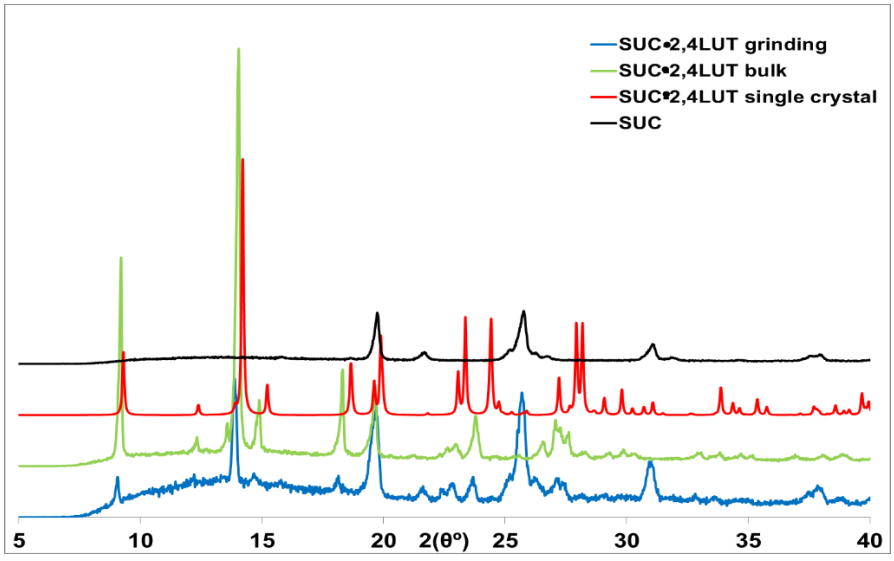

Figure 3.1.14 PXRD patterns for the pure acid (SUC, black), the single crystal structure (SUC•2,4LUT single crystal, red), the crystalline bulk material (SUC•2,4LUT bulk, green) and the result of the grinding experiment (SUC•2,4LUT grinding, blue).

3.1.d Crystal structure of succinic acid with 3.5-lutidine (SUC•3,5LUT)

Similarly to the previous crystals of SUC, this crystal structure was published earlier (RESHIS[1]) and the compound was recrystallized for further analysis. The succinic acid (SUC) was introduced into a vial of 3,5LUT (ca. 4 ml) and the mixture was stirred continuously (**figure 3.1.15**). The solid dissolved easily and the solution became clear after a few minutes. The solution was left to crystallize at room temperature and resulted colorless block shape crystals in two weeks. A selected crystal with dimensions of 0.18 x 0.22 x 0.56 mm was subjected to single crystal X-ray structure analysis.

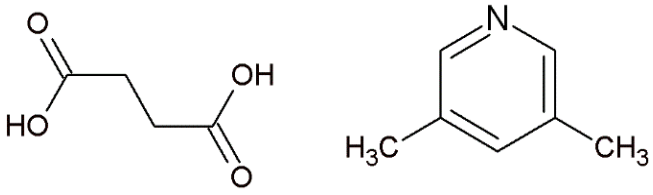

Figure 3.1.15 Structural line diagram of succinic acid (SUC) and 3,5-lutidine (3,5LUT).

The structure was solved in the monoclinic achiral space group $P2_1/c$ with $C_{18}H_{24}N_2O_4$ molecular formula and it was refined to R_1= 0.0404 and wR_2=0.1152. The asymmetric unit contains half SUC molecule (located at *Wyckoff position d*) hydrogen bonded to one 3,5LUT molecule (**figure 3.1.16**) via **C5-H5...O8B** (3.236(2) Å, 130.5°) and **O8A-H8...N1** (2.676(1) Å, 176.4°) hydrogen bonds which are presented in **figure 3.1.16**.

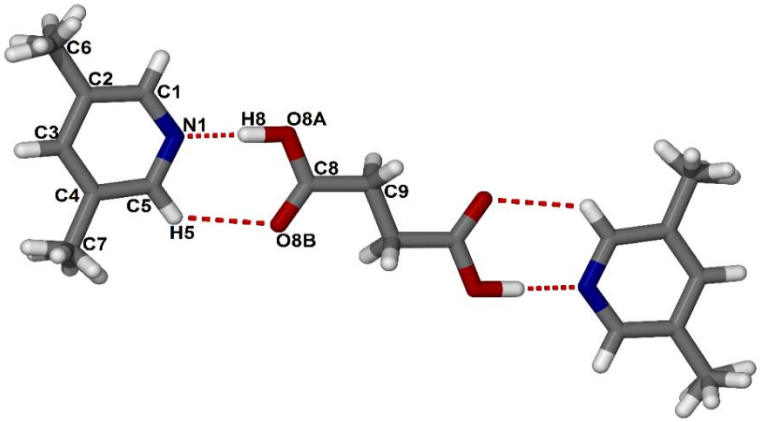

Figure 3.1.16 The structure of SUC•3,5LUT consists of hydrogen bonded molecular associates in the way that one SUC bonds to two 3,5LUTs. Only the asymmetric unit is labelled for clarity.

Similarly to the SUC•2,4LUT structure, the methyl groups of the lutidine are disordered and were modelled in two equal positions. The hydrogen bonded units are arranged into 1D molecular tapes similarly observed in the structure of SUC•4PIC (**figure 3.1.3**). Again, there are no strong secondary interactions, such as hydrogen bonds, observed between the neighbouring units forming these tapes (**figure 3.1.17**). The tapes of molecules packed in zigzag motifs running along the *a* axis (**figure 3.1.18**). This packing diagram looks similar to the one described for SUC•3,4LUT (**figure 3.1.9)** in term of motif but with the lack of the hydrogen bonds between the molecules.

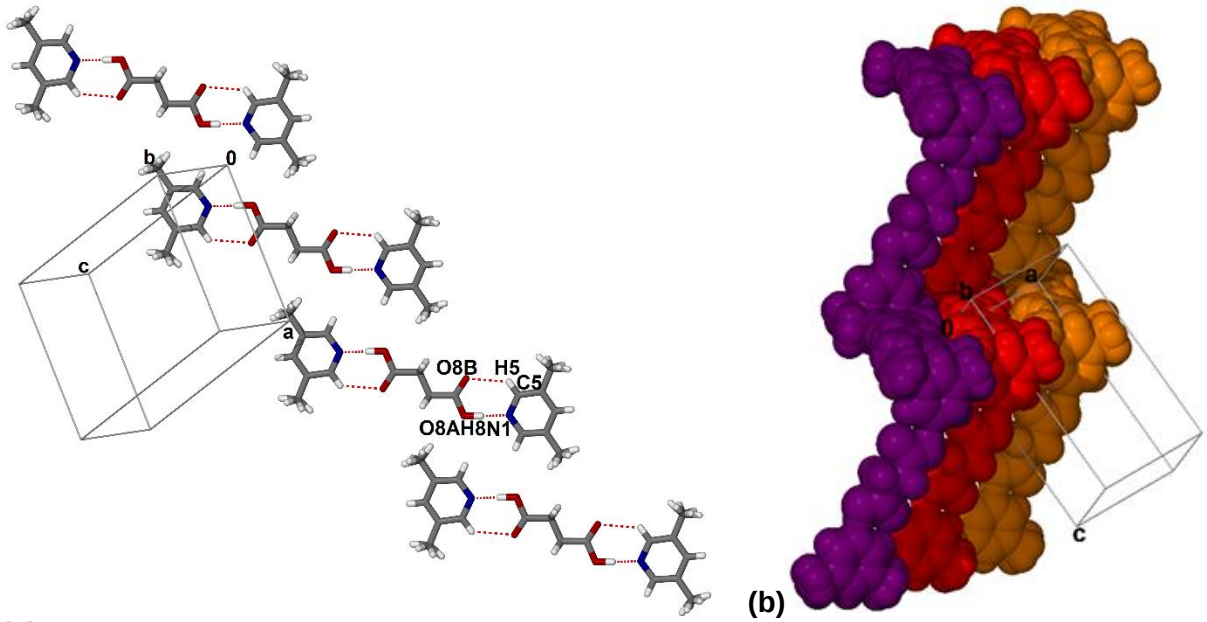

Figure 3.1.17 (a) Packing diagram of SUC•3,5LUT showing the layers of molecular associates. Note the lack of hydrogen bonds between the acid-amine units forming these 1D tape structure. (Only the hydrogen bonds in the asymmetric unit are labelled for clarity.) (b) Packing diagram of SUC•3,5LUT presenting a zigzag motif shown from the direction of [100].

PXRD analysis was used to prove that the single crystal structure detected (**figure 3.1.18** SUC•3,5LUT single crystal, red) and the bulk material (**figure 3.1.18** SUC•3,5LUT, green) are the same. The grinding method (**figure 3.1.18** SUC•3,5LUT grinding, blue) resulted a mixture of the starting material and the inclusion compound, thus the experiment was not successful (**figure 3.1.18** SUC•3,5LUT grinding, blue staring material SUC, black).

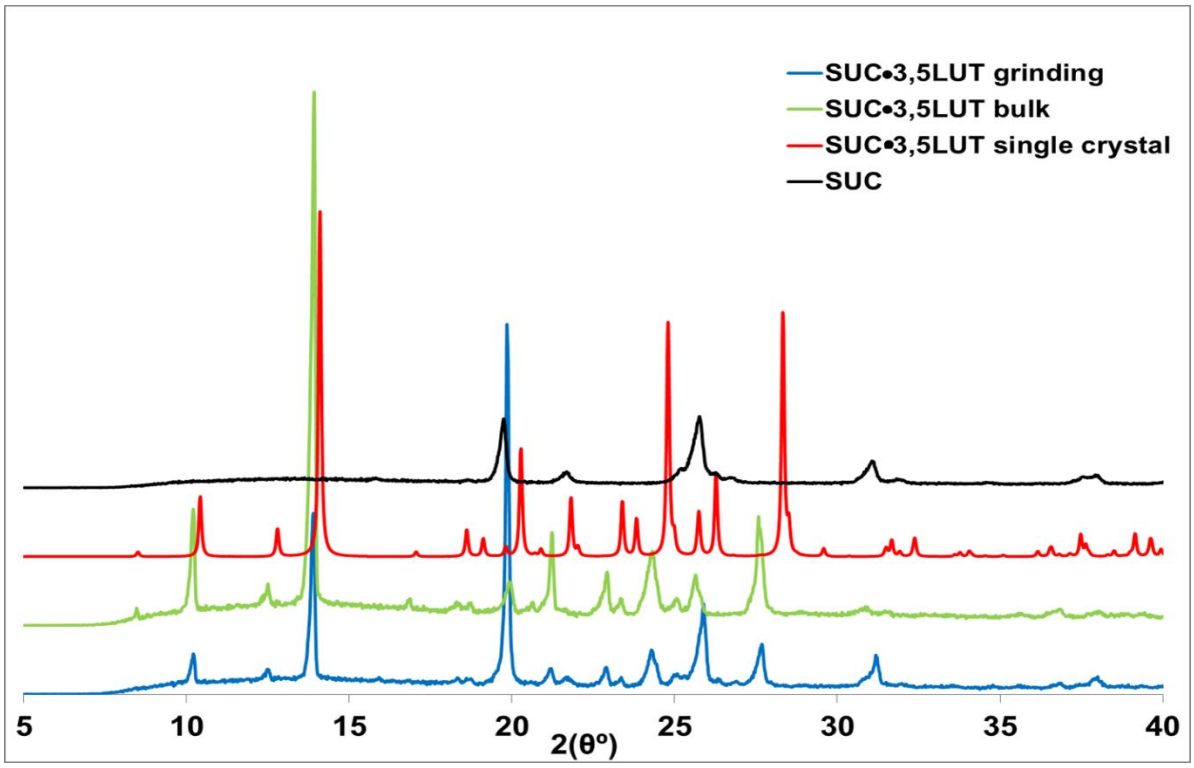

Figure 3.1.18 PXRD patterns for the pure acid (SUC, black), the single crystal structure (SUC•3,5LUT single crystal, red), the crystalline bulk material (SUC•3,5LUT bulk, green) and the result of the grinding experiment (SUC•3,5LUT grinding, blue).

3.2. Crystals of adipic acid (ADP) with substituted pyridines

In the following section, single crystal structures of adipic acid (ADP) obtained from its solutions of substituted pyridines, such as 4-picoline (4PIC), 3,4-lutidine (3,4LUT), 2,4-lutidine (2,4LUT) and 3,5-lutidine (3,5LUT) will be discussed. All the crystal structure data of the adipic acid inclusions compounds (ADP•4PIC, ADP•3,4LUT, ADP•2,4LUT and ADP•3,5LUT) were collected on a Bruker APEX II diffractometer and summarized in **table 3.2** and their hydrogen bonding details are presented in **table 3.2.1**.

Table 3.2 Crystal data for ADP•4PIC, ADP•3,4LUT, ADP•2,4LUT and ADP•3,5LUT crystals.

Crystal data				
Compounds	**ADP•4PIC**	**ADP•3,4LUT**	**ADP•2,4LUT**	**ADP•3,5LUT**
Molecular formula	$C_{18}H_{24}N_2O_4$	$C_{20}H_{28}N_2O_4$	$C_{20}H_{28}N_2O_4$	$C_{20}H_{28}N_2O_4$
Formula weight (g.mol^{-1})	332.39	360.45	360.45	360.45
Crystal system	Triclinic	Triclinic	Triclinic	Monoclinic
Space group	*P*1	$P\bar{1}$	$P\bar{1}$	$P2_1/n$
a (Å)	6.948(1)	10.699(2)	7.437(2)	12.007(2)
b (Å)	7.162(1)	11.862(2)	8.705(2)	6.508(1)
c (Å)	10.509(2)	12.731(3)	8.982(2)	12.702(3)
α (°)	78.17(3)	109.09(3)	92.14(3)	90.00
β (°)	73.89(3)	101.58(3)	102.95(3)	90.13(3)
γ (°)	62.48(3)	96.97(3)	114.85(3)	90.00
V (Å^3)	443.8(2)	1464.9(5)	508.5(2)	992.6(3)
Z	1	3	1	2
ρ_{calc} (g.cm^{-3})	1.2437	1.2256	1.1770	1.2059
μ (MoKα) (mm^{-1})	0.088	0.085	0.082	0.084
F (000)	178	582	194	388
Crystal size (mm)	0.12 x 0.13 x 0.24	0.12 x 0.13 x 0.24	0.18 x 0.22 x 0.29	0.12 x 0.28 x 0.31
Temperature (K)	173(2)	173(2)	173(2)	173(2)
Radiation (Å)	MoKα, 0.71073	MoKα, 0.71073	MoKα, 0.71073	MoKα, 0.71073
Theta min-max (°)	2.03; 28.36	1.75; 27.56	4.39; 27.54	2.33; 28.43
Dataset	-9;9;-9:9;-13:13	-13: 13; -15: 15; -14: 16	-9:0; -10: 11; -11: 11	-16:16;-8:8;-16:16
Final R indices [I>2.0(I)]	0.0385; 0.1066	0.0538; 0.1356	0.0426; 0.1122	0.0399; 0.1044
R indices [all data]	0.0477; 0.1161	0.1001; 0.1624	0.0578; 0.1224	0.0501; 0.1126
Tot., uniq. data, R (int)	8148; 3653; 0.0183	17350; 3914; 0.0405	2292; 1803; 0.0000	12126; 2012; 0.0321
N_{ref}, N_{par}	4379; 222	6739; 360	2292; 118	2483; 120
S	1.038	0.993	1.050	1.049
Max.and av. Shift/error	4.852/0.133	0.000/0.007	0.000/0.000	0.000/0.000
Min. and max. resd. dens. (Å^3)	-0.181/0.271	-0.256; 0.279	-0.179; 0.253	-0.186; 0.293

Table 3.2.1 Hydrogen bonds in ADP•4PIC, ADP•2,4LUT, ADP•3,4LUT and ADP•3,5LUT

Crystals	D-H···A	d(D-H) (Å)	d(H··· A) (Å)	d(D··· A) (Å)	D-H···A (º)	Symmetry operator
ADP•4PIC	O7A-H7...N1	0.90	1.79	2.688(4)	176.2	
	C5-H5…O7B	0.95	2.58	3.277(4)	130.2	
	C1-H1…O12A	0.95	2.57	3.390(4)	144.2	x-1, y, z-1
	C4-H4…O12B	0.95	2.44	3.321(4)	153.5	x-1, y-1, z
	C13-H13…O7A	0.95	256	3.370(4)	143.2	1+x, y, 1+z
	C16-H16…O7B	0.95	2.42	3.300(4)	154.5	1+x, 1+y, z
	C17-H17…O12B	0.95	2.55	3.265(4)	132.6	
ADP•3,4LUT	O8A-H8...N1	0.94	1.69	2.631(2)	174.6	
	O18A-H18...N2	0.98	1.69	2.666(2)	173.0	
	O23A-H23...N3	1.01	1.63	2.631(2)	175.3	
	C1-H1…O8A	0.95	3.18	3.923(2)	136.3	1-x, 1-y, 1-z
	C4-H4...O8B	0.95	2.43	3.362(2)	165.7	1-x, -y, 1-z
	C5-H5...O8B	0.95	2.57	3.253(2)	128.8	
	C11-H11…O23A	0.95	3.03	3.870(2)	148.2	x, 1+y, 1+z
	C14-H14…O23B	0.95	2.40	3.337(2)	167.6	x, y, 1+z
	C15-H15...O18B	0.95	2.53	3.232(2)	130.9	
	C22-H22…O8A	0.99	2.67	3.655(2)	171.7	x, y, z
	C24-H24...O18A	0.95	3.10	3.887(2)	141.4	x, y-1, z-1
	C27-H27...O18B	0.95	2.44	3.339(2)	157.5	x, y, z-1
ADP•2,4LUT	O8A-H8...N1	0.99	1.67	2.661(2)	173.3	
ADP•3,5LUT	C1-H1...O8B	0.95	2.78	3.421(2)	125.8	
	O8A-H8...N1	0.98	1.68	2.654(1)	173.8	

3.2.a Crystal structure of adipic acid with 4-picoline (ADP•4PIC)

The ADP•4PIC structure was previously published by our research group[2]. For the completeness of this work, this structure is discussed in details again. Originally the compound was prepared by dissolving 100 mg of adipic acid (ADP) in 4 ml of 4-picoline (4PIC) and the mixture was stirred until the acid dissolved (**figure 3.2**). After a few minutes, the solution became clear and it was left to crystalize at room temperature. After two weeks, well-shaped block crystals were obtained. A selected crystal with dimensions of 0.12 x 0.33 x 0.58 mm was subjected to single crystal X-ray structure analysis.

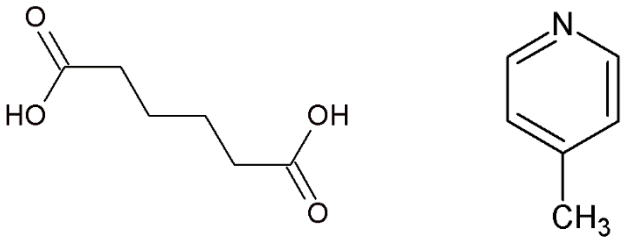

Figure 3.2 Structural line diagram of adipic acid (ADP) and 4-picoline (4PIC).

The ADP•4PIC solvate was solved in the triclinic chiral space group *P*1 with $C_{18}H_{24}N_2O_4$ molecular formula. The inclusion compound ADP•4PIC was refined to R_1= 0.0385 and wR_2= 0.1161. During the structure solution, the E-statistics indicated a $P\ \bar{1}$ space group however the refinement resulted disordered methyl groups on the picoline moiety. Then the structure was refined in *P*1 space group and interestingly, the hydrogen atoms of the methyl groups showed no disorder and were not related by the pseudo centre of symmetry located at the centre of the ADP methylene chain. Consequently it was concluded that the structure is non-centrosymmetric only by virtue of the different orientation of the methyl hydrogen atoms of the picoline. The structure showed that the diacid ADP captured two molecules of the 4PICs, and the asymmetric unit contains one full ADP located in a general position and two 4PIC molecules. The main supramolecular unit consist of a ADP molecule hydrogen bonded to two 4PICs via the two carboxylic acid moieties through **O7A-H7···N1** hydrogen bond (2.688(4) Å, 176.2°), **C5-H5···O7B** hydrogen bond (3.277(4) Å, 130.2°) and **C17-H17···O12B** hydrogen bond (3.265(4) Å, 132.6°) (**figure 3.2.1**). These hydrogen bonded assemblies are arranged in hydrogen bonded sheets via **C1-H1…O12A** (3.390(4) Å, 144.2°), **C4- H4…O12B** (3.321(4) Å, 153.5°), **C13-H13…O7A** (3.370(4) Å, 143.2°) and **C16-H16…O7B** (3.300(4) Å, 154.5°) hydrogen bonds presented in figure 3.2.2.

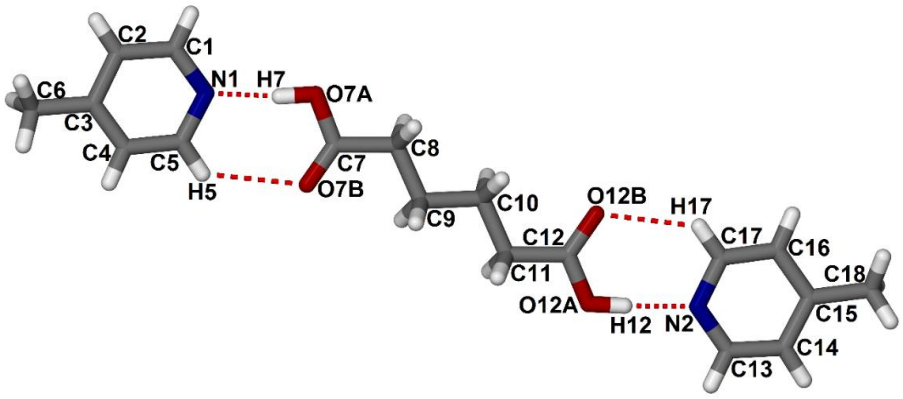

Figure 3.2.1 The structure of ADP•4PIC consists of hydrogen bonded molecular associates in the manner that one ADP bonds to two 4PICs.

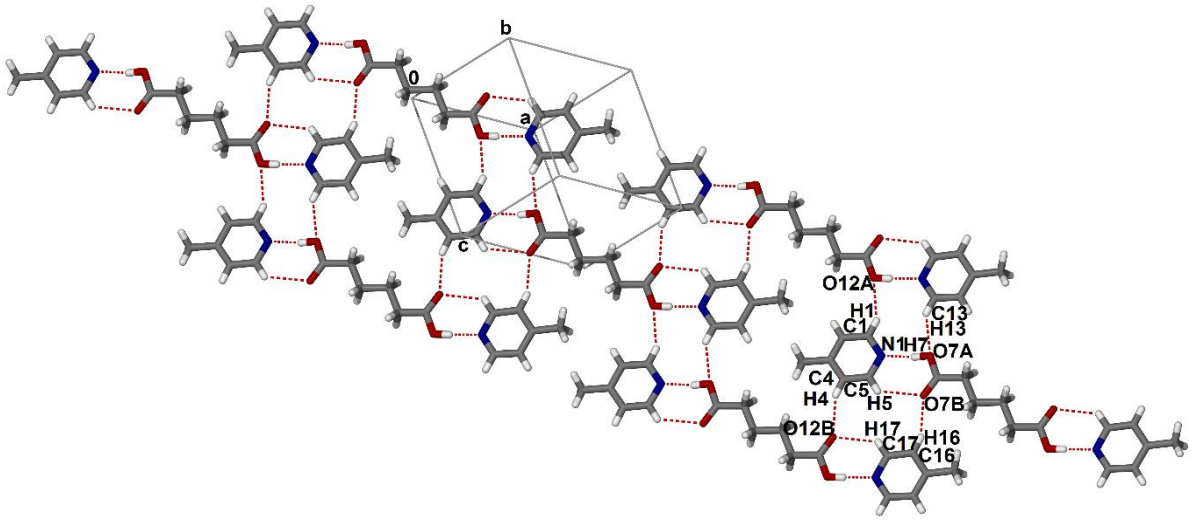

Figure 3.2.2 Packing diagram of ADP•4PIC showing the hydrogen bonded layer formation from the acid-amine units. Only atoms involved in hydrogen bonds are labelled for clarity.

PXRD analysis was used to demonstrate that the structure of the single crystal (**figure 3.2.3** ADP•4PIC single crystal, red) is illustrative of the bulk material (**figure 3.2.3** ADP•4PIC, green). Grinding was used to produce the ADP•4PIC solvate by adding three drops of 4PIC. The obtained pattern was compared to the pattern of the bulk (**figure 3.2.3** ADP•4PIC grinding, blue and **figure 3.2.3** ADP, green). The pattern of the single crystal matches with the bulk, thus the collected single crystal structure is representative to the bulk material. The ground material shows similarities with the bulk but contains some peaks related to the starting acid, therefore the grinding experiment was partially successful.

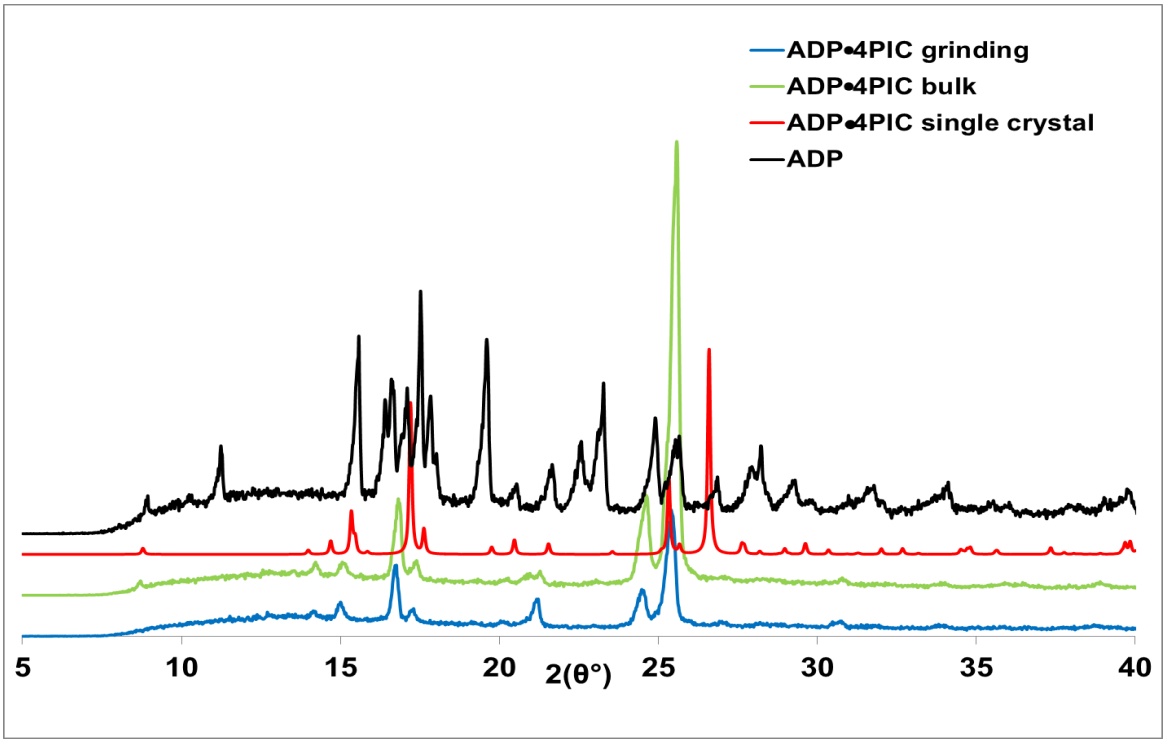

Figure 3.2.3 PXRD patterns for the pure acid (ADP, black), the single crystal structure (ADP•4PIC single crystal, red), the crystalline bulk material (ADP•4PIC bulk, green) and the result of the grinding experiment (ADP•4PIC grinding, blue).

3.2.b Crystal structure of adipic acid with 3,4-lutidine (ADP•3,4LUT)

The host, adipic acid (ADP) was introduced into 4 ml 3,4-lutidine (3,4LUT) and the mixture became clear after a few minutes of continuous stirring. The solution was left to crystallize at room temperature and resulted colorless block shape crystals in two weeks (**figure 3.2.4**) and a selected crystal with dimensions of 0.12 x 0.13 x 0.24 mm was subjected to single crystal X-ray structure analysis.

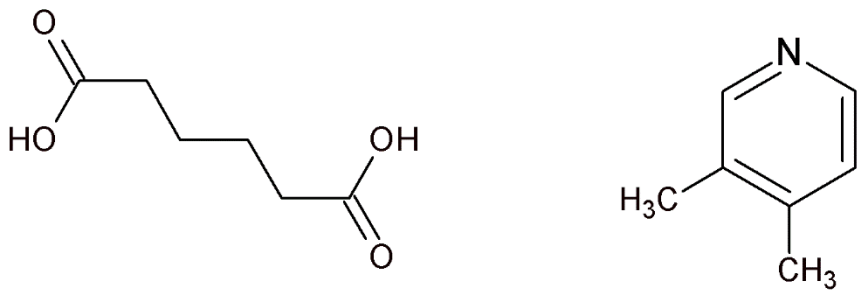

Figure 3.2.4 Structural line diagram of adipic acid (ADP) and 3,4-lutidine (3,4LUT).

The ADP•3,4LUT was solved in the triclinic achiral space group $P\bar{1}$ with $C_{20}H_{28}N_2O_4$ molecular formula and it was refined to R_1= 0.0538 and wR_2= 0.1624. The asymmetric unit contains one and a half of ADPs and three 3,4LUTs. The single crystal structure analysis showed that two ADPs captured four molecules of the 3,4LUT. There are two types of hydrogen bonded associates are present in the structure, namely molecular unit A is in a general position and the centrosymmetric unit B is in a *Wycoff position d.* The carboxylic acid moieties hydrogen bond via **O8A-H8···N1** bond (2.631(2)Å, 174.6º), **O18A-H18···N2** bond (2.666(2)Å, 173.0º), **C15-H15···O18B** (3.232(2) Å, 130.9°) and **O23A-H23···N3** (2.64(2) Å, 175.3°) to two 3,4-lutidines (**figure 3.2.5**).

The hydrogen bonded molecular assemblies (A and B) form two different sheets of molecules in the manner of A-B-A-A-B-A pattern (**figure 3.2.6**). The interactions in these sheets are slightly different (**figure 3.2.6**) and may be described with a series of hydrogen bonds for 'sheet A' (blue) **C11-H11···23A** (3.870(2) Å, 148.2°), **C14-H14···O23B** (3.337(2) Å, 167.6º), **C24-H4···O18A** (3.887(2) Å, 141.4°) and **C27-H27···O18B** (3.339(2) Å, 157.5°) (**figure 3.2.7.a**). 'Sheet B' builds from **C1-H1···O8A** (3.923(2) Å, 136.3°) and **C4-H4···O8B** (3.362(2) Å, 165.7°) (**figure 3.2.7.b**). Sheet A and B are only connected via **C22-H22A···O8A (**3.655(2) Å, 171.7º) hydrogen bond (**figure 3.2.8**). This weak interaction is present only between sheets of A and B, and cannot be found between layers from the same type (**figure 3.2.8)**.

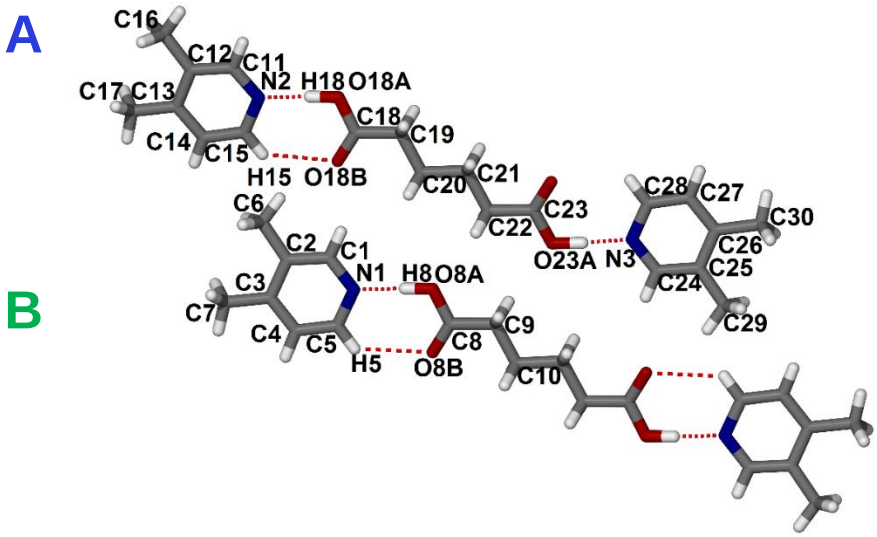

Figure 3.2.5 The structure of ADP•3,4LUT consists of hydrogen bonded molecular associates in the manner that two ADPs bond to four 3,4LUTs. Only the asymmetric unit is labelled for clarity.

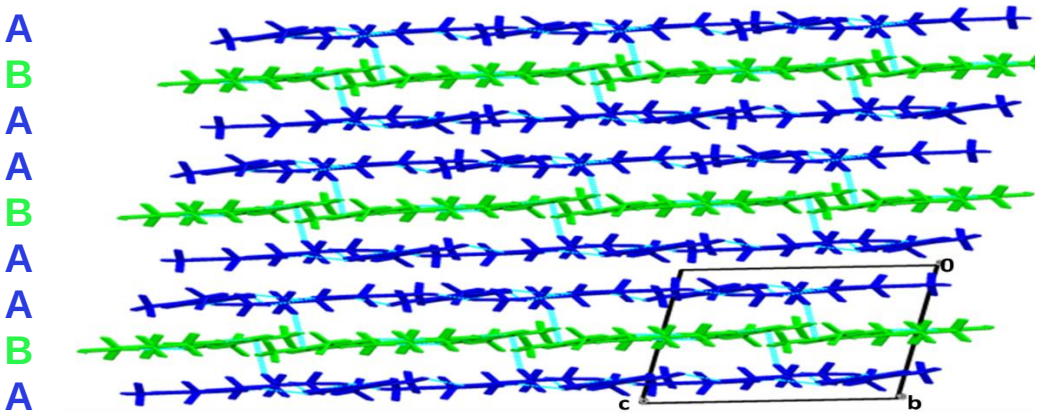

Figure 3.2.6 The two distinct hydrogen bonded molecular assemblies, A (blue) and B (green) form two different hydrogen bonded sheets in the manner of A-B-A-A-B-A pattern in the [100] crystallographic direction.

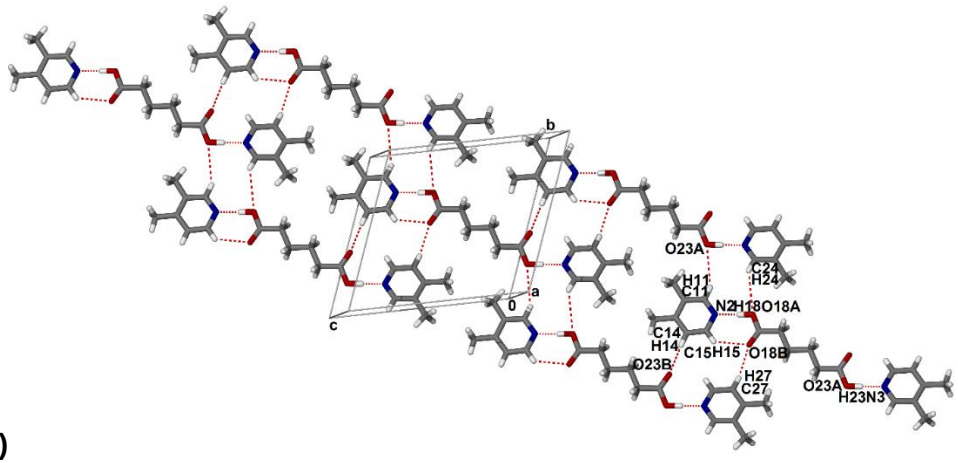

(a)

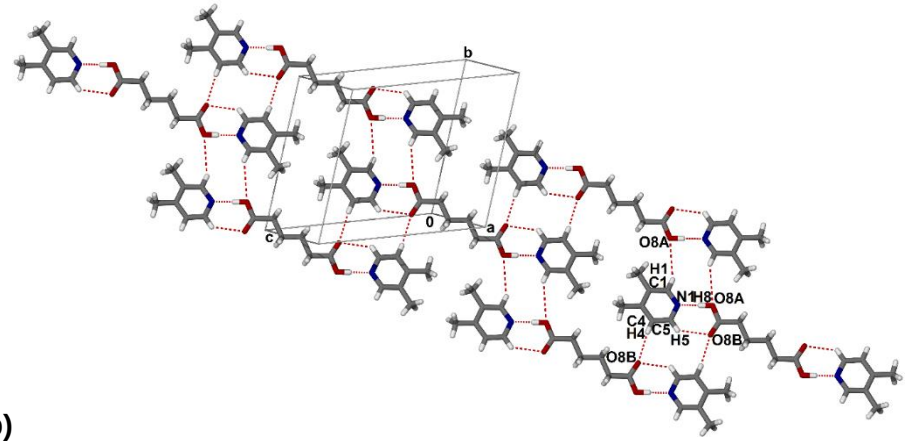

(b)

Figure 3.2.7 (a) Packing diagram of ADP•3,4LUT showing the hydrogen bonds arranged in layer A (only hydrogens involved in bonds are labeled). (b) packing diagram of ADP•3,4LUT representing hydrogen bonds arranged in sheet B (only hydrogens involved in hydrogen bonds are labeled).

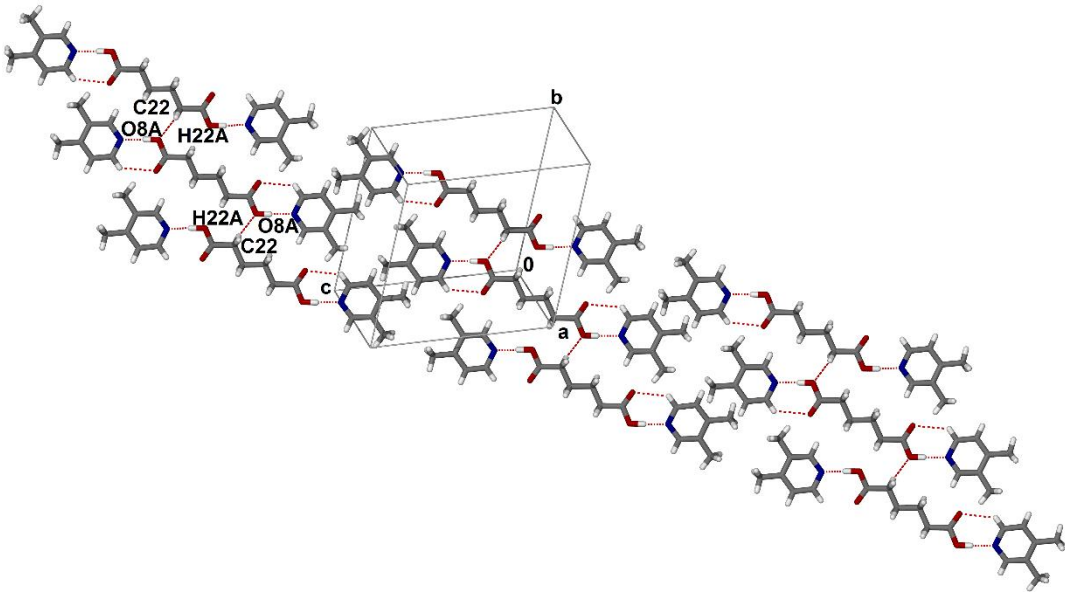

Figure 3.2.8 Packing diagram of ADP•3,4LUT representing the interaction between sheet A and B (only hydrogens involved in hydrogen bonds are labeled).

PXRD analysis was used to prove that the single crystal structure is representative to the bulk material. Indeed, the structure detected on one crystal (**figure 3.2.9** ADP•3,4LUT single crystal, red) and the pattern of the bulk material (**figure 3.2.9** ADP•3,4LUT, green) showed good agreement. Some peaks of the starting material can be recognized in the pattern of the ground product (**figure 3.2.9** ADP•3,4LUT grinding, blue). Thus it may be concluded that the ground product is a mixture of the starting material and the inclusion compound.

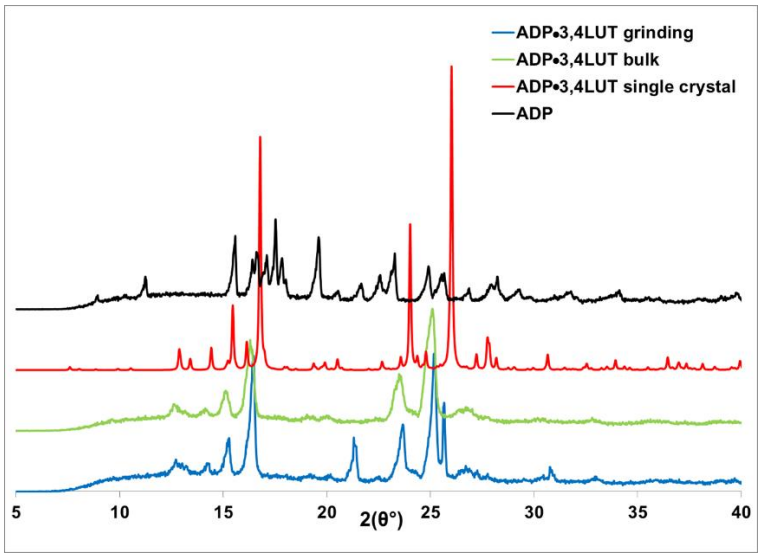

Figure 3.2.9 PXRD patterns for the pure acid (ADP, black), the single crystal structure (ADP•3,4LUT single crystal, red), the crystalline bulk material (ADP•3,4LUT bulk, green) and the result of the grinding experiment (ADP•3,4LUT grinding, blue).

3.2.c Crystal structure of adipic acid with 2,4-lutidine (ADP•2,4LUT)

The adipic acid (ADP) was introduced into a vial of 2,4LUT (ca. 4 ml) and the mixture was stirred continuously (**figure 3.2.10**). The acid dissolved easily and the solution became clear after a few minutes. The solution was left to crystallize at room temperature and resulted colorless block shape crystals in two weeks. A selected crystal with dimensions of 0.18 x 0.22 x 0.29 mm was subjected to single crystal X-ray structure analysis.

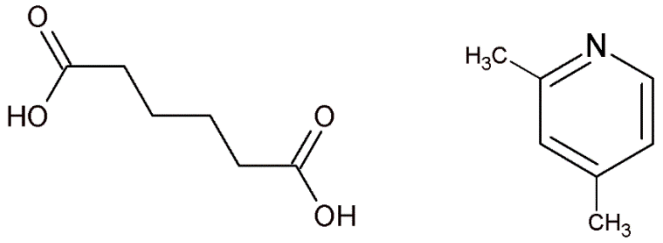

Figure 3.2.10 Structural line diagram of adipic acid (ADP) and 2,4-lutidine (2,4LUT).

The structure was solved in the triclinic achiral space group $P\ \bar{1}$ with $C_{10}H_{14}NO_2$ molecular formula and it was refined to R_1= 0.0426 and wR_2= 0.1224. The asymmetric unit contains half an ADP molecule (*Wyckoff position e*) hydrogen bonded to one 2,4LUT molecule (**figure 3.2.11**) via **O8A-H8···N1** (2.661(2) Å, 173.3°) hydrogen bonds which are presented in **figure 3.1.11**. The carboxylic acid group and the aromatic ring are not coplanar (19.13°) thus only one hydrogen bond forms between these moieties. The ADP•2,4LUT structure, the methyl groups of the lutidine are disordered and were modelled in two equal positions. These hydrogen bonded assemblies packed into layers in the crystal structure and there is secondary interactions via **C4-H4···O8B** (3.317(2) Å, 155.5°) between the neighbouring units forming these sheet motif (**figure 3.1.12**).

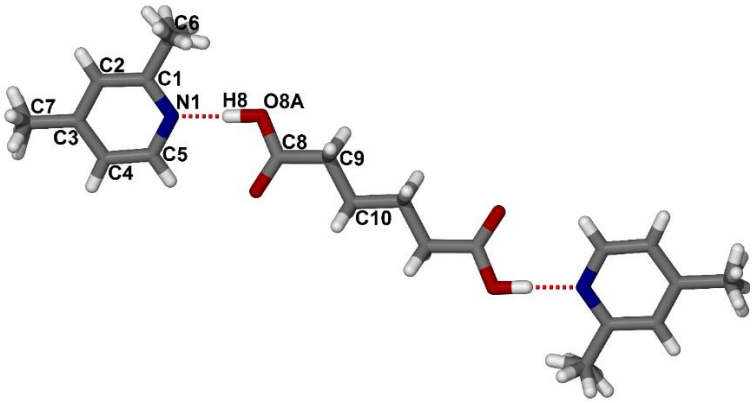

Figure 3.2.11 The structure of ADP•2,4LUT consists of hydrogen bonded molecular associates in the manner that one ADP bond to two 2,4LUTs. Only the asymmetric unit is labelled for clarity.

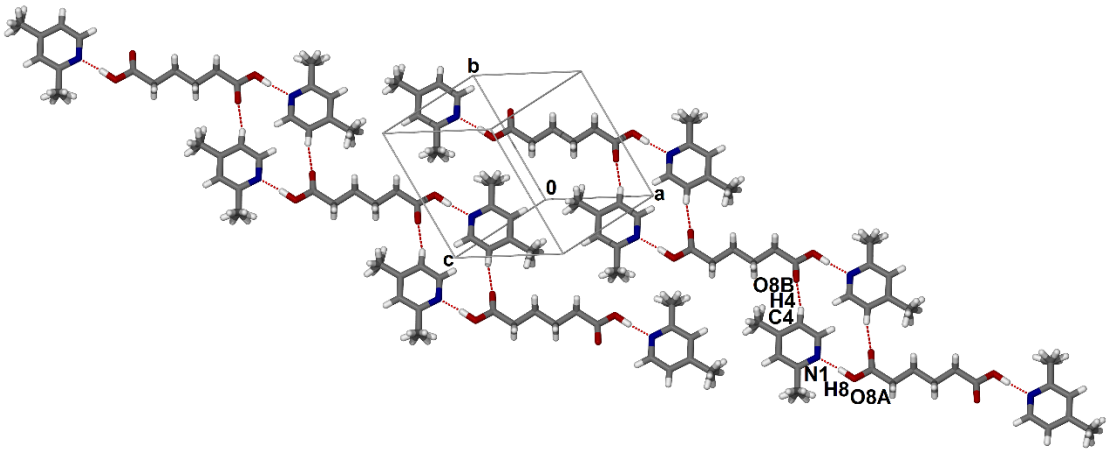

Figure 3.2.12 Packing diagram of ADP•2,4LUT showing the layers of molecular associates. Only atoms involved in hydrogen bonds are labelled for clarity.

PXRD analysis was used to reveal that the single crystal (**figure 3.2.13** ADP•2,4LUT single crystal, red) is illustrative of the bulk material (**figure 3.2.c.3** ADP•4PIC, green). The pattern of ground material was compared to the pattern of the pure acid (**figure 3.2.13** ADP•2,4LUT grinding, blue and **figure 3.2.13** ADP, black). The pattern of the single crystal shows agreement with the bulk material, consequently the collected single crystal structure is representative to the bulk material. The pattern of the ground material shows good agreement with the single crystal. Therefore, the grinding experiment was successful.

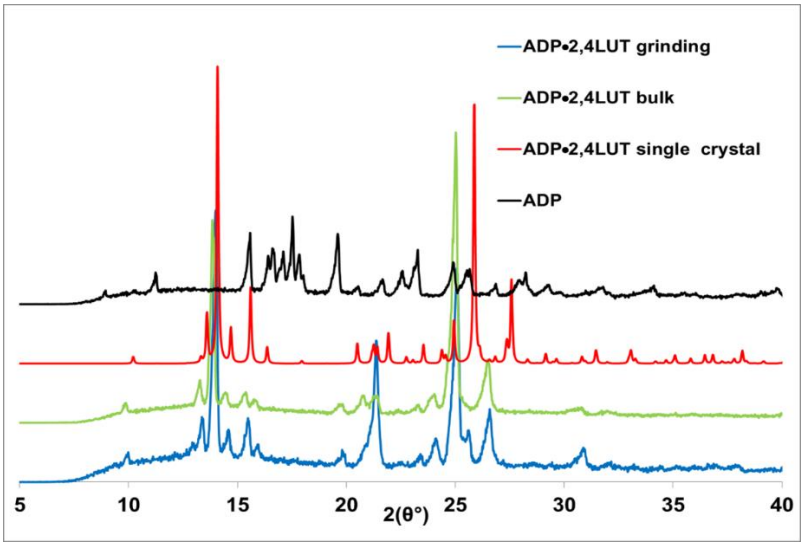

Figure 3.2.13 PXRD patterns for the pure acid (ADP, black), the single crystal structure (ADP•2,4LUT single crystal, red), the crystalline bulk material (ADP•2,4LUT bulk, green) and the result of the grinding experiment (ADP•2,4LUT grinding, blue).

3.2.d Crystal structure of adipic acid with 3,5-lutidine (ADP•3,5LUT)

The host, adipic acid (ADP) was introduced into a vial of 4 ml 3,5-lutidine (3,5LUT) and the mixture became clear after a few minutes of continuous stirring. The solution was left to crystallize at room temperature and resulted colorless block shape crystals in two weeks (**figure 3.2.14**). A selected crystal with dimensions of 0.12 x 0.28 x 0.31 mm was subjected to single crystal X-ray structure analysis.

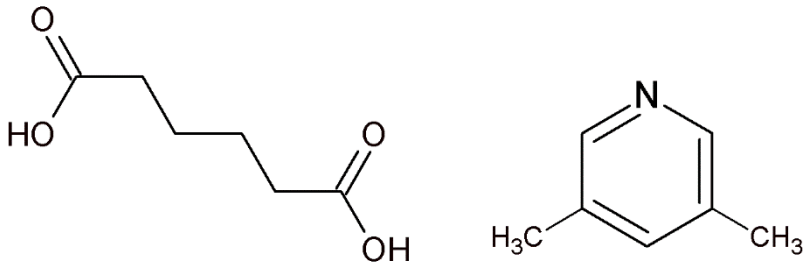

Figure 3.2.14 Structural line diagram of adipic acid (ADP) and 3,5-lutidine (3,5LUT).

The structure was solved in the monoclinic achiral space group $P2_1/n$ with a molecular formula of $C_{10}H_{14}NO_2$ and it was refined to R_1= 0.0399 and wR_2= 0.1126. The asymmetric unit contains half an ADP molecule (*Wyckoff position d*) hydrogen bonded to one 3,5LUT molecule (**figure 3.2.15**) via **O8A-H8···N1** (2.654(1) Å, 173.8°) and **C1-H1···O8B** (3.421(2) Å, 125.8º) hydrogen bonds which are presented in **figure 3.2.15**. The methyl groups are disordered in two equal positions, similarly to the previous structure. These hydrogen bonded base-acid-base assemblies are arranged in columns and no obvious hydrogen bonding can be recognized between these neighbouring units (**figure 3.2.16**).

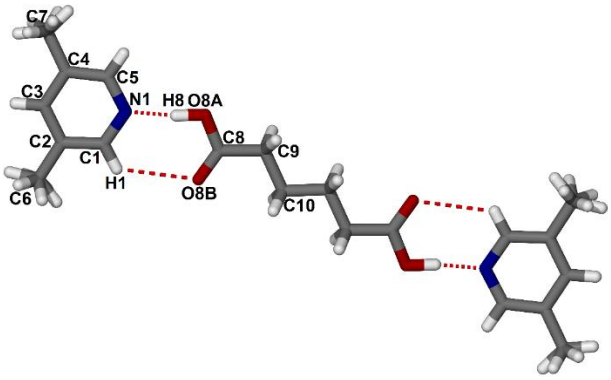

Figure 3.2.15 The structure of ADP•3,5LUT consists of hydrogen bonded molecular associates in the manner that one ADP bonds to two 3,5LUTs. Only the asymmetric unit is labelled for clarity.

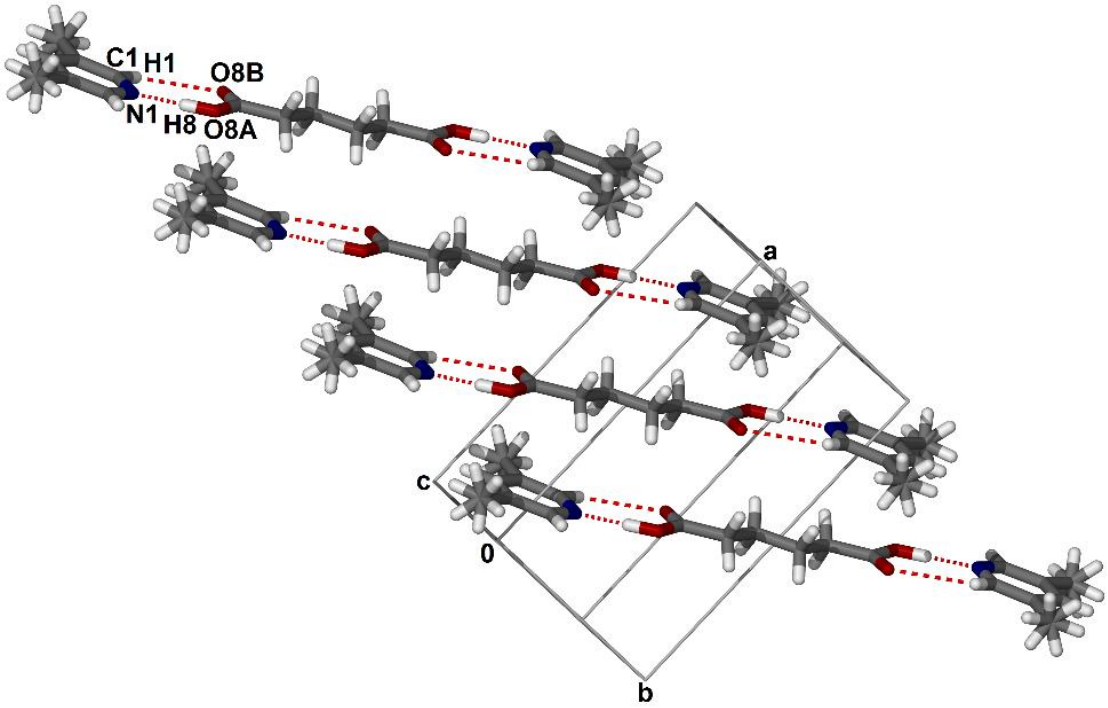

Figure 3.2.16 Packing diagram of ADP•3,5LUT presenting columns of molecular associates. Note the lack of hydrogen bonds between the acid-amine units forming the sheet motif. Only atoms involved in hydrogen bonds are labelled for clarity.

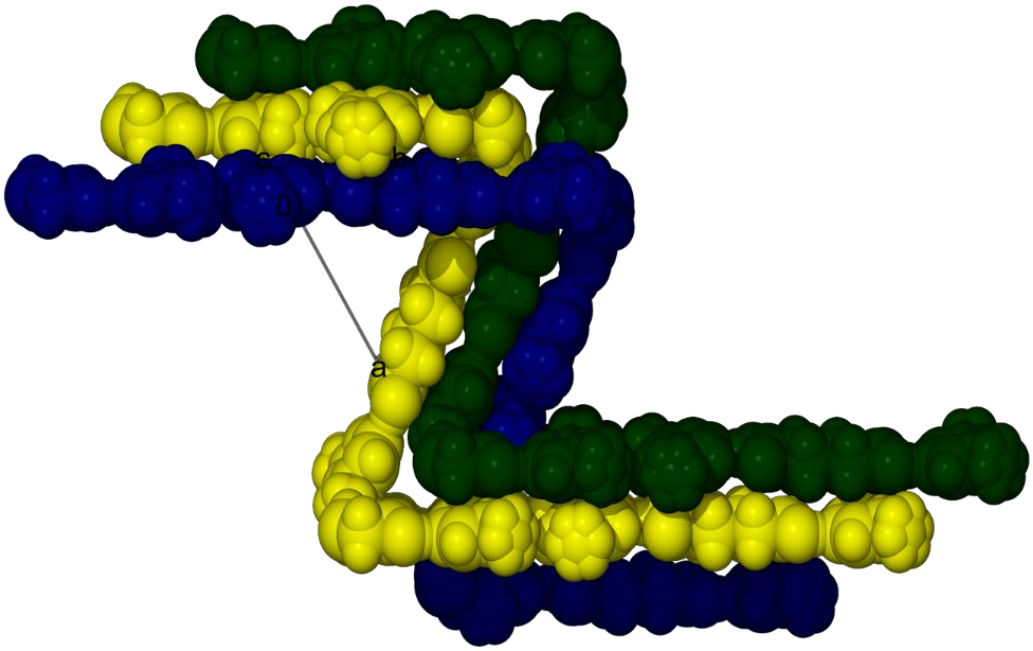

Figure 3.2.17 Packing diagram of ADP•3,5LUT showing a zigzag motif shown from the direction of [100].

PXRD analysis was used to show that the single crystal structure detected (**figure 3.2.18** ADP•3,5LUT single crystal, red) and the bulk material (**figure 3.2.18** ADP•3,5LUT, green) are the same. The ground material (**figure 3.2.18** ADP•3,5LUT grinding, blue) shows some peaks of the starting material and some peaks of the inclusion compound. Thus the grinding experiment was not successful (**figure 3.2.18** ADP•3,5LUT grinding, blue staring material ADP, black).

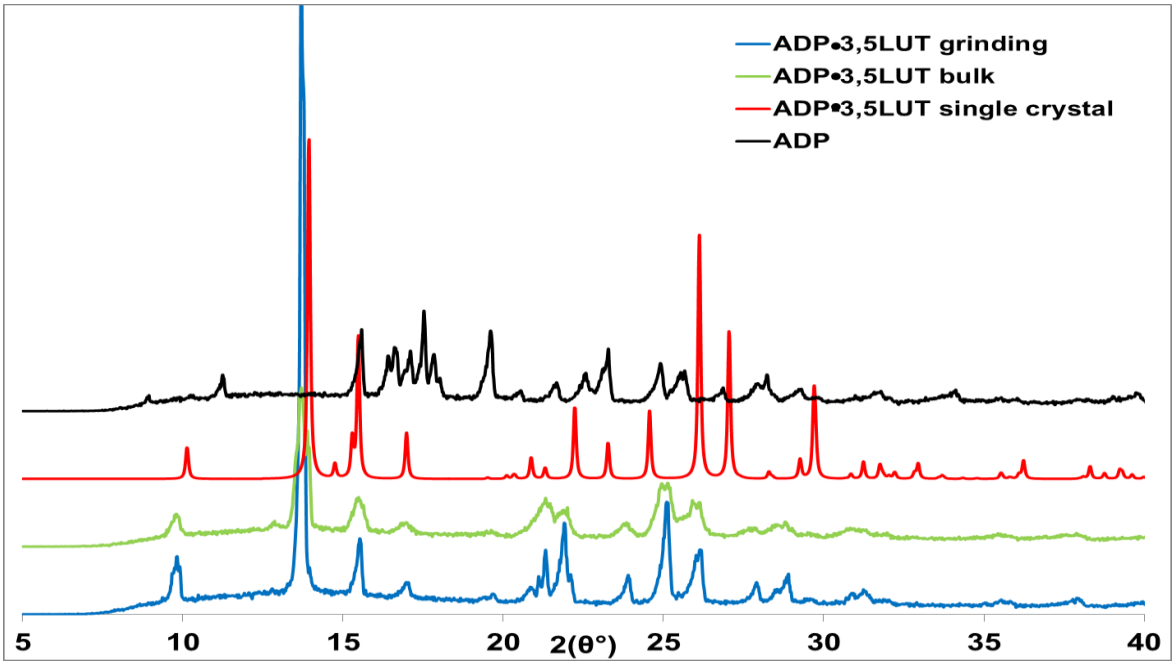

Figure 3.2.18 PXRD patterns for the pure acid (ADP, black), the single crystal structure (ADP•3.5LUT single crystal, red), the crystalline bulk material (ADP•3,5LUT bulk, green) and the result of the grinding experiment (ADP•3,5LUT grinding, blue).

3.3. Crystals of suberic acid (SUB) with substituted pyridines

In the following section, single crystal structures of suberic acid (SUB) obtained from its solutions of substituted pyridines, such as 4-picoline (4PIC), 3,4-lutidine (3,4LUT), 2,4-lutidine (2,4LUT) and 3,5-lutidine (3,5LUT) will be discussed. The crystal data of SUB•4PIC, SUB•2,4LUT and SUB•3,5LUT were collected on a Bruker APEX II diffractometer and SUB•3,4LUT was collected on a Nonius Kappa CCD single crystal diffractometer. The relevant data are summarized in **table 3.3** and their hydrogen bonding details are presented in **table 3.3.1**.

Table 3.3. Crystal data for SUB•4PIC, SUB•3,4LUT, SUB•2,4LUT and SUB•3,5LUT crystals.

Crystal data				
Compounds	**SUB•4PIC**	**SUB•3,4LUT**	**SUB•2,4LUT**	**SUB•3,5LUT**
Molecular formula	$C_{20}H_{28}N_2O_4$	$C_{22}H_{32}N_2O_4$	$C_{22}H_{32}N_2O_4$	$C_{22}H_{32}N_2O_4$
Formula weight (g.mol^{-1})	360.44	388.50	388.50	388.50
Crystal system	Triclinic	Triclinic	Monoclinic	Monoclinic
Space group	$P\bar{1}$	$P\bar{1}$	$P2_1/c$	$P2_1/c$
a (Å)	7.509(2)	7.468(2)	9.374(2)	6.949(1)
b (Å)	7.875(2)	11.541(2)	15.229(3)	21.199(4)
c (Å)	9.426(2)	13.919(3)	7.615(2)	7.465(2)
α (°)	91.08(3)	68.64(3)	90.00	90.00
β (°)	108.81(3)	80.23(3)	92.70(3)	95.16(3)
γ (°)	107.44(3)	72.61(3)	90.00	90.00
V (Å^3)	499.2(2)	1063.7(4)	1085.9(4)	1095.3(4)
Z	1	2	2	2
ρ_{calc} (g.cm^{-3})	1.1989	1.2129	1.1881	1.1779
μ (MoKα) (mm^{-1})	0.083	0.083	0.081	0.081
F (000)	194	420	420	420
Crystal size (mm)	0.20 x 0.42 x 0.53	0.14 x 0.17 x 0.29	0.17 x 0.59 x 0.60	0.05 x 0.40 x 0.48
Temperature (K)	173(2)	173(2)	173(2)	173(2)
Radiation (Å)	MoKα, 0.71073	MoKα, 0.71073	MoKα, 0.71073	MoKα, 0.71073
Theta min-max (°)	2.30; 28.33	1.96; 27.48	2.18; 28.38	1.92; 28.46
Dataset	-10:10;-10:10-12:12	-9:9;-14:14;-18:18	-12:12;-20:20;-10:10	-9:7;-28:24;-10:9
Final R indices [I>2.0(I)]	0.0383; 0.1110	0.0476; 0.1030	0.0406; 0.1189	0.0462; 0.1131
R indices [all data]	0.0430; 0.1162	0.1160; 0.1299	0.0470; 0.1254	0.0662; 0.1240
Tot., uniq. data, R (int)	12293; 2175; 0.0174	9658; 2637; 0.0524	23086; 2329; 0.0268	8625; 2002 ; 0.0327
N_{ref}, N_{par}	2461; 121	4854; 259	2715; 129	2732; 128
S	1.059	1.002	1.073	1.038
Max.and av. Shift/error	0.000/0.010	0.000/ 0.000	0.000/0.001	0.001/0.000
Min. and max. resd. dens. (Å^3)	-0.210; 0.303	-0.240; 0.273	-0.234; 0.316	-0.195; 0.234

Table 3.3.1 Hydrogen bonds in SUB•4PIC, SUB•2,4LUT, SUB•3,4LUT and SUB•3,5LUT

Crystals	D-H···A	d(D-H) (Å)	d(H··· A) (Å)	d(D··· A) (Å)	D-H··· A (°)	Symmetry operator
SUB•4PIC	C2-H2…O7B	0.95	2.53	3.307(2)	139.4	-x, -y, 1-z
	C5-H5...O7A	0.95	2.50	3.403(2)	157.9	1-x, 1-y, 2-z
	O7A-H7...N1	0.88	1.76	2.632(1)	171.1	
SUB•3,4LUT	C1-H1...O8A	0.95	2.83	3.725(3)	156.8	-x, 1-y, -z
	C4-H4...O8B	0.95	2.49	3.402(3)	161.9	1-x, -y, 1-z
	C5-H5…O8B	0.95	2.46	3.159(3)	130.2	
	C12-H12…O19B	0.95	2.47	3.170(3)	130.4	
	C13-H13…O19B	0.95	2.46	3.391(3)	166.7	-x, 1-y, 1-z
	C16-H16…O19A	0.95	2.79	3.679(3)	157.1	1-x, -y, 1-z
	O8A-H8...N1	1.00	1.66	2.664(3)	176.6	
	O19A-H19…N2	1.14	1.56	2.692(3)	173.6	
SUB•2,4LUT	C4-H4...O8B	0.95	3.02	3.934(1)	161.8	1-x, 1-y, -z
	C2-H2…O8A	0.95	2.36	3.309(1)	174.3	-x, y-1/2, 1/2-z
	C5-H5…O8B	0.95	2.61	3.276(1)	127.3	
	O8A-H8...N1	0.91	1.76	2.676(1)	175.4	
SUB•3,5LUT	C1-H1…O8A	0.95	2.96	3.903(2)	173.0	-x, 1-y, -z
	C3-H3…O8B	0.95	2.89	3.837(2)	173.3	x-1, 3/2-y, z-1/2
	O8A-H8...N1	0.97	1.70	2.663(2)	174.5	

3.3.a Crystal structure of suberic acid with 4-picoline (SUB•4PIC)

The suberic acid (SUB) was introduced into a vial of 4PIC (ca. 4 ml) and the mixture was stirred continuously (**figure 3.3.**). It dissolved easily and the solution became clear after a few minutes. The solution was left to crystallize at room temperature and resulted colorless block shape crystals in two weeks. A selected crystal with dimensions of 0.20 x 0.42 x 0.53 mm was subjected to single crystal X-ray structure analysis.

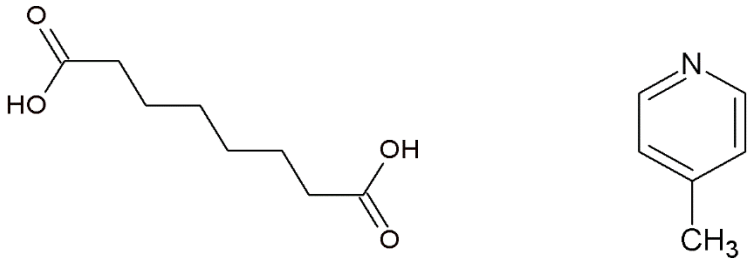

Figure 3.3. Structural line diagram of suberic acid (SUB) and 4-picoline (4PIC).

The solvate SUB•4PIC was solved in the triclinic achiral space group $P\ \bar{1}$ with $C_{20}H_{28}N_2O_4$ molecular formula. The inclusion compound SUB•4PIC was refined to R_1= 0.0383 and wR_2= 0.1162. The structure presented that the diacid, SUB captured two molecules of the 4PICs, and the asymmetric unit consist of half a SUB and one 4PIC molecule. The SUB is located on *Wyckoff position d*. The main supramolecular unit is hydrogen bonded in the manner of base-acid-base through **O7A-H7···N1** hydrogen bond (2.632(1) Å, 171.1°) (**figure 3.3.1**). The carboxylic acid group and the aromatic ring are not coplanar (13.69°) thus only one hydrogen bond forms between these moieties. The hydrogen bonded assemblies are packed in layers via **C2-H2···O7B** (3.307(2) Å, 139.4°) and **C5-H5···O7A** (3.403(2) Å, 157.9°) hydrogen bonds (**figure 3.3.2 (a)**). These assemblies are arranged into sheets which are layered in the [010] crystallographic direction (figure **3.3.2 (b)**.

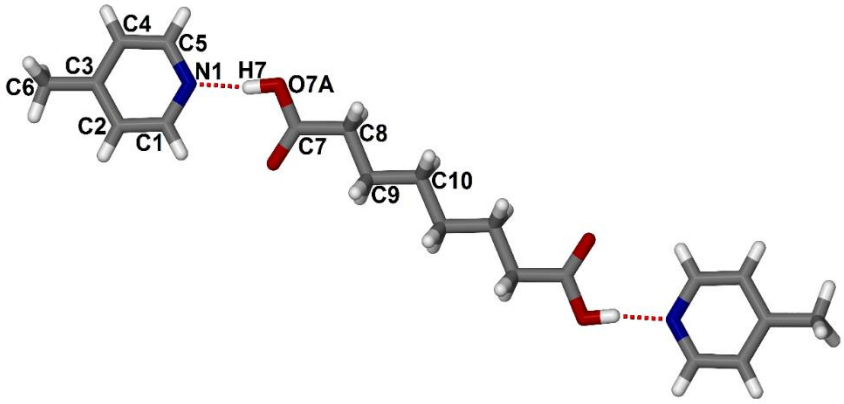

Figure 3.3.1 The structure of SUB•4PIC consists of hydrogen bonded molecular associates in the manner that one SUB bonds to two 4PIC. Only the asymmetric unit is labelled for clarity.

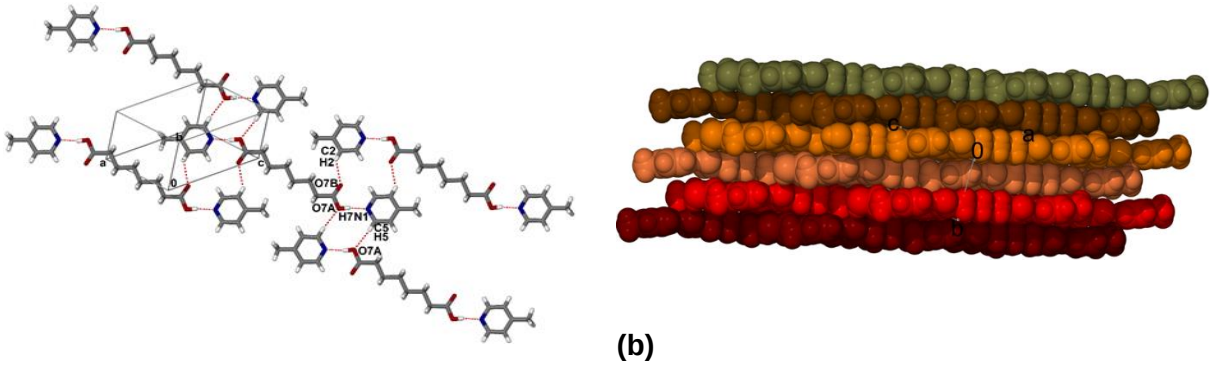

(a) **(b)**

Figure 3.3.2 (a) Packing diagram of SUB•4PIC showing sheet motif of molecular associates. Only atoms involved in hydrogen bonds are labelled, (b) Packing diagram of SUB•4PIC showing the sheet motif.

PXRD analysis was used to prove that the single crystal structure is illustrative to the bulk material. The structure detected on one crystal (**figure 3.3.3** SUB•3,4LUT single crystal, red) and the pattern of the bulk material (**figure 3.3.3** SUB•3,4LUT, green) showed good agreement. Some peaks of the starting material can be recognized in the pattern of the ground material (**figure 3.3.3** SUB•3,4LUT grinding, blue). Definitely, the ground product is a mixture of the starting material and the inclusion compound.

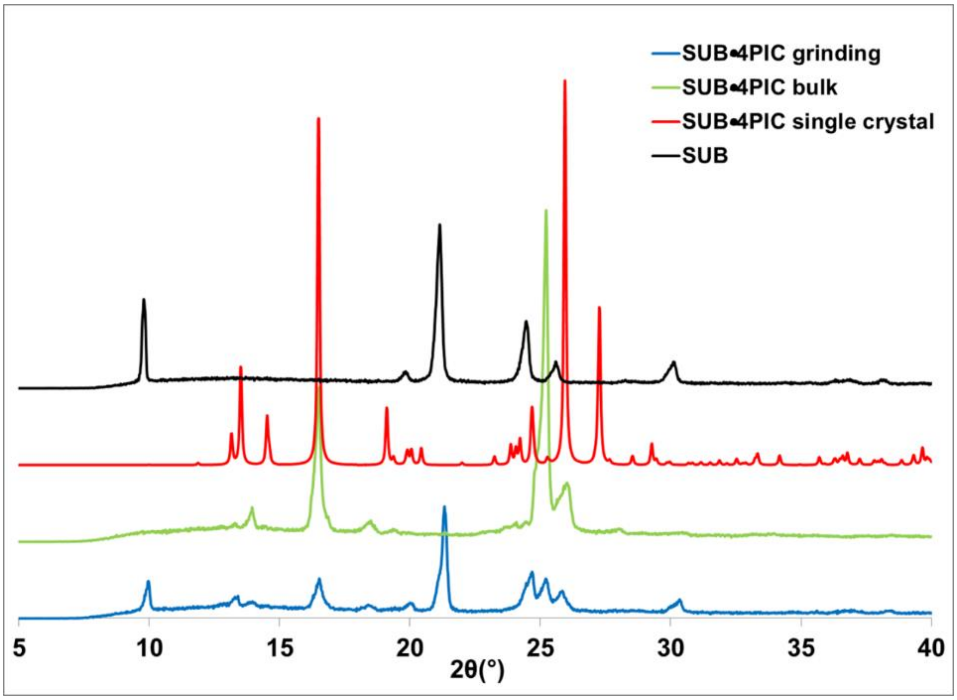

Figure 3.3.3 PXRD patterns for the pure acid (SUB, black), the single crystal structure (SUB•4PIC single crystal, red), the crystalline bulk material (SUB•4PIC bulk, green) and the result of the grinding experiment (SUB•4PIC grinding, blue).

3.3.b Crystal structure of suberic acid with 3,4-lutidine (SUB•3,4LUT)

The host, suberic acid (SUB) was introduced into 4 ml 3,4-lutidine (3,4LUT) and the mixture became clear after a few minutes of continuous stirring. The solution was left to crystallize at room temperature and resulted colorless block shape crystals in two weeks (**figure 3.3.4**) and a selected crystal with dimensions 0.14 x 0.17 x 0.29 mm was subjected to single crystal X-ray structure analysis.

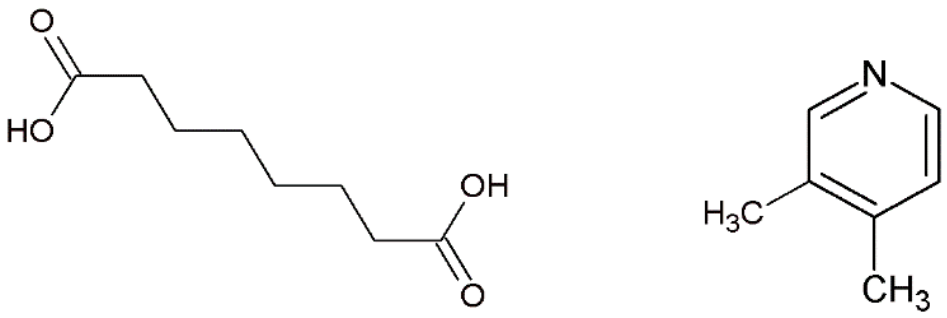

Figure 3.3.4 Structural line diagram of suberic acid (SUB) and 3,4-lutidine (3,4LUT).

The SUB•3,4LUT was solved in the triclinic achiral space group $P\ \bar{1}$ with $C_{22}H_{32}N_2O_4$ molecular formula and it was refined to R_1= 0.0476 and wR_2= 0.1299. The asymmetric unit consists of two half SUBs and two 3,4LUTs. The single crystal structure analysis showed that two symmetrically independent SUBs crystallized with four molecules of the 3,4LUTs. There are two types of hydrogen bonded associates which are present in the structure, namely the symmetry generated (A) is in *Wycoff* position *b* and the symmetry generated unit (B) is located on *Wycoff* position *a*. The carboxylic acid moieties hydrogen bond via **O8A-H8**···**N1** bond (2.664(3) Å, 176.6º), **C5-H5**···**O8B** bond (3.159(3) Å, 130.2º), **O19-H19**···**N2** (2.692(3) Å, 173.6°) and **C12-H12**···**O19B** (3.170(3) Å, 130.4°) to two 3,4-lutidines (**figure 3.3.5**).

The hydrogen bonded molecular assemblies (A and B) combine two different sheets of molecules in the manner of A-B-A-B-A-B pattern (figure 3.3.b.2). The interactions in these sheets are slightly different **(figure 3.3.6)** and can be described with a series of hydrogen bonds for the sheet A (red) **C13-H13**···**O19B** (3.391(3) Å, 166.6°), **C16-H16**···**O19A** (3.679(3) Å, 157.1º) (**figure 3.3.7.a**) and sheet B (yellow) **C4-H4**···**O8B** (3.402(3) Å, 161.9°), **C5-H5**···**O8B** (3.159(3)Å, 130.2°) and **C1-H1**···**O8A** (3.725(3) Å, 156.6°) (**figure 3.3.7.b**). No strong hydrogen bonds were found between sheets A and B.

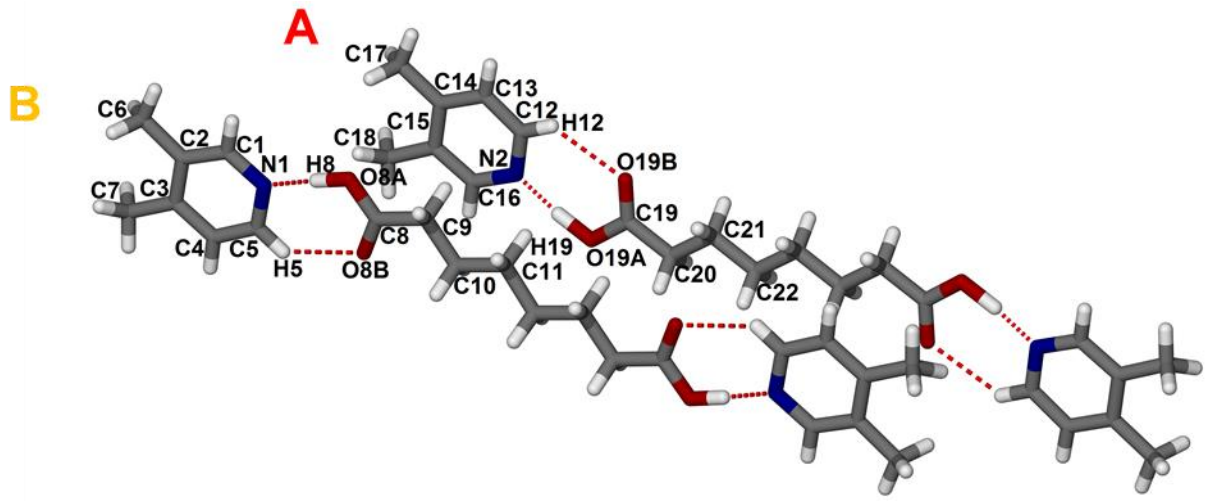

Figure 3.3.5 The structure of SUB•3,4LUT consists of hydrogen bonded molecular associates in the manner that two SUBs bond to four 3,4LUTs. Only the non hydrogen atoms in the asymmetric unit are labelled for clarity.

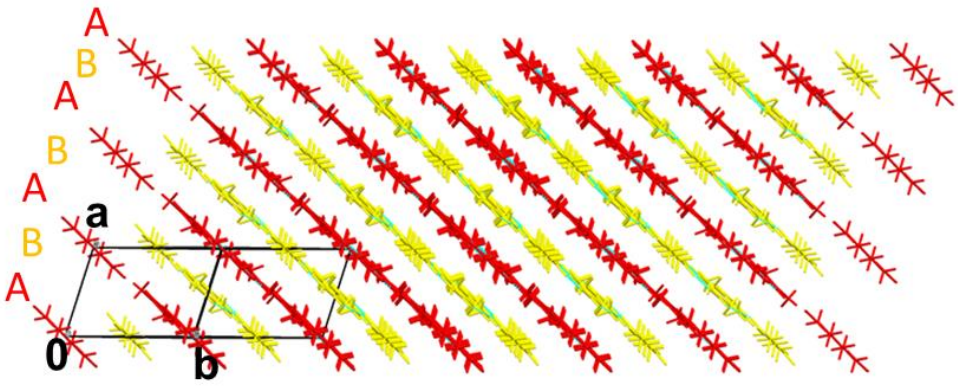

Figure 3.3.6 The two distinct hydrogen bonded molecular assemblies, A (red) and B (yellow) form two different hydrogen bonded sheets in the manner of A-B-A-B-A-B pattern in the [100] crystallographic direction.

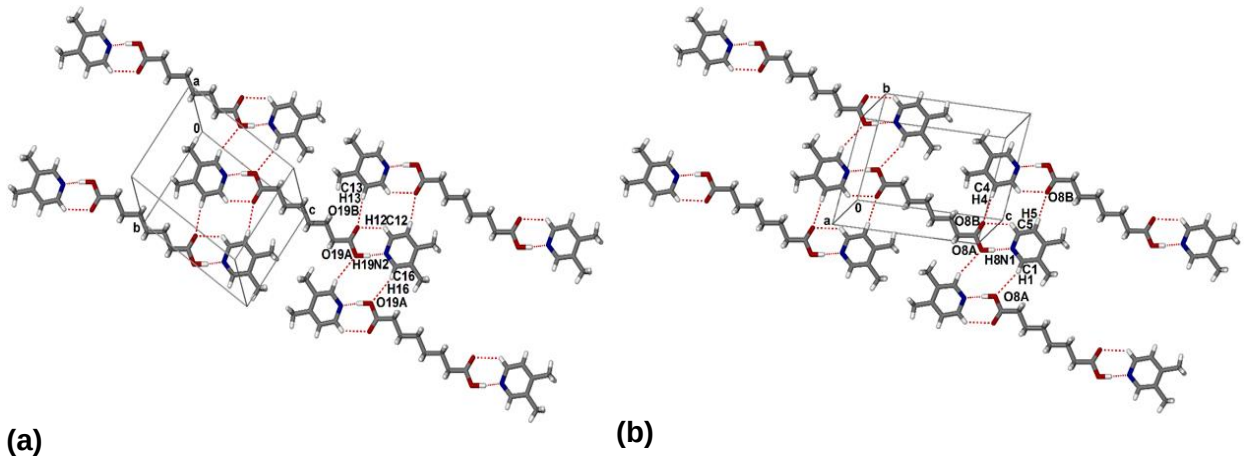

(a) **(b)**

Figure 3.3.7 Packing diagram of SUB•3,4LUT showing the two distinct layers built from molecular associates A (a) and B (b) (Only atoms involved in hydrogen bonds are labelled).

PXRD analysis was used to demonstrate that the single crystal (**figure 3.3.8** SUB•3,4LUT single crystal, red) is illustrative of the bulk material (**figure 3.3.8** SUB•3,4LUT, green). The grinding method was used to produce SUB•3,4LUT solvate with three drops of the (3,4LUT) and was compared to the PXRD pattern of the pure acid (**figure 3.3.8** SUB•3,4LUT grinding, blue and **figure 3.3.8** SUB, black). The pattern of the single crystal agrees with the bulk material, thus the collected single crystal structure is representative to the bulk material. The pattern of the ground product lacks some peaks related to single crystal but significantly differ to the starting material. Therefore, the experiment may a partial success.

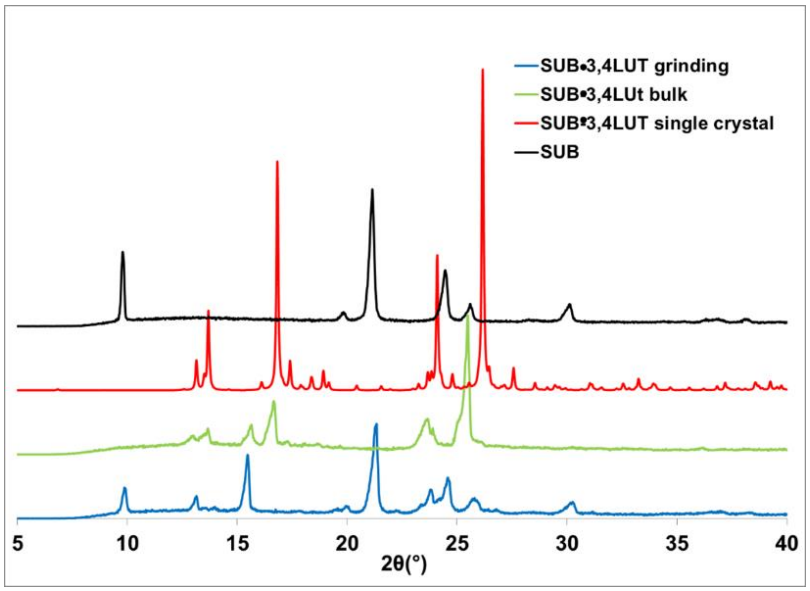

Figure 3.3.8 PXRD patterns for the pure acid (SUB, black), the single crystal structure (SUB•3,4LUT single crystal, red), the crystalline bulk material (SUB•3,4LUT bulk, green) and the result of the grinding experiment (SUB•3,4LUT grinding, blue).

3.3.c Crystal structure of suberic acid with 2,4-lutidine (SUB•2,4LUT)

Suberic acid (ca. 100 mg) was introduced into a vial of 4 ml of 2,4-lutidine and the mixture was stirred until the acid dissolved. The solution became clear after a few minutes and it was left to crystallize at room temperature and after two weeks, well-shaped block crystals were obtained (**figure 3.3.9**). A selected crystal was subjected to single crystal X-ray analysis with dimensions of 0.17 x 0.59 x 0.60 mm.

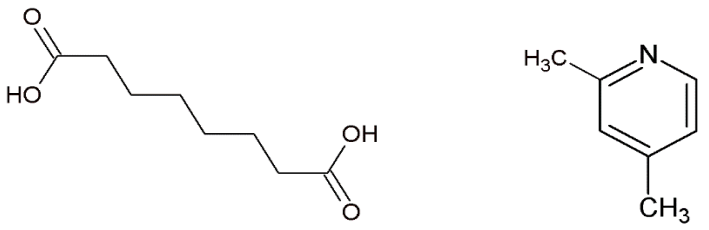

Figure 3.3.9 Structural line diagram of suberic acid (SUB) and 2,4-lutidine (2,4LUT).

The SUB•2,4LUT solvate was solved in the monoclinic achiral space group $P2_1/c$ with $C_{22}H_{32}N_2O_4$ molecular formula. The inclusion compound SUC•2,4LUT was refined to R_1= 0.0406 and wR_2= 0.1254. The asymmetric unit contains a half SUB molecule (located on *Wyckoff position*

b) and one 2,4LUT molecule hydrogen bonded via **O8A-H8···N1** (2.676(1)Å, 175.4°) and **C5-H5···O8B** (3.276(2)Å,127.3°) (**figure 3.3.10**). The methyl groups of the lutidine molecules showed disorder and were modelled in two positions with equal site occupancies. The hydrogen bonded assemblies packed in layers via **C2-H2···O8A** (3.309(1) Å, 174.3°) and **C4-H4···O8B** (3.935(1) Å, 161.8°) hydrogen bonds (**figure 3.3.11 a**). The hydrogen bonded assemblies are packed in layers in a V-shape manner and the layers are assemble in the third dimension without noticable hydrogen bond formations. (**figure 3.3.11.(b)**).

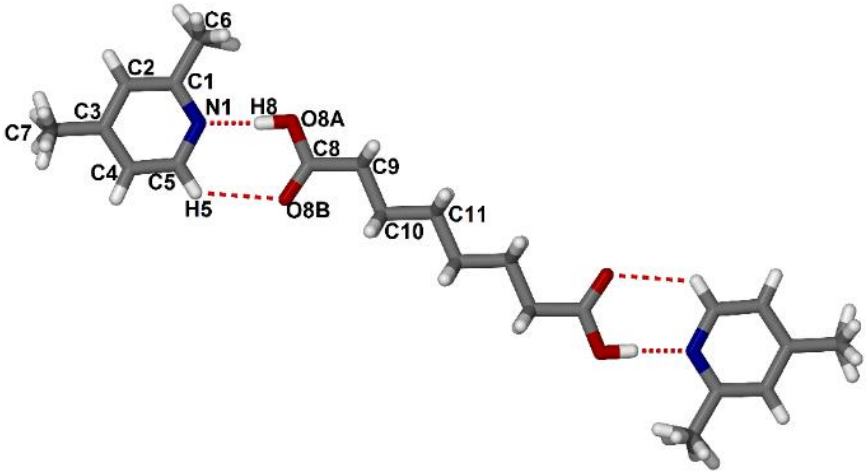

Figure 3.3.10 The structure of SUB•2,4LUT consists of hydrogen bonded molecular associates in the manner that one SUB bonds to two 2,4LUTs. Only the asymmetric unit is labelled for clarity.

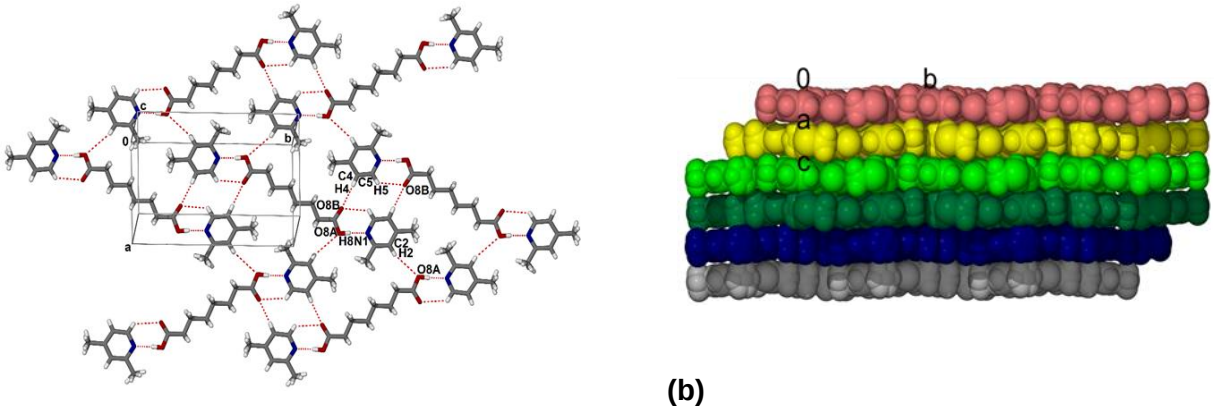

(a) **(b)**

Figure 3.3.11(a) Packing diagram of SUB•2,4LUT showing the molecular sheet form with labels of the atoms involved in hydrogen bonding. (b) Sheets of hydrogen bonded molecules are packed down [001].

PXRD analysis was used to prove that the single crystal structure is illustrative to the bulk material. The structure detected on one crystal (**figure 3.3.12** SUB•2,4LUT single crystal, red) and the pattern of the bulk material (**figure 3.3.12** SUB•2,4LUT, green) match well. Some peaks of the starting material can be identified in the pattern of the ground material (**figure 3.3.12** SUB•2,4LUT grinding, blue). As a result the ground product is a mixture of the starting material and the inclusion compound.

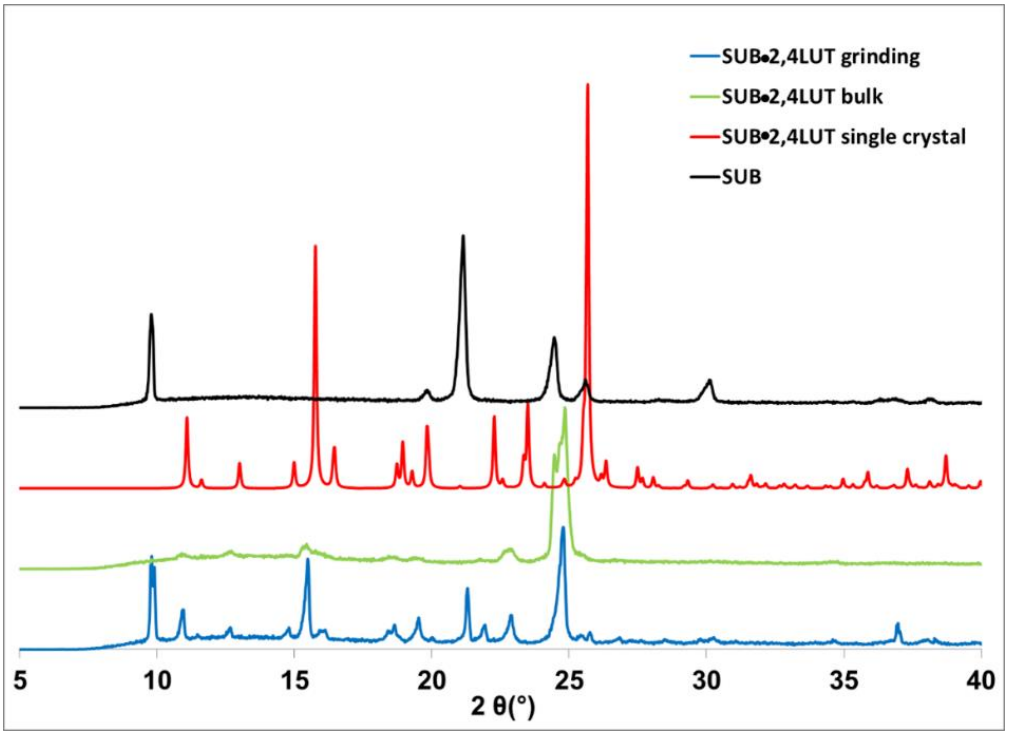

Figure 3.3.12 PXRD patterns for the pure acid (SUB, black), the single crystal structure (SUB•2,4LUT single crystal, red), the crystalline bulk material (SUB•2,4LUT bulk, green) and the result of the grinding experiment (SUB•2,4LUT grinding, blue).

3.3.d Crystal structure of suberic with 3,5-lutidine (SUB•3,5LUT)

Suberic acid (SUB) was introduced into a vial of 3,5LUT (3,5LUT) in 4 ml and the mixture was stirred continuously. It dissolved easily and the solution became clear after a few minutes. The solution was left to crystallize at room temperature and resulted colorless block shape crystals in two weeks (**figure 3.3.13**). A selected crystal with dimensions of 0.05 x 0.40 x 0.48 mm was subjected to single crystal X-ray structure analysis.

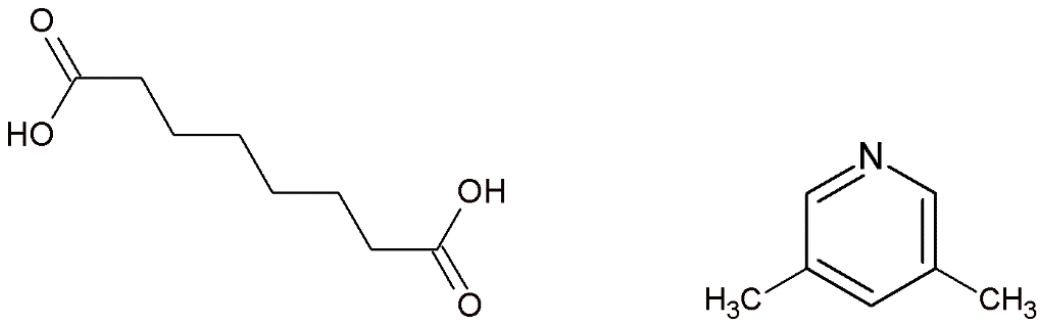

Figure 3.3.13 Structural line diagram of suberic acid (SUB) and 3,5-lutidine (3,5LUT).

The structure was solved in the monoclinic achiral space group $P2_1/c$ with $C_{22}H_{32}N_2O_4$ molecular formula and it was refined to R_1= 0.0462 and wR_2= 0.1240. The asymmetric unit contains half SUB molecule (*Wyckoff position a*) hydrogen bonded to one 3,5LUT molecule (**figure 3.3.14**) via **O8A-H8···N1** (2.663(1) Å, 174.5°) hydrogen bond (**figure 3.1.14**). The carboxylic acid group and the aromatic ring are not coplanar (12.70°) thus only one hydrogen bond forms between these moieties. The methyl groups of the lutidine are also disordered like the previous structure SUB•2,4LUT and were modelled in two equal positions. The hydrogen bonded units are arranged into 2D molecular sheets similarly observed in the structure of SUB•2,4LUT (**figure 3.3.11 a**). These hydrogen bonded assemblies packed in layers via **C1-H1···O8A** (3.903(2) Å, 173.0°) and **C3-H3···O8B** (3.837(2)Å, 173.3°) hydrogen bonds (**figure 3.3.15**).

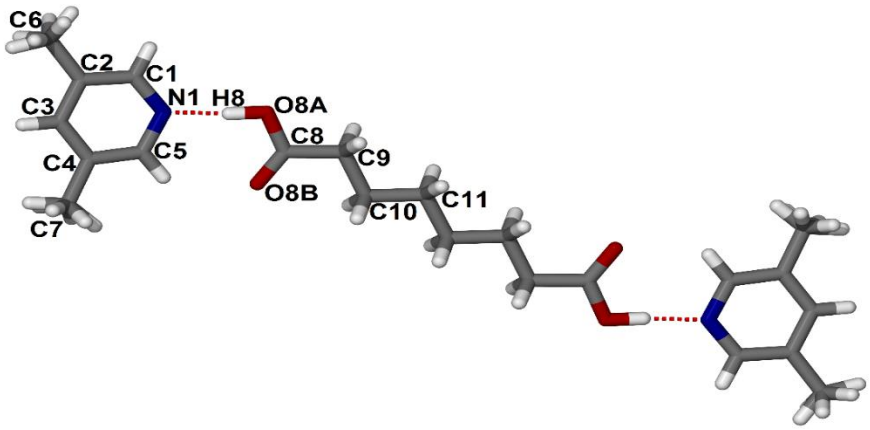

Figure 3.3.14 The structure of SUB•3,5LUT consists of hydrogen bonded molecular associates in the manner that one SUB bonds to two 3,5LUTs.

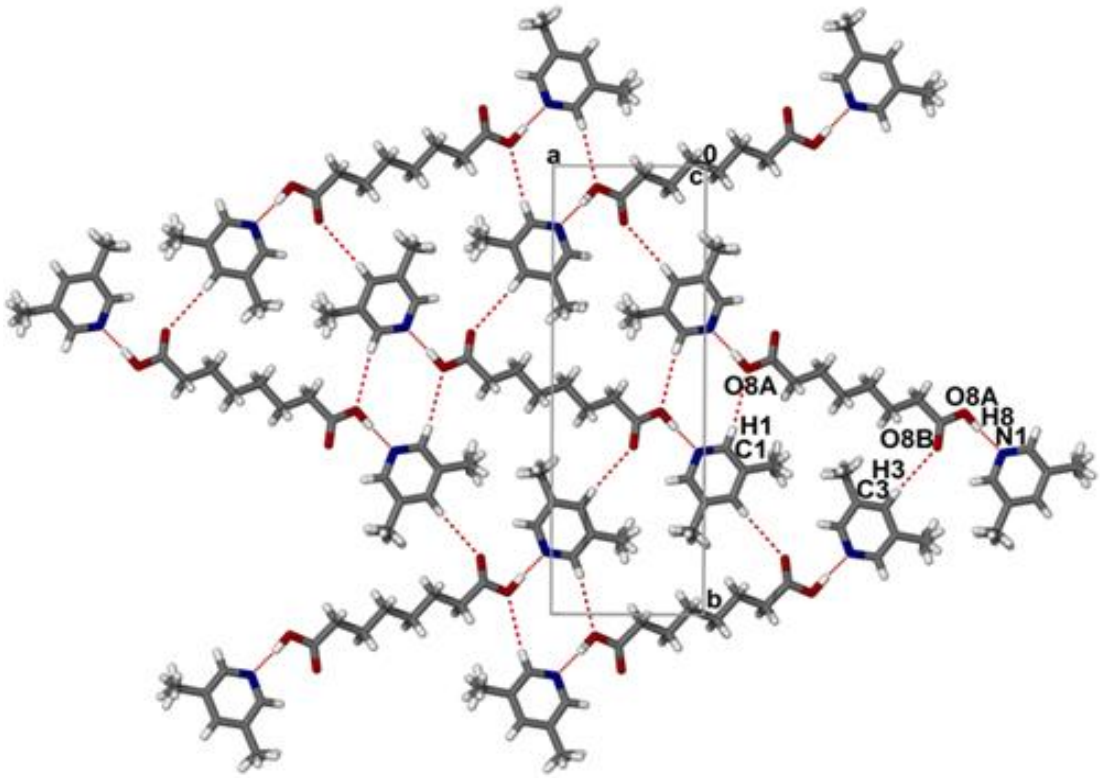

Figure 3.3.15 Packing diagram of SUB•3,5LUT showing the hydrogen bonded molecular sheets.

PXRD analysis was used to demonstrate that the single crystal (**figure 3.3.16** SUB•3,5LUT single crystal, red) is representative of the bulk material (**figure 3.3.16** SUB•3,5LUT, green). The ground product was compared to the pattern of the pure acid (**figure 3.3.16** SUB•3,5LUT grinding, blue and **figure 3.3.16** SUB, black). The pattern of the single crystal shows good agreement with the bulk material, thus the collected single crystal structure is representative to the bulk material. The pattern of the ground product lacks some peaks when compared to the single crystal patters but significantly differ to the starting material. Therefore, the experiment was partially successful.

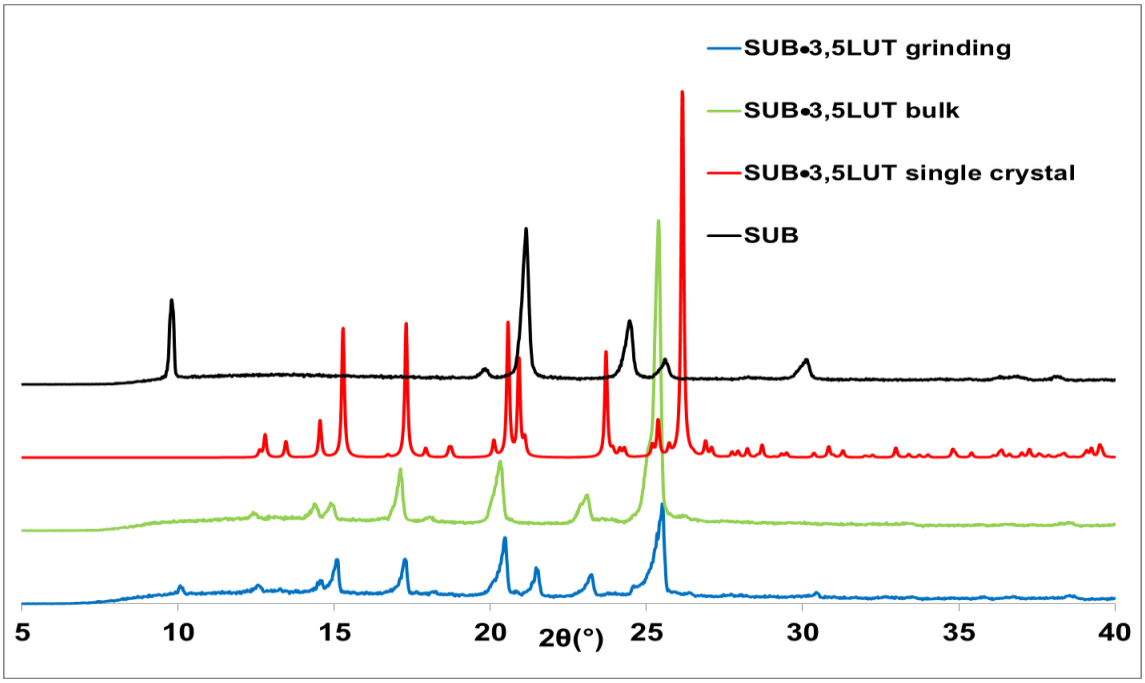

Figure 3.3.16 PXRD patterns for the pure acid (SUB, black), the single crystal structure (SUB•3,5LUT single crystal, red), the crystalline bulk material (SUB•3,5LUT bulk, green) and the result of the grinding experiment (SUB•3,5LUT grinding, blue).

In summary, twelve multicomponent crystals were investigated and their crystal structure was analyzed with the focus on (i) how the diacid hydrogen bonds to the aromatic amines, (ii) are the methyl moieties of the amines show disorders and (iii) how the base-acid-base units hydrogen bond to each other to form the 3D structure. It may be concluded that in all cases, the diacids crystallized with the bases in a 1:2 manner, as it was expected. In some cases, the anticipated formation of the double hydrogen bond between the aromatic amine and the carboxylic acid moiety was not reached and only two single hydrogen bond formation was observed in the base-acid-base units. Also, in several structures, disorder of the methyl functional groups were noted. The highly anticipated hydrogen bond formation between the base-acid-base supramolecular units were not observed in all the structures. (**Table 3.4**)

Attempts were made to resynthesize the twelve inclusion compounds via liquid assisted grinding. The solubility of the diacids were extremely high in the picoline derivatives and even the addition of a few drops of solvent dissolved the acid completely. Thus it may be concluded that perhaps the required host:guest ratio was not reached in these experiments.

Table 3.4. Summary of structural features of the analyzed inclusion compounds.

	SUC•4PIC	**SUC•3,4LUT**	**SUC•2,4LUT**	**SUC•3,5LUT**
disorder?	yes	no	yes	yes
H-bond in molecular unit	single	double	double	double
H-bond between units?	no	yes	no	no
	ADP•4PIC	**ADP•3,4LUT**	**ADP•2,4LUT**	**ADP•3,5LUT**
disorder	no	no	yes	yes
H-bond in molecular unit	double	double	single	double
H-bond between units?	yes	yes	yes	no
	SUB•4PIC	**SUB•3,4LUT**	**SUB•2,4LUT**	**SUB•3,5LUT**
disorder?	no	no	yes	yes
H-bond in molecular unit	single	double	double	single
H-bond between units?	yes	yes	yes	yes

References

[1] Haynes, D.A; Jones, W; Motherwell, W.D.S. *CrystEngComm,* 2006, 8, 830-840.

[2] Batisai, E; Ayamine, A; Youdaga Kilinkissa, O.E; Báthori, N.B. *CrystEngComm*, 2014, 16, 9992-9998.

Chapter 4

Hirshfeld Surface Analysis

Chapter 4: Hirshfeld Surface Analysis

Crystal Explorer is a software to analyse crystal structures via the generation of Hirshfeld surfaces of selected molecular units.[1] The Hirshfeld surface[2] of a molecule in a crystal is constructed by partitioning space into regions where the electron distribution of a sum of spherical atoms for the molecule (the promolecule) dominates the corresponding sum over the crystal (the procrystal). Simply said, the region where the promolecule contribution to the procrystal electron density exceeds that from all other molecules in the crystal. (Figure 4) The shape of the Hirshfeld surface depends on the interactions between molecules in the crystal and different properties can be encoded on it. The interpretation of the 3D Hirshfeld surface is not straight forward when comparing two or more surfaces. Thus, generally the 2D representation of the surface, the so called 'fingerprint plot'[3] simplifies the 3D information and provide a visual summary. For each point on the Hirshfeld surface d_e (distance from the surface to the nearest external atom) and d_i (distance from the surface to the nearest internal atom) is determined. Each point on the 2D fingerprint plot corresponds to a unique (d_e+d_i) pair, and the colour of each point corresponds to the relative area of the surface. All fingerprint plots are coloured on the same relative scale, so the obtained plots of different moieties are comparable. [4]

In this chapter, Hirshfeld surfaces were generated to the base-acid-base moieties of all crystal structures and the related fingerprint plots were generated. In case of structures when two symmetrically independent base-acid-base moieties were found, both Hirshfeld surfaces were calculated and the corresponding fingerprint plots are presented. When structures had disordered methyl groups, the Hirshfeld surfaces were calculated to the two disordered moieties separately, the fingerprints are presented individually and the specific interactions were averaged. The crystals analysed in this work contain mainly H···H, O···H and C···H interactions and these are labelled as **1**, **2** and **3** on Figure 4A-G, respectively. The quantitative information of these interactions are summarized in Table 4.

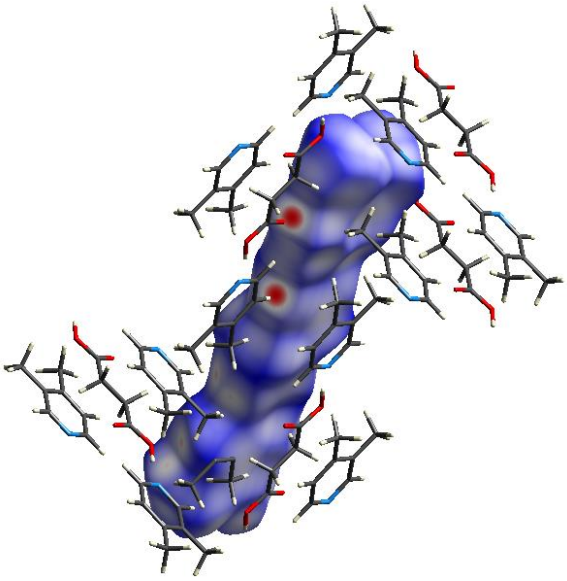

Figure 4. Hirshfeld surface calculated for SUC•3,4LUT base-acid-base complex surrounded by neighboring molecules.

4.1.a Intermolecular interactions of succinic acid inclusion compounds

For SUC•4PIC two plots were generated because the methyl group of the 4-picoline is disordered (Disorder 1 and 2, Fig. 4.1A and B). The two fingerprint plots differ in the H···H interactions because Dis1 (Disorder 1) presents a very short H···H contact (Fig. 4.1A, spike 1). The rest of the plots are similar in that manner that in both orientations the C···H interactions, the so called 'chicken wings' are present (Fig. 4.1A and B, area 3). Also the base-acid-base units are loosely packed and this results the 'clouds' of interactions at higher d_e and d_i vales. SUC•3,4LUT has one ordered base-acid-base unit in the structure which presents symmetrical prominent O···H (Fig. 4.1C, spike 2) and C···H (Fig. 4.1C, area 3) interactions. In the structure of SUC•3,4LUT the base-acid-base units may be in two positions hence the methyl groups of the lutidines are disordered (Fig. 4.1D and E). The difference between the two disorders is significant because Dis1 have a short H···H contact (Fig. 4.1D, spike 1) while in Dis2 the O···H interactions are more significant (Fig. 4.1E, spike 2). The C···H interactions are similar in case of both arrangement (Fig. 4.1D and E, area 3). In the structure of SUC•3,5LUT (Fig. 4.1F and G) the methyl group of the lutidines are disordered similarly to the previous examples but no prominent short contacts may be recognized on the plots. Interestingly, quantitative comparisons of the interactions (Table 4) does not show significant differences in how the disorders occupy the crystal space.

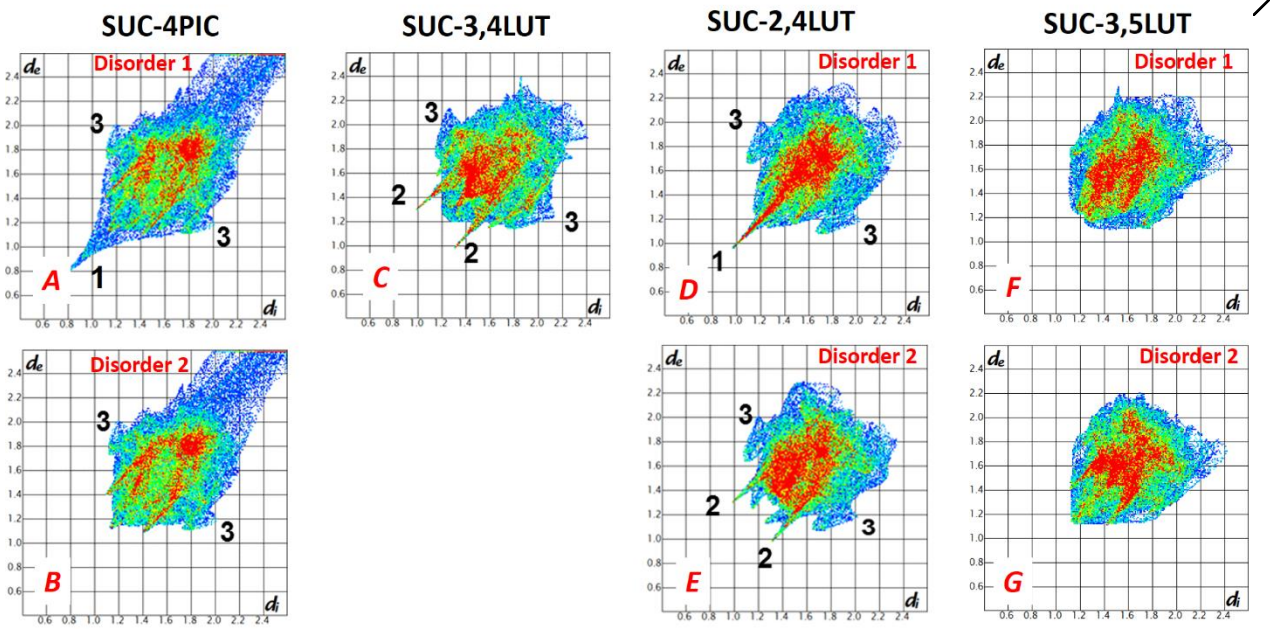

Figure 4.1 Fingerprint plots of base-succinic acid-base moieties.

4.1.b Intermolecular interactions of adipic acid inclusion compounds

ADP•4PIC has built from one ordered base-acid-base unit with some close H···H contacts (Fig. 4.2A, spike 1) and symmetrical O···H and C···H interactions (Fig. 4.2A, spikes 2 and 3, respectively) ADP•3,4LUT has two symmetry independent base-acid-base units and the generated plots are revealing similar O···H interactions but more prominent C···H interactions for Mol A (Fig.4.2B and C, respectively). These differences are obvious from the quantitative comparison hence the C···H interactions differ by 2.8% and the O···H by 1.6% (Table 4). ADP•2,4LUT is a disordered structure but the two plots are almost identical (Fig. 4.2D and E). Interestingly, the quantitative comparison shows some differences in the % distribution of the interactions, namely the C···H interactions differ by 0.9% and the N···H by 0.6%. Although ADP•3,5LUT is also disordered via the methyl group but in case of Dis1 a short H···H contact may form (Fig. 4.2F, spike 1) which does not appear in the arrangement involving Dis2 (Fig. 4.2G). Interestingly this visual difference does not manifest in the % interactions; the values are basically the same for both disorders.

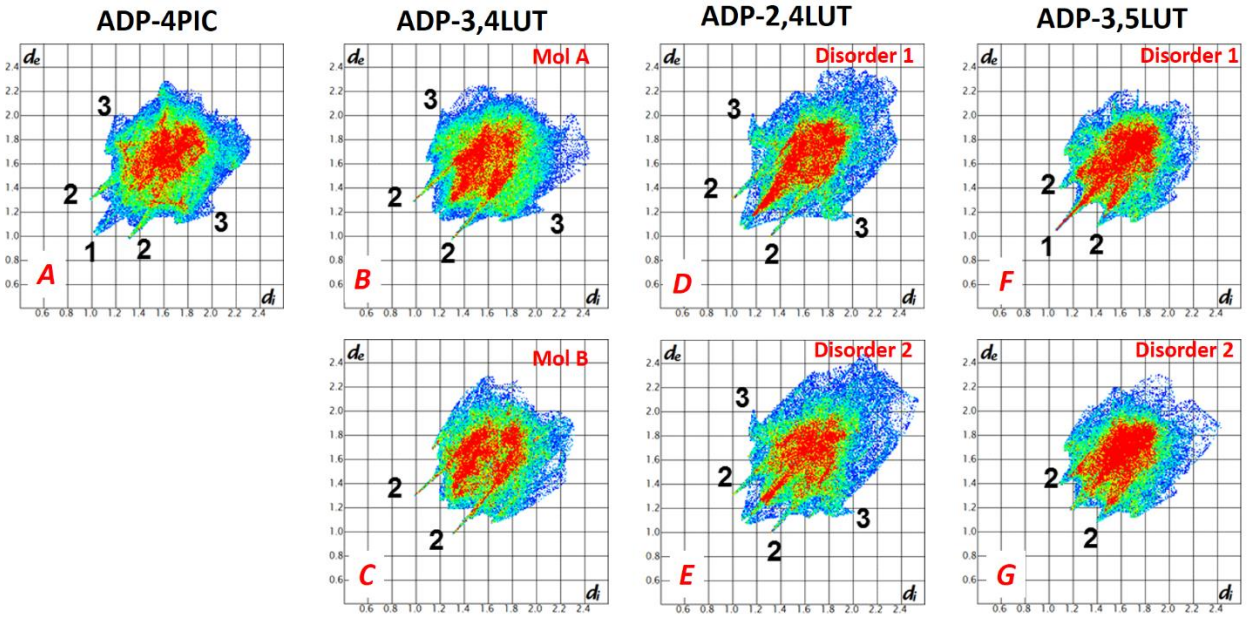

Figure 4.2. Fingerprint plots of base-adipic acid-base moieties.

4.1.c Intermolecular interactions of suberic acid inclusion compounds

SUB•4PIC is an ordered structure and built form a single type of base-acid-base unit. The typical interactions between the units are the O···H and the C···H contacts (Fig. 4.3A, spikes 2 and areas 3, respectively). SUB•3,4LUT structure is similar to ADP•3,4LUT structure in the manner that has two symmetry independent base-acid-base units (Mol A and B, Fig. 4.3B and C). The generated plots are revealing similar O···H interactions but the 'chicken wings' related to the C···H interactions are asymmetrical, and looks complementary on the two plots. Quantitative comparison of the interactions shows Mol A and B carry similar % of the different types of interactions. The SUB•2,4LUT structure has disordered methyl groups on the lutidines. The plots generated for the two possible positions are different. Although in both cases the O···H interactions are present (Fig. 4.3D and E, spikes 2) but short H···H contacts appear around Dis 1 (Fig. 4.3D, spike 1) and more prominent C···H contacts form around Dis 2 (Fig. 4.3E, areas 3). SUB•3,5LUT is also disordered and molecules in the two positions have similar H···H interactions but in case of Dis 1 prominent C···H interactions can be describe (Fig. 4.3F and G, spikes 1 and areas 3, respectively). The quantitative comparison of the disordered structures reflect the previously described differences (Table 4).

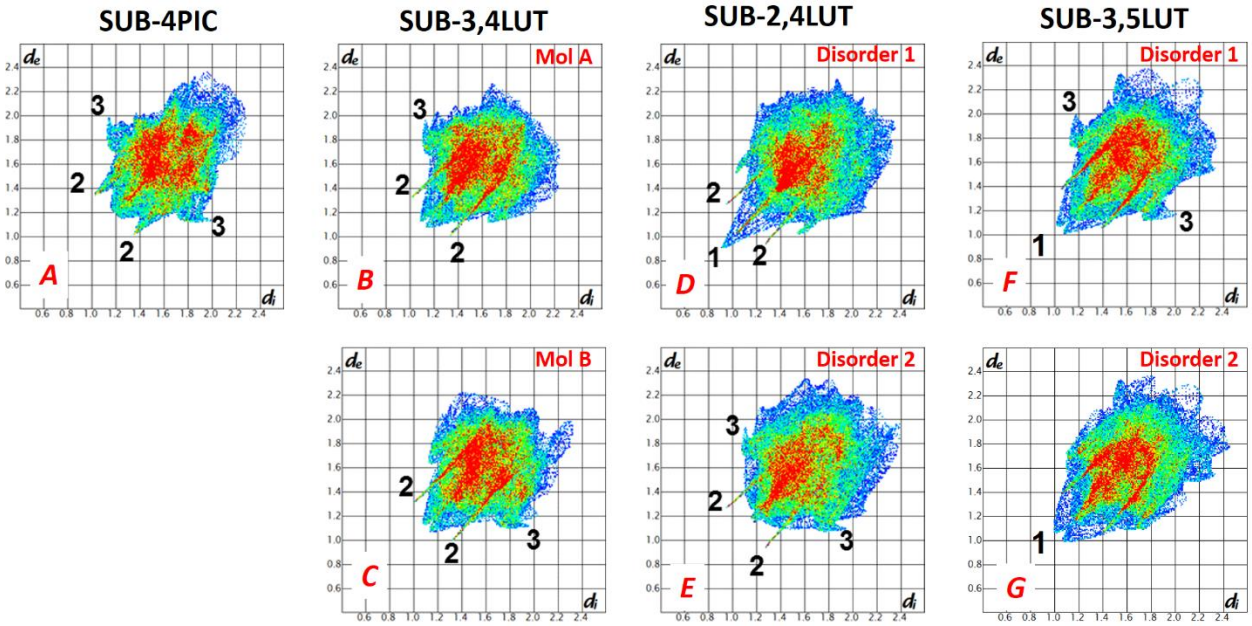

Figure 4.3 Finger print plots of base-suberic acid-base moieties.

A rough analysis of the values of the contribution (Table 4) shows that the % H···H interactions are increasing with the increasing aliphatic carbon chain of the dicarboxylic acid but no further numerical comparison reveals trends in the changes.

The visual comparison of the fingerprint plots and the quantitation of the % contribution of the different interactions reveal insight information about the packing of the structures but it may be concluded that comparison of these similar structures are a challenging process. A typical example to support this statement is when a plot shows short H···H contacts for one of the calculated units (Disorder 1 in SUC•4PIC) while the other unit lacks of this feature (SUC•4PIC, Dis 2) but this visually noticeable difference could not be seen when the % contributions are compared for the two units (SUC•4PIC, Dis1 and 2).

The calculated differences between the interactions presented by two symmetry independent molecules or disorders are relatively small thus averaging the % contribution of the interactions for a pair or molecules are possible and these values may be used to describe the selected structures.

Table 4 Quantitative summary of various interactions (differences are bold if larger than 0.5%)

structures	C…H (%)	O…H (%)	N…H (%)	C…C (%)	H…H (%)	others (%)
SUC•4PIC Disorder 1	12.0	27.1	3.3	3.8	51.0	2.8
SUC•4PIC Disorder 2	12.1	27.4	3.0	3.6	51.0	2.9
difference	*0.1*	*0.3*	*0.3*	*0.2*	*0.0*	*0.1*
<SUC•4PIC>	**12.1**	**27.3**	**3.2**	**3.7**	**51.0**	**2.9**
SUC•3,4LUT	**13.4**	**18.9**	**4.9**	**1.3**	**57.9**	**3.6**
SUC•2,4LUT Disorder 1	13.2	17.0	3.1	1.3	59.5	5.9
SUC•2,4LUT Disorder 2	13.5	17.2	2.9	1.2	59.8	5.4
difference	*0.3*	*0.2*	*0.2*	*0.1*	*0.3*	*0.5*
<SUC•2,4LUT >	**13.4**	**17.1**	**3.0**	**1.3**	**59.7**	**5.7**
SUC•3,5LUT Disorder 1	13.7	18.4	3.5	1.2	58.6	4.6
SUC•3,5LUT Disorder 2	14.0	18.5	3.4	1.2	58.8	4.1
difference	*0.3*	*0.1*	*0.1*	*0.0*	*0.2*	*0.5*
<SUC•3,5LUT >	**13.9**	**18.5**	**3.5**	**1.2**	**58.7**	**4.3**
ADP•4PIC	**13.8**	**20.0**	**4.7**	**2.5**	**56.6**	**2.4**
ADP•3,4LUT Mol A	13.7	18.5	4.3	2.1	60.0	1.4
ADP•3,4LUT Mol B	10.9	20.1	4.3	3.0	60.1	1.6
difference	***2.8***	***1.6***	*0.0*	***0.9***	*0.1*	*0.2*
<ADP•3,4LUT >	**12.3**	**19.3**	**4.3**	**2.6**	**60.1**	**1.5**
ADP•2,4LUT Disorder 1	12.1	18.4	3.1	2.7	61.7	2.0
ADP•2,4LUT Disorder 2	13.0	18.5	3.7	2.4	60.8	1.6
difference	***0.9***	*0.1*	***0.6***	*0.3*	***0.9***	*0.4*
<ADP•2,4LUT >	**12.6**	**18.5**	**3.4**	**2.6**	**61.3**	**1.8**
ADP•3,5LUT Disorder 1	9.2	18.4	3.8	4.2	62.6	1.8
ADP•3,5LUT Disorder 2	9.1	18.4	3.9	4.2	62.6	1.8
difference	0.1	0.0	0.1	0.0	0.0	0.0
<ADP•3,5LUT >	**9.2**	**18.4**	**3.9**	**4.2**	**62.6**	**1.8**
SUB•4PIC	**11.9**	**21.4**	**4.3**	**3.4**	**58.7**	**0.3**
SUB•3,4LUT Mol A	14.2	17.3	4.1	1.1	62.6	0.7
SUB•3,4LUT Mol B	14.6	17.4	3.7	1.1	62.7	0.5
difference	*0.4*	*0.1*	*0.4*	*0.0*	*0.1*	*0.2*
<SUB•3,4LUT >	**14.4**	**17.4**	**3.9**	**1.1**	**62.7**	**0.6**
SUB•2,4LUT Disorder 1	14.5	17.5	4.1	0.3	62.4	1.2
SUB•2,4LUT Disorder 2	15.4	18.0	3.5	0.1	61.7	1.3
difference	***0.9***	***0.5***	***0.6***	*0.2*	***0.7***	*0.1*
<SUB•2,4LUT >	**15.0**	**17.8**	**3.8**	**0.2**	**62.1**	**1.3**
SUB•3,5LUT Disorder 1	13.1	17.8	3.6	1.3	63.4	0.8
SUB•3,5LUT Disorder 2	13.6	18.7	3.8	1.2	62.3	0.4
difference	***0.5***	***0.9***	*0.2*	*0.1*	***1.1***	*0.4*
<SUB•3,5LUT >	**13.4**	**18.3**	**3.7**	**1.3**	**62.9**	**0.6**

References

[1] McKinnon, J,J; Jayatilaka, D; Spackman, M.A. *Chem.Comm*, 2007, **37**, 3814-3816.
[2] McKinnon, J.J; Spackman, M.A; Mitchell, AS. *Acta Cryst. B*, 2004, **60**, 627-668.
[3] Spackman, M.A; McKinnon, J.J. *CrystEngComm*, 2002, **4**, 378-392.
[4] Spackman, M.A; McKinnon, J.J; Jayatilaka, J. *CrystEngComm*, 2008, **10**, 377-388.

Chapter 5

Thermoanalysis vs interaction

Chapter 5: Thermoanalytical results and their relation to the intermolecular interactions

All the crystals were analyzed with Thermogravimetry (TG) and Differential Scanning Calorimetry (DSC) to obtain host-guest (solvent) ratios and accurate melting temperatures. A summary of the obtained values are presented in **Table 5** and the original data is shown in the Appendix.

The TG results were compared to the calculated values (based on the single crystal structures) and the occasional difference of these values were used to judge the thermal stability of the crystals. In all crystal structures the main building units are the base-acid-base associates and therefore the host:guest ratios are 1:2. The analysis of the bulk material showed good agreement between the calculated and the measured H:G ratio in case of crystals of adipic and suberic acids. However, the inclusion compounds formed with succinic acid showed non-stoichiometric ratios of H:G for the bulk material. The crystals of SUC•4PIC contained ca. 17% less 4PIC as expected and the crystals of lutidines are also contained ca. 9% less solvents. This significant difference cannot be explained with any unique structural features of the crystal packing. It more likely was caused by the overdue analysis* of the bulk material after formation and this particular sets of crystals started to decompose already. (There were no difficulties with the thermoanalytical analysis of the other two batches of crystal and the obtained results were satisfactory.)

The thermal behavior of the crystals are represented by the onset and the peak temperature of the melting and the concomitant enthalpy change. The visual analysis of the DSC curves (i. e. the lack of the endotherm related to the melting of the host after the decomposition of the inclusion compound) suggests congruent melting. Namely, the melting of these inclusion compounds leads directly to a liquid region with solid-liquid coexistence at a single temperature, the actual melting point. The melting temperatures revealed that the inclusion formation significantly decreased the melting points of the pure dicarboxylic acids (**Table 2.1 and 5**). It is also noticeable that the melting points of the inclusion compounds for the same acid are vary significantly; the largest difference (Δ= 36.6°C) was recorded between the inclusion compounds of adipic acid with 2,4LUT (T_{on}= 48.14°C) and with 3,4LUT (T_{on}= 84.73°C). This is understandable because however the main difference between these two structures is the position of one methyl group on

* The TG equipment was out of order for 3 months and great difficulties were experienced with the analysis of the SUC crystals.

the lutidine moiety but there are significantly more hydrogen bonds can be recognized in the structure of ADP•3,4LUT.

Table 5: Melting point measurement and thermogrametric values for multicomponents crystals.

Acids	Amines	TG					DSC			
		Measured %	Calculated %	Difference %	H:G Ratio		Melting point			
					TG	SCXR	Onset ºC	Peak ºC	ΔH J/g	ΔH J/mol
SUC	4PIC	50.34	68.33	-17.19	1:1.5	1:2	61.10	64.50	111.00	0.36
	3,4LUT	55.23	64.47	-9.24	1:1.7	1:2	71.30	73.43	80.78	0.24
	2,4LUT	54.69	64.47	-9.78	1:1.7	1:2	60.65	64.56	160.46	0.48
	3,5LUT	55.47	64.47	-9.00	1:1.7	1:2	84.01	87.49	183.73	0.55
ADP	4PIC	52.56	56.13	-3.57	1:1.9	1:2	49.84	52.65	24.81	0.07
	3,4LUT	58.27	59.45	-1.18	1:2	1:2	84.73	88.48	141.07	0.39
	2,4LUT	58.55	59.45	-0.90	1:2	1:2	48.14	51.04	140.71	0.39
	3,5LUT	59.35	59.45	-0.10	1:2	1:2	69.55	72.60	128.12	0.35
SUB	4PIC	51.95	51.67	0.28	1:2	1:2	84.35	87.44	193.57	0.53
	3,4LUT	55.49	55.16	0.33	1:2	1:2	83.90	89.06	150.03	0.53
	2,4LUT	55.32	55.16	0.16	1:2	1:2	74.14	77.12	171.82	0.44
	3,5LUT	57.39	55.16	2.23	1:2	1:2	57.07	58.13	1258.00	3.23

To understand how the different intermolecular interactions may influence the property of these multicomponent crystal, the melting points and the % contribution of the various intermolecular interactions were plotted (**Fig. 5.1-5.3**). A similar approach was used in our previous work[1] when inclusion compounds of adipic and fumaric acids were analyzed.

A closer inspection of the melting points vs. interactions graph for the succinic acid inclusion compounds (**Fig. 5.1**) shows no correlation between the increasing melting points and any of the specific interactions of the crystals. The melting points of the inclusion compounds increasing in the order of SUC•4PIC → SUC•2,4LUT → SUC•3,4LUT → SUC•3,5LUT. The previous crystal structure analysis revealed that SUC•4PIC, the lowest melting crystal, is a disordered structure and the diacid forms only single H-bonds with the PICs and no H-bonds were formed between the base-acid-base units. SUC•2,4LUT has also disordered lutidines but the diacid forms the typical double H-bonds with the two lutidines, however the base-acid-base units do not H-bond to each other, similarly to SUC•4PIC. As the melting point of the crystals increasing, it noticeable that H-bonds are formed between the now ordered base-acid-base units in

SUC•3,4LUT. It is interesting to note that the structure SUC•3,5LUT does not follow this logic hence the lutidines are disordered and no strong H-bonds can be noted between the base-acid-base units.

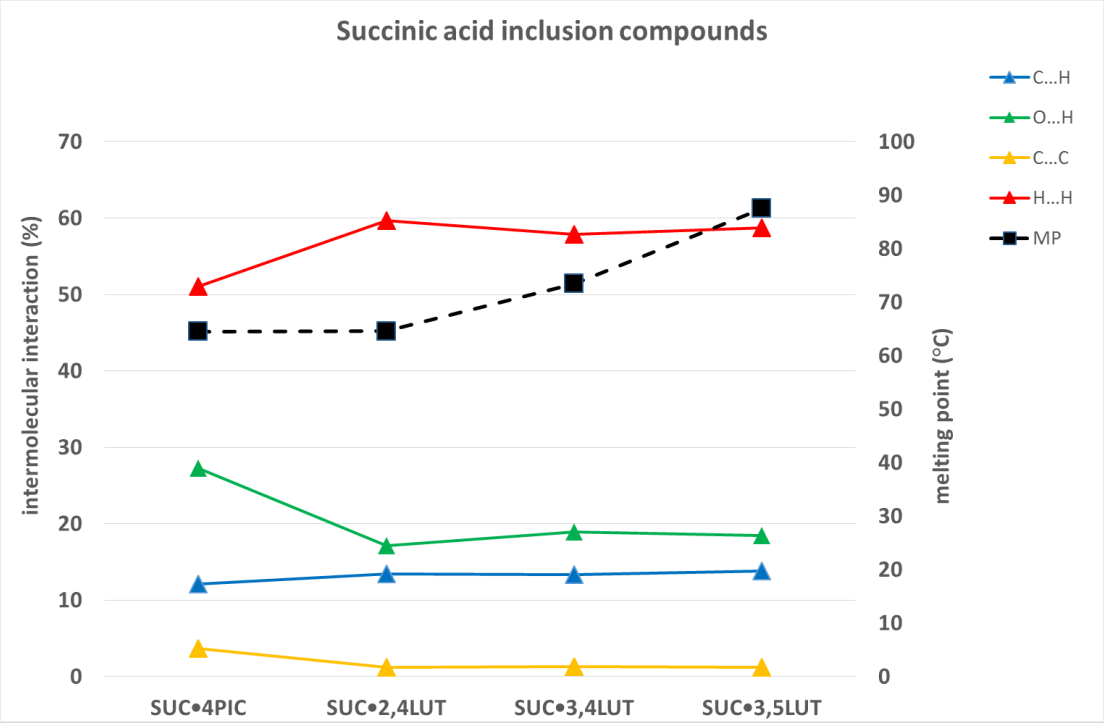

Figure 5.1 Various intermolecular interaction and the melting points of succinic acid inclusion compounds.

The melting points vs. interactions graph for the adipic acid inclusion compounds (**Fig. 5.2**) shows no correlation between the increasing melting points and the selected interactions of the crystals. The melting points of the inclusion compounds increasing in a slightly different order than in case of the succinic acid structures: ADP•2,4LUT → ADP•4PIC → ADP•3,5LUT → ADP•3,4LUT. The lowest melting point of ADP•2,4LUT may be explained by the disorder and the single H-bond formation between the diacid and the lutidines. In contrast, the ADP•4PIC has ordered lutidines and double H-bonds are formed between the diacid and the bases, thus the structures of the base-acid-base units differ significantly. However, in both crystals H-bonds are formed between these units and their melting points are virtually the same. Interestingly, the melting point of ADP•3,5LUT is significantly higher but the structure is disordered and there are no strong H-bonds formed between the base-acid-base units. The highest melting point of

ADP•3,4LUT crystals may be explained with its ordered structure, double H-bond formation between the acid and the bases and the extended H-bonding between these units.

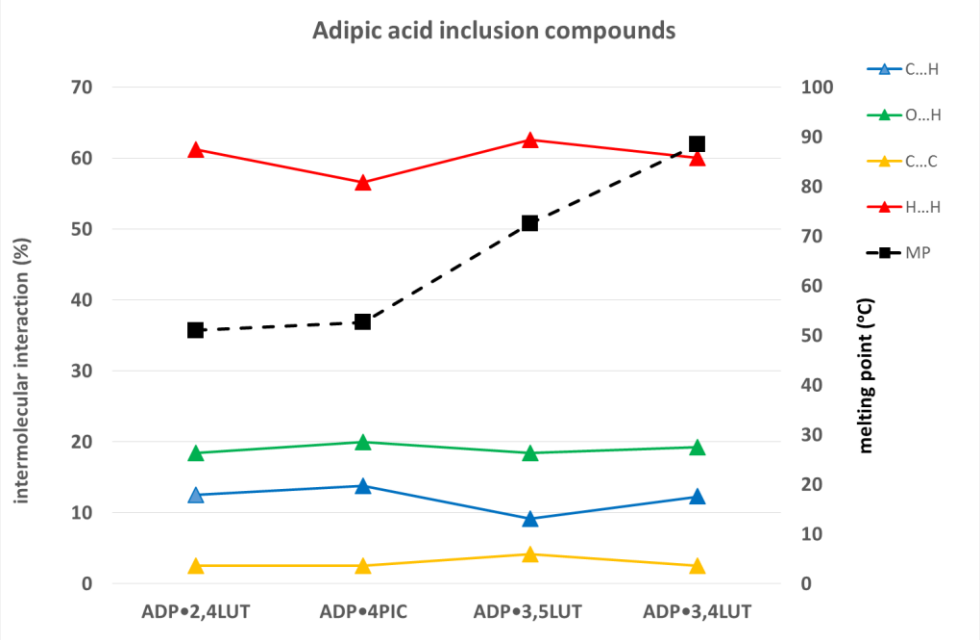

Figure 5.2 Various intermolecular interaction and the melting points of adipic acid inclusion compounds.

The melting points vs. interactions graph for the suberic acid inclusion compounds (**Fig. 5.3**) again, shows no correlation between the increasing melting points and the selected interactions. The melting points of the inclusion compounds increasing in a different order, namely: SUB•3,5LUT → SUB•2,4LUT → SUB•4PIC → SUB•3,4LUT. The lowest melting SUB•3,5LUT is disordered, only single H-bonds are formed between the acid and the bases. In SUB•2,4LUT the lutidines are disordered but double H-bonds are formed between the acid and the bases. SUB•4PIC is an ordered structure but only single H-bonds formed between the acid and the bases while the highest melting ordered SUB•3,4LUT forms double H-bonds. In all structures the base-acid-base units H-bond together. It may be concluded that the most logical correlation between the melting points and the crystal structures could be find in the series of suberic acid crystals.

In conclusion, the previously successful approach of correlating the change in melting points to changes in certain intermolecular interactions of a series of closely related crystals was unsuccessful. It may be concluded that the selection of these congruently melting systems were

not ideal, however whether a material melts congruently or incongruently depends on multiple factors and cannot be predicted.

The multicomponent crystals of lutidines (if 4PIC is excluded) form a series of constitutional isomers of these host:guest systems. It is interesting to note that these very similar molecular building blocks can arrange into a 3D structure that will give rise to significant differences in their melting points.

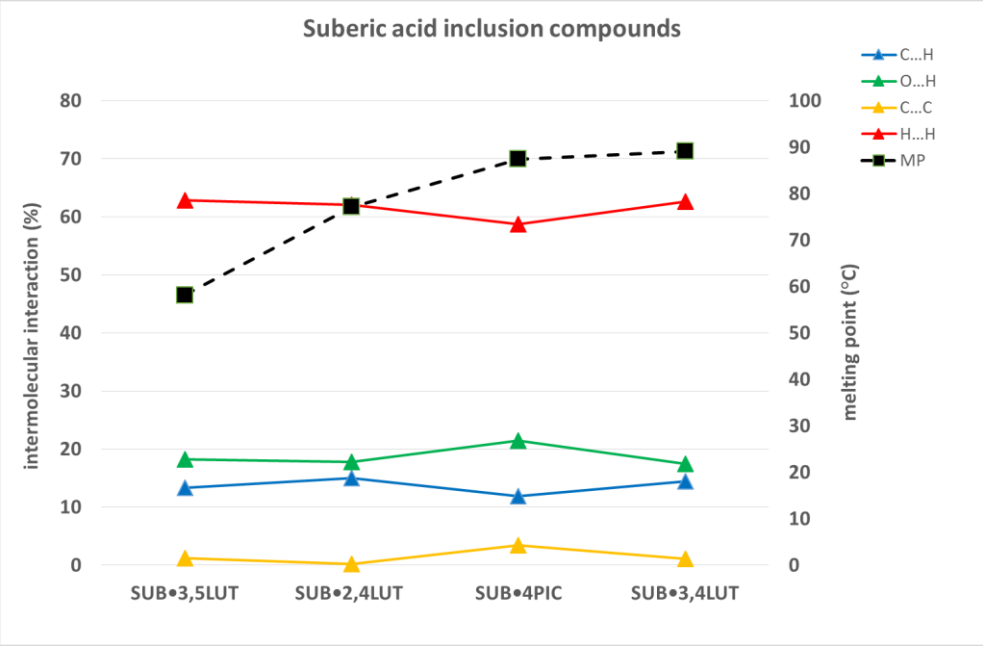

Figure 5.3 various intermolecular interaction and the melting points of suberic acid inclusion compounds.

References

[1] Batisai, E; Ayamine, A; Youdaga Kilinkissa, O.E; Báthori, N.B. 2014. *CrystEngComm*, 2014, 16, 9992-9998.

Chapter 6

Summary and Conclusion

Chapter 6: Summary and Conclusion

Multicomponent model-crystals, a simplified versions of the pharmaceutical co-crystals or salt, may be formed by replacing the API with a simple molecular unit. Thus a model crystal has the ability to present the same type of supramolecular behavior as a pharmaceutical co-crystal but the interpretation of the structure is simpler and the understanding of the structure-property relations of these crystals expected to be easier.

Melting point is one of the physical properties to characterize a compound and it is defined by the temperature at which the solid phase is at equilibrium with liquid phase. To find a suitable solid form of a drug substance which can have superior properties is one of the big challenges in pharmaceutical development.

Applying model crystals we may simplify the nature of the intermolecular forces and restrict the degrees of freedom and this may lead us to understand how a certain interaction influences the melting point of the crystalline material.

This project was designed to find correlation between the melting point and structural features of the selected multicomponent crystals. Twelve solvates were crystallized via combining succinic acid (SUC), adipic acid (ADP) and suberic acid (SUB) with the 4-picoline (4PIC), 2,4-lutidine (2,4LUT), 3,4-lutidine (3,4LUT) and 3,5-lutidine (3,5LUT). The solvates of SUC•2,4LUT (CSD refcode: RESGAY), SUC•3,4LUT (RESHAZ), SUC•3,5LUT (RESHIZ) were known previously and APD•4PIC was made by our research group, but were remade for completeness and to obtain accurate melting temperatures. The acids were selected because of their systematically increasing chain lengths and the selection of the picoline derivatives were based on the systematic variation of the positions of the methyl groups around the pyridine moiety.

The crystalline material obtained were analyzed with single crystal X-ray diffraction. In all crystals the diacids crystallized with the bases in the expected 1:2 ratio. Although the formation of double H-bond between the aromatic amine and the carboxylic acid moiety was expected exclusively, occasionally this was not reached and only two single H-bond formation was observed in the base-acid-base units. In some of the structures H-bond formation were observed between the base-acid-base supramolecular units but occasionally there was no obvious H-bond formed between them and the units interact via C…H and C…C interactions.

Parallel to the solution crystallizations, grinding experiments were carried out to prepare the aimed inclusion compounds by using much less of the solvents. The liquid assisted grinding

(LAG) yielded the 1:2 H:G product exclusively only in the case of. ADP•2,4LUT while the other experiments were unsuccessful. The solubility of the diacids are very high in the picoline derivatives and by adding only several drops of solvent, the acids dissolve almost immediately. It is more likely that a 1:1 or a non stoichiometric ratio of the materials were ground together and resulted in the formation of new solid phases.

Thermogravimetry was used to confirm the solvent content of the bulk material and showed good agreement between the calculated and the measured H:G ratios in case of crystals of adipic and suberic acids. The crystals formed with succinic acid showed significantly lower solvent content than anticipated and this likely was caused by the unfortunate overdue analysis of the bulk material.

Differential scanning calorimetry was used to obtain information about the melting process: the onset and the peak temperature of the melting and the associated enthalpy change. The melting temperatures revealed that the inclusion formation significantly decreased the melting points of the staring materials and the melting points of the inclusion compounds for the same acid differ significantly. This observation lead to further analysis of the structural features of the multicomponent crystals.

Hirshfeld surfaces of the base-acid-base moieties were calculated for all crystal structures and the related fingerprint plots were generated. The structures were compared both qualitatively (shapes of the fingerprint plots) and quantitatively (percentage contribution of the different intermolecular interaction). To understand how the different intermolecular interactions may influence the property of these multicomponent crystal, the melting points were plotted against the percentage contribution of the various intermolecular interactions. This data treatment was successfully used previously to correlate the change in melting points to the observed changes in certain intermolecular interactions of a series of closely related crystals. These crystals of lutidines (with the exclusion of 4PIC) form a series of constitutional isomers of multicomponent crystals and although their main building blocks are the base-acid-base units, the way how these common units have been arranged in the crystal give rise to significant differences in their melting points.

Our hope is that this work contributes to the bulk knowledge of supramolecular chemistry and a great addition to the subset of research focused on structure-property relationships of multicomponent crystals and their property alteration via solid state modification.

Appendix

Appendix

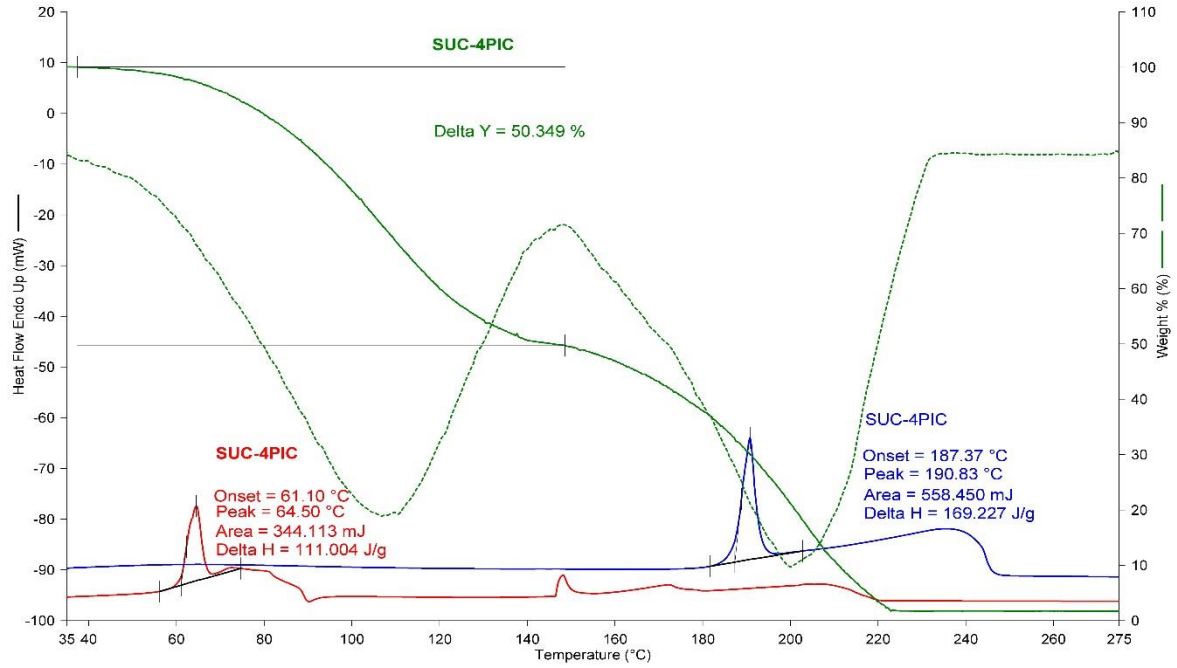

Figure A 1 DSC and TG curve of SUC•4PIC and the individual starting material, SUC.

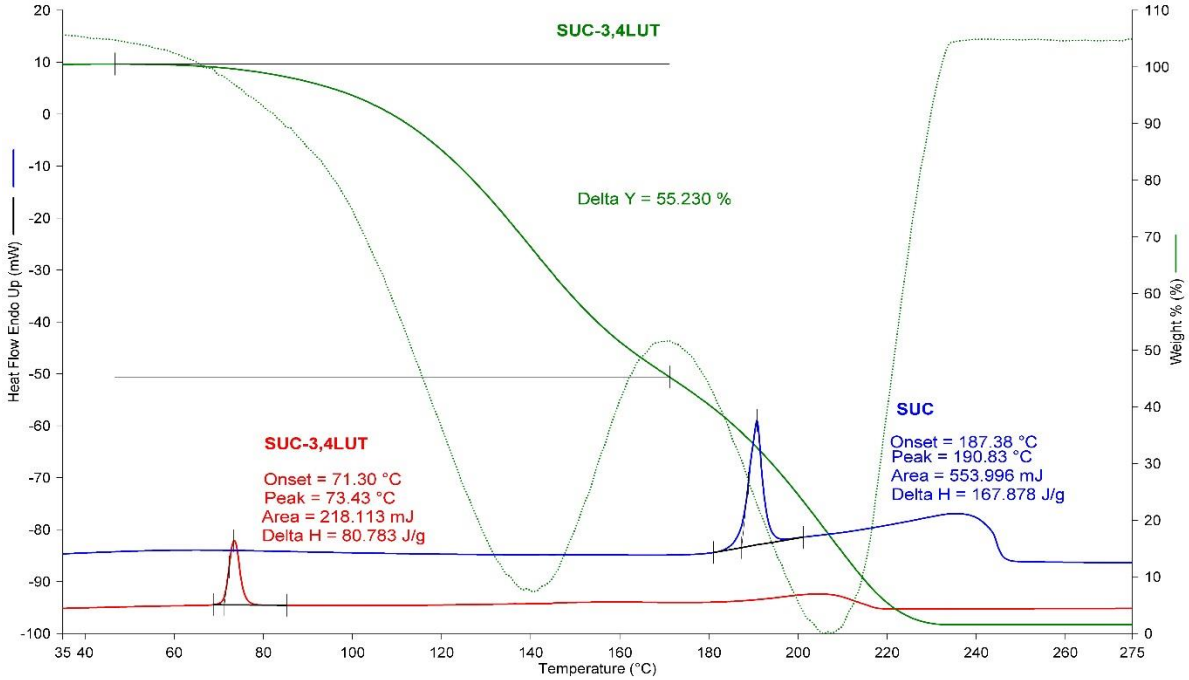

Figure A 2 DSC and TG curve of SUC•3,4LUT and the individual starting material, SUC.

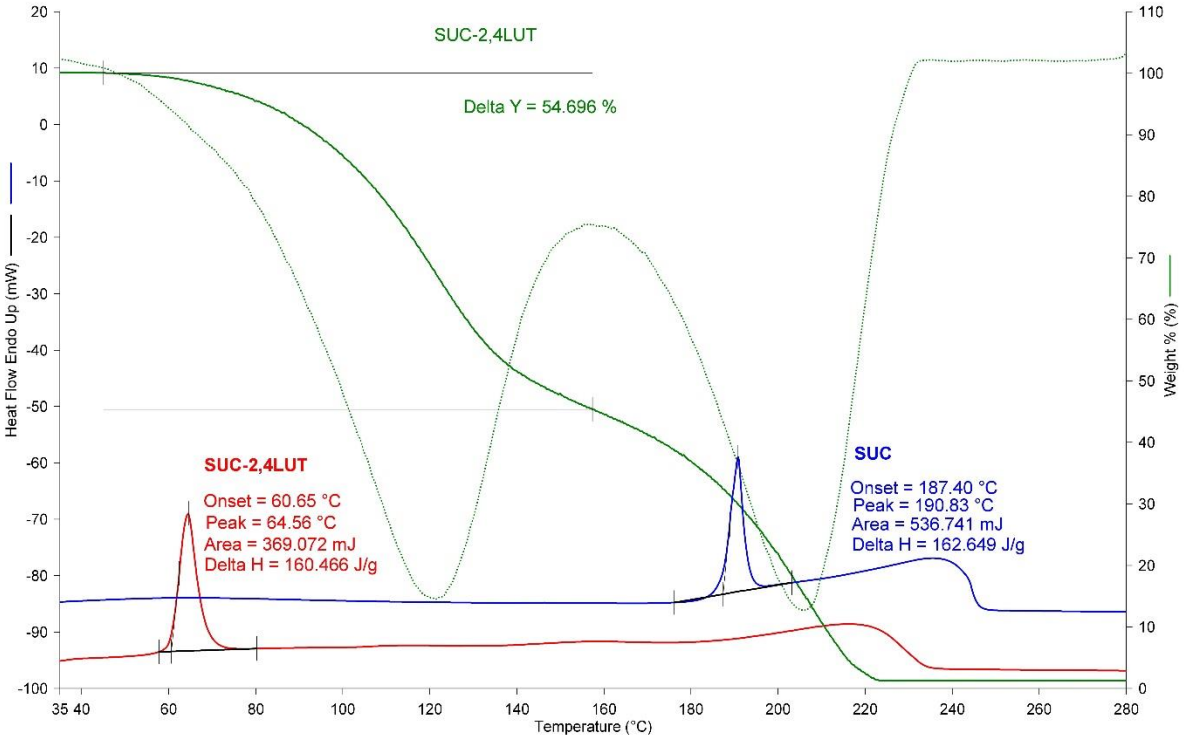

Figure A 3 DSC and TG curve of SUC•2,4LUT and the individual starting material, SUC.

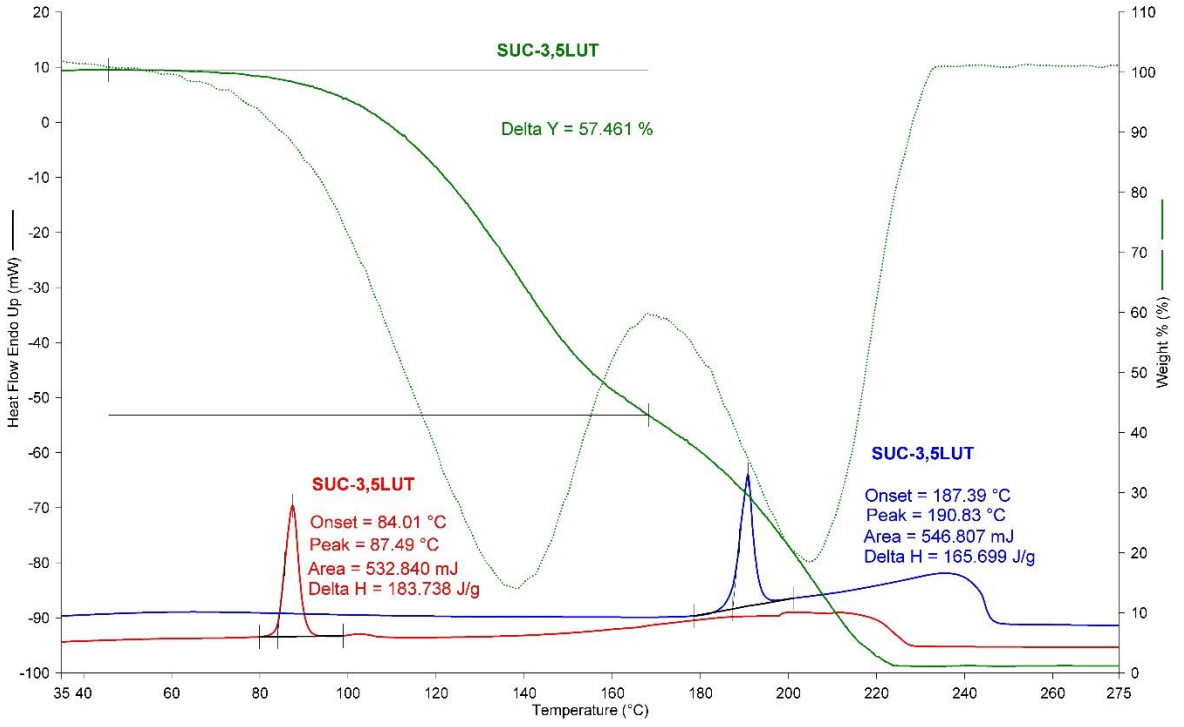

Figure A 4 DSC and TG curve of SUC•3,5LUT and the individual starting material, SUC.

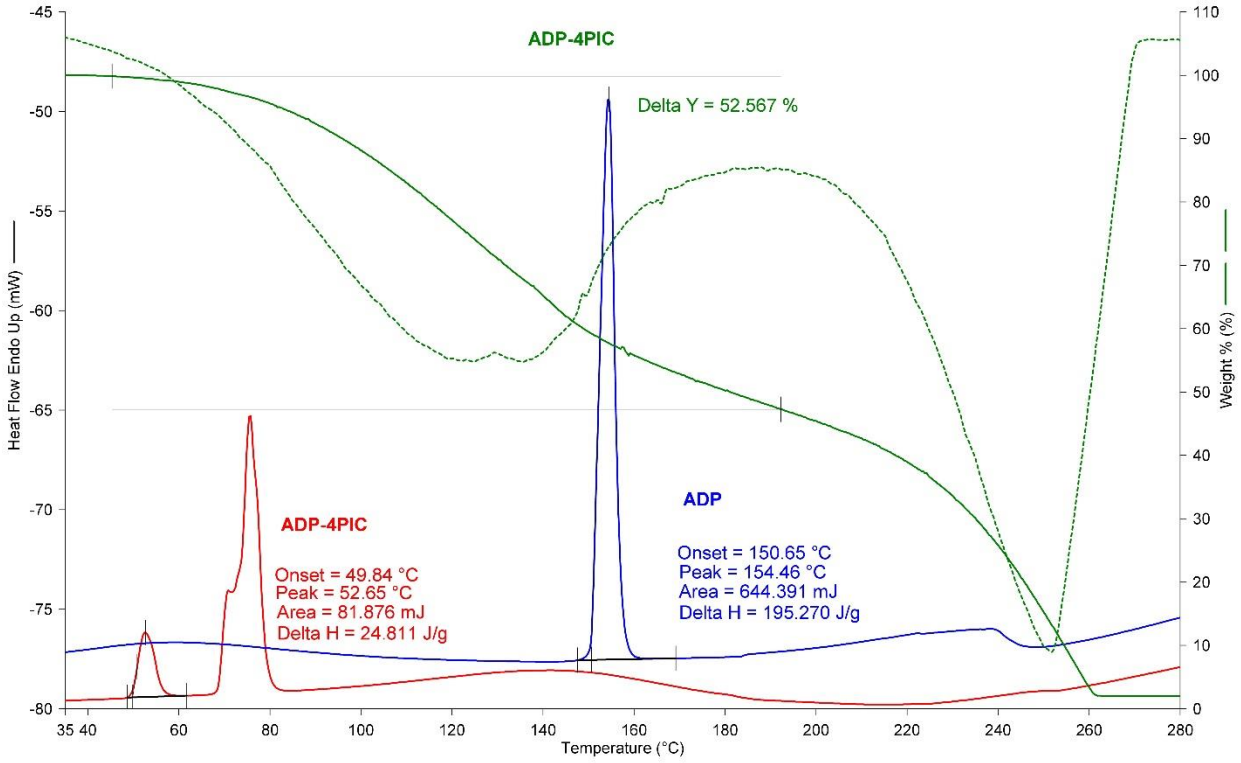

Figure A 5 DSC and TG curve of ADP•4PIC and the individual starting material, ADP.

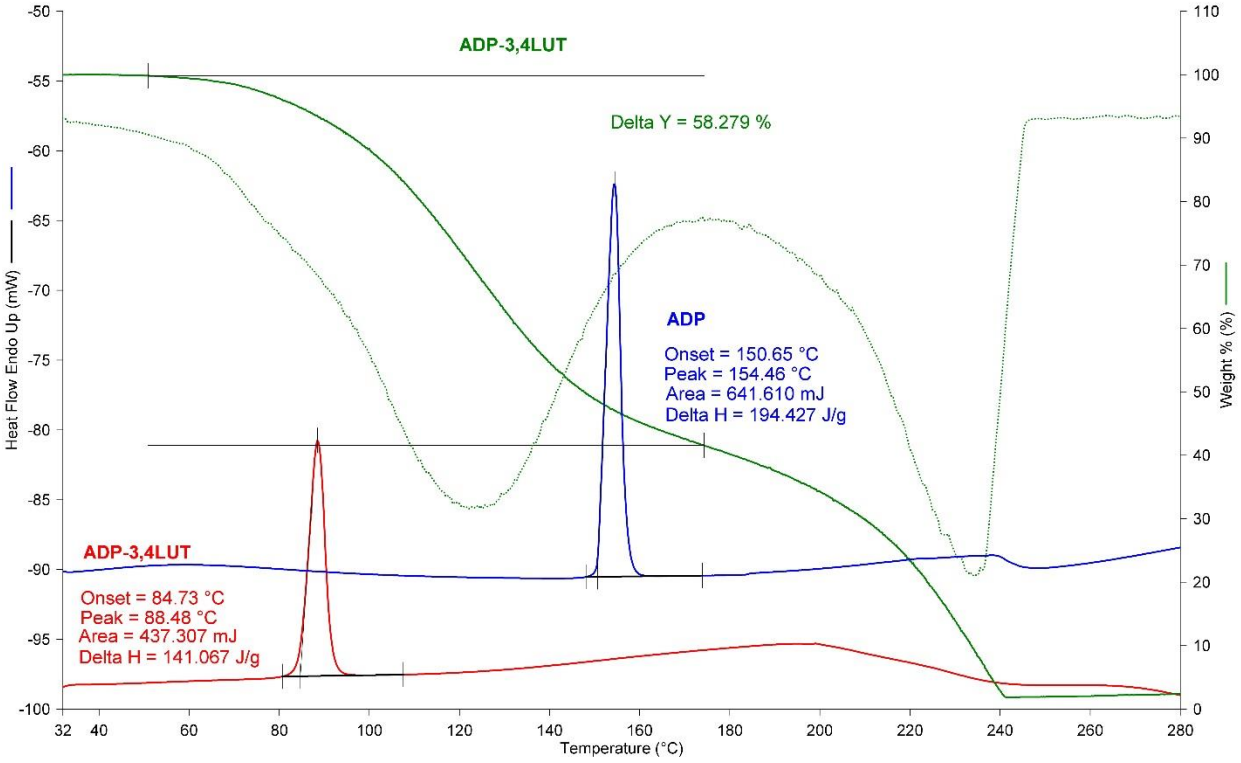

Figure A 6 DSC and TG curve of ADP•3,4LUT and the individual starting material, ADP.

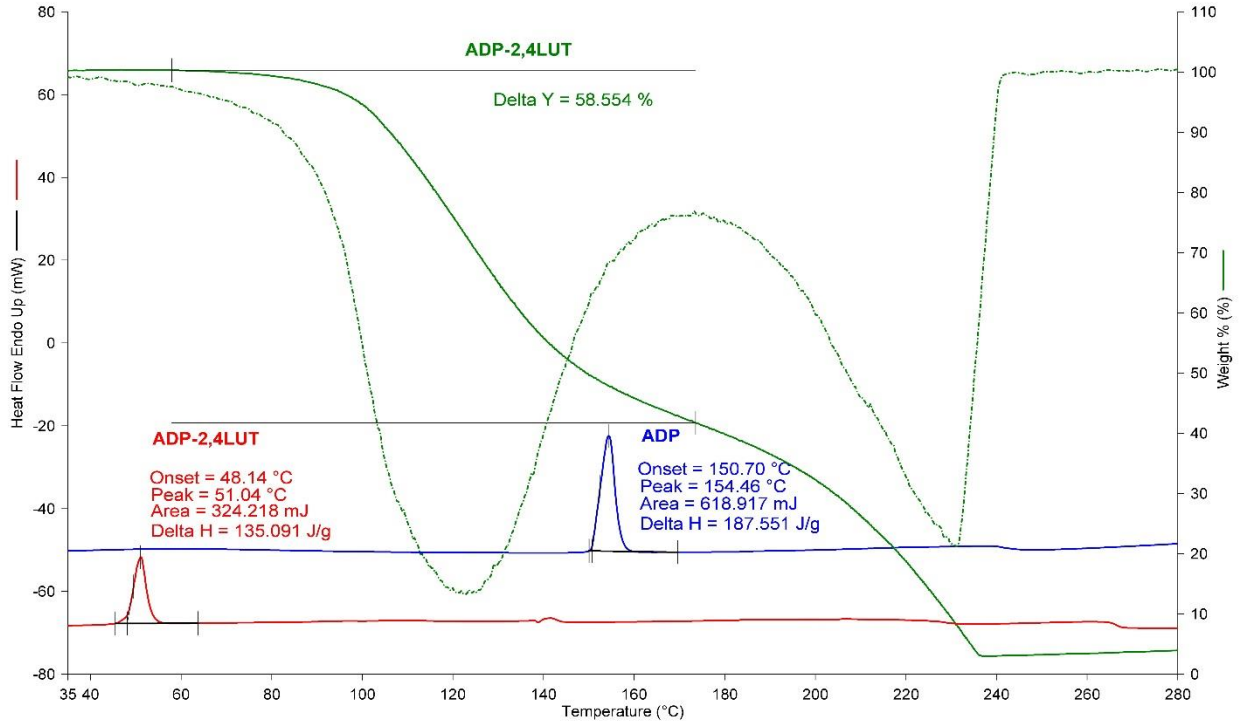

Figure A 7 DSC and TG curve of ADP•2,4LUT and the individual starting material, ADP.

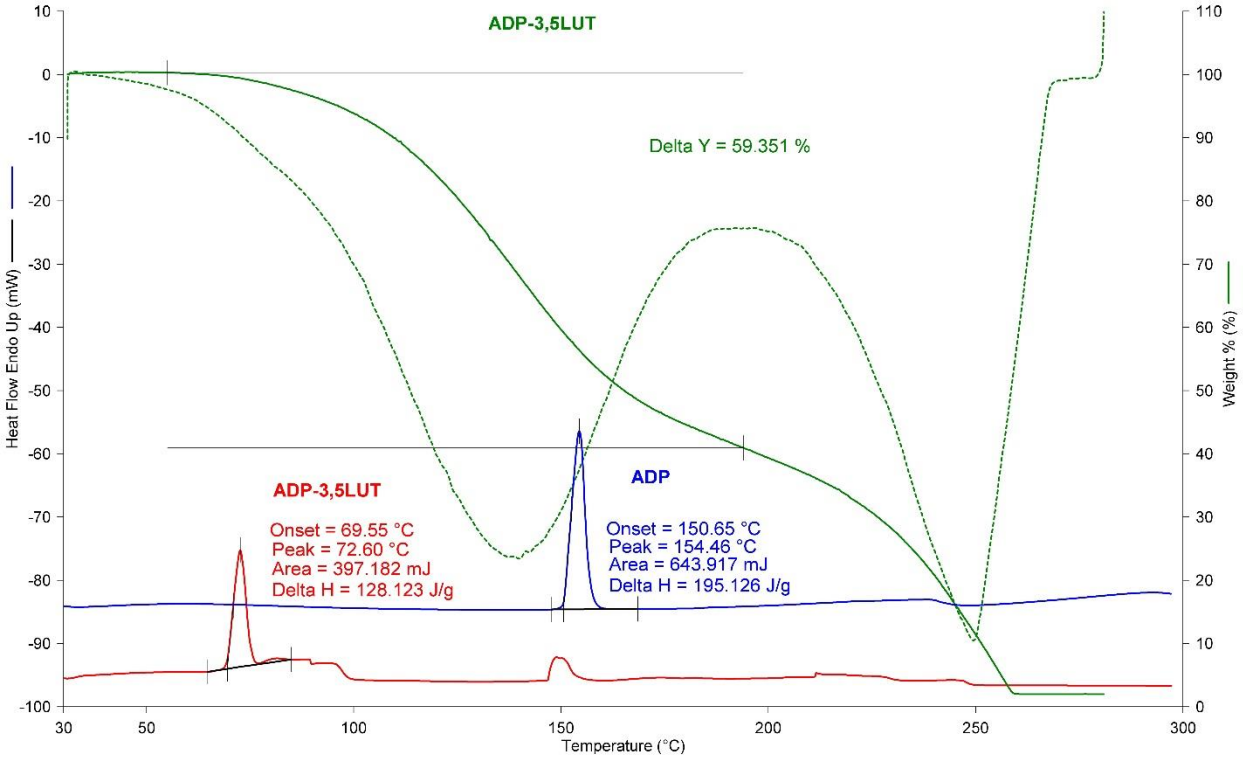

Figure A 8 DSC and TG curve of ADP•3,5LUT and the individual starting material, ADP.

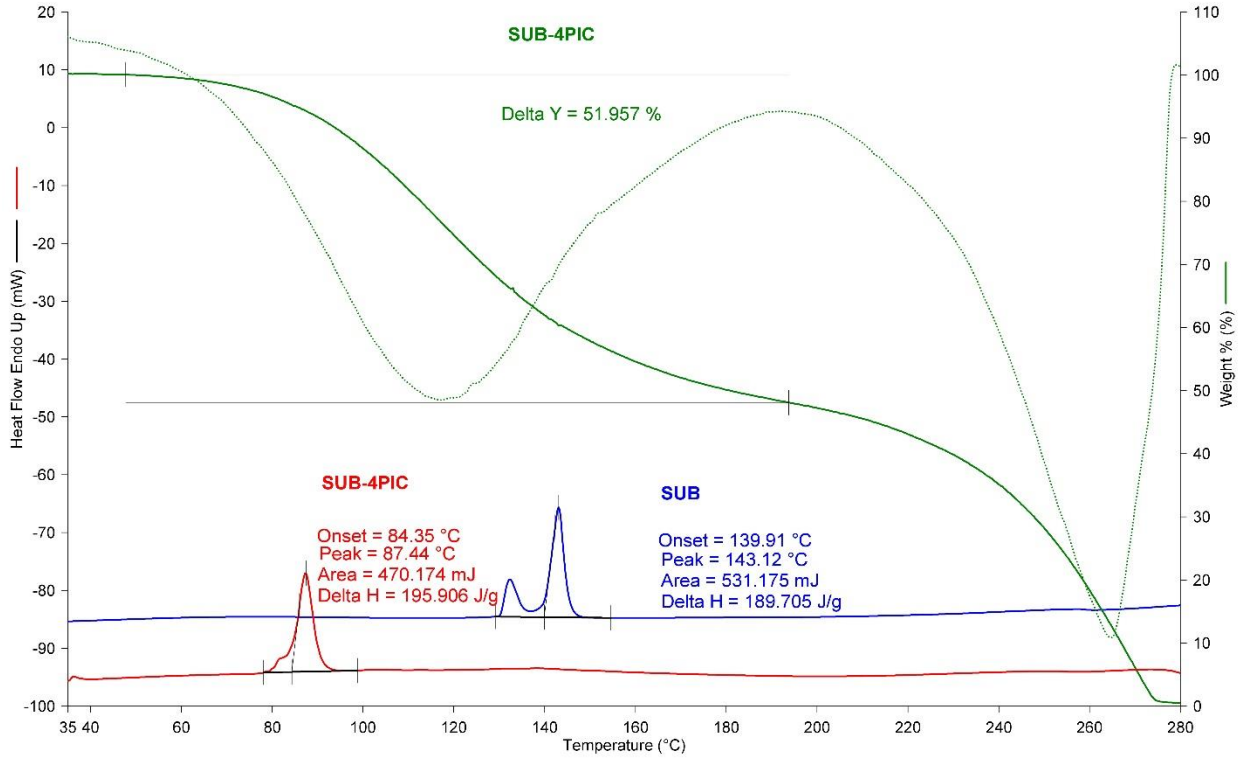

Figure A 9 DSC and TG curve of SUB•4PIC and the individual starting material, SUB.

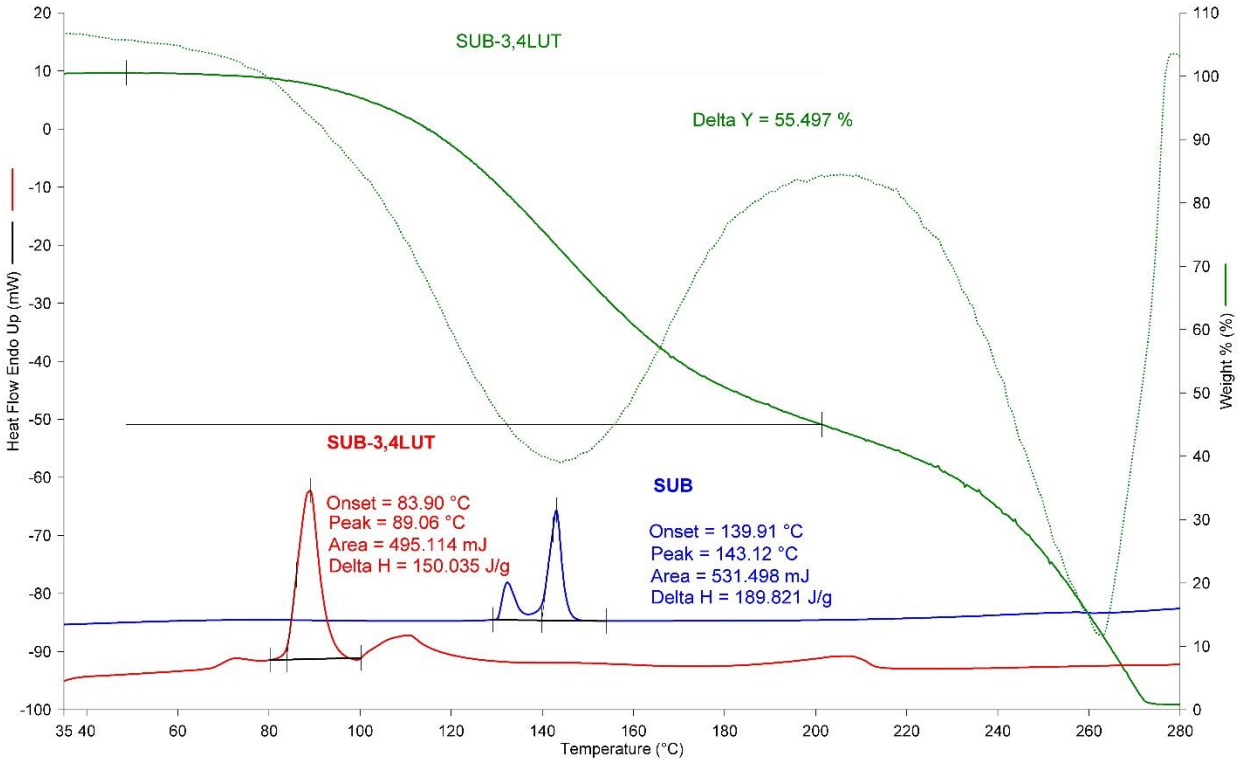

Figure A 10 DSC and TG curve of SUB•3,4LUT and the individual starting material, SUB.

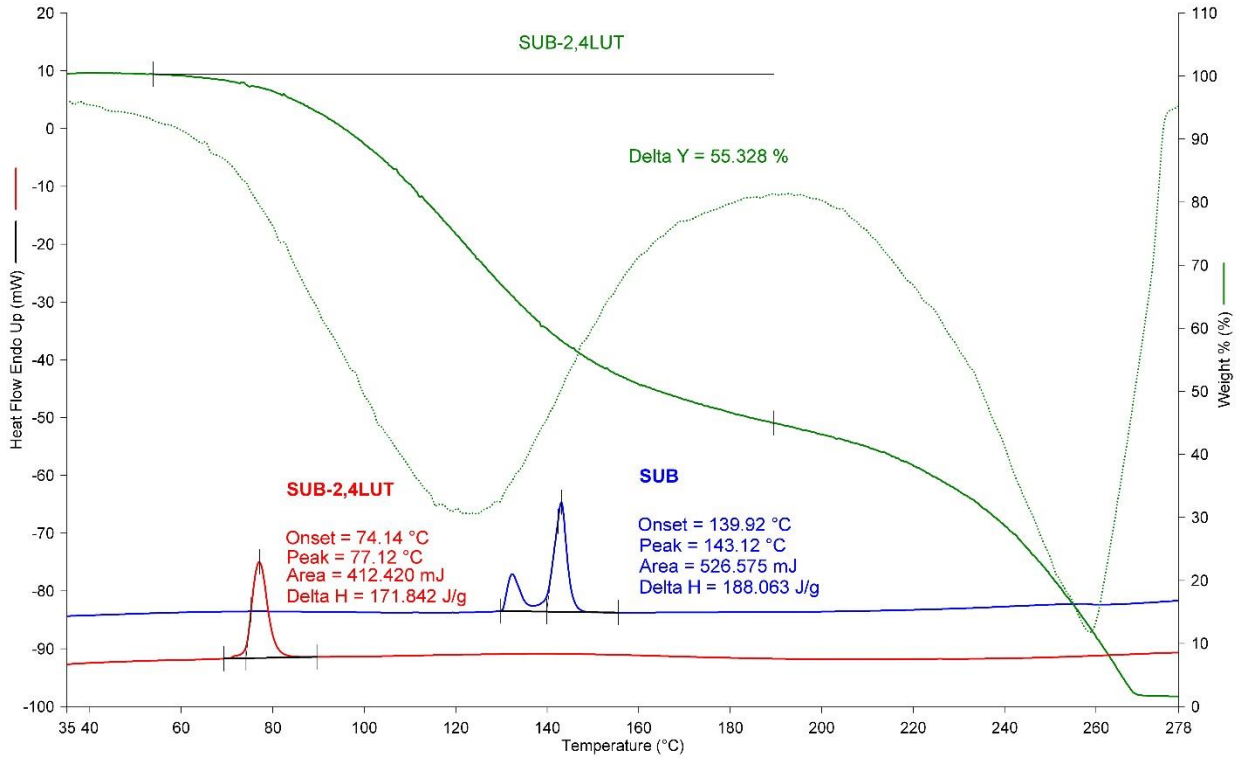

Figure A 11 DSC and TG curve of SUB•2,4LUT and the individual starting material, SUB.

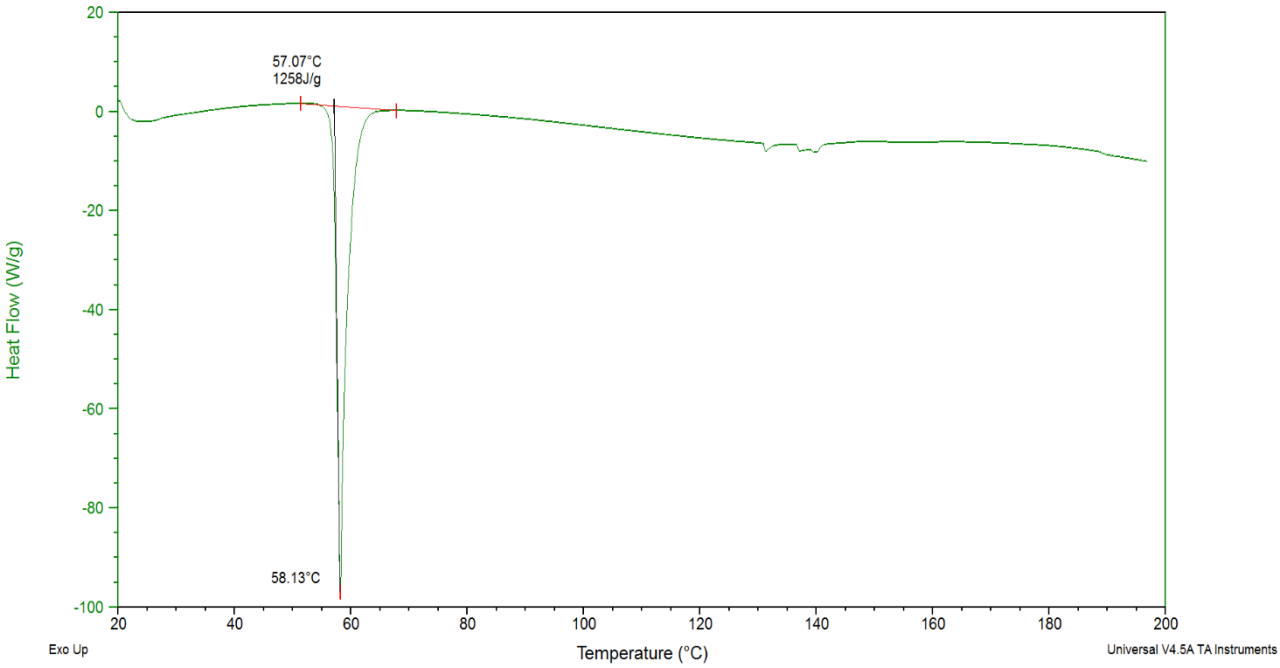

Figure A 12 DSC curve of SUB•3,5LUT and the individual starting material, SUB.

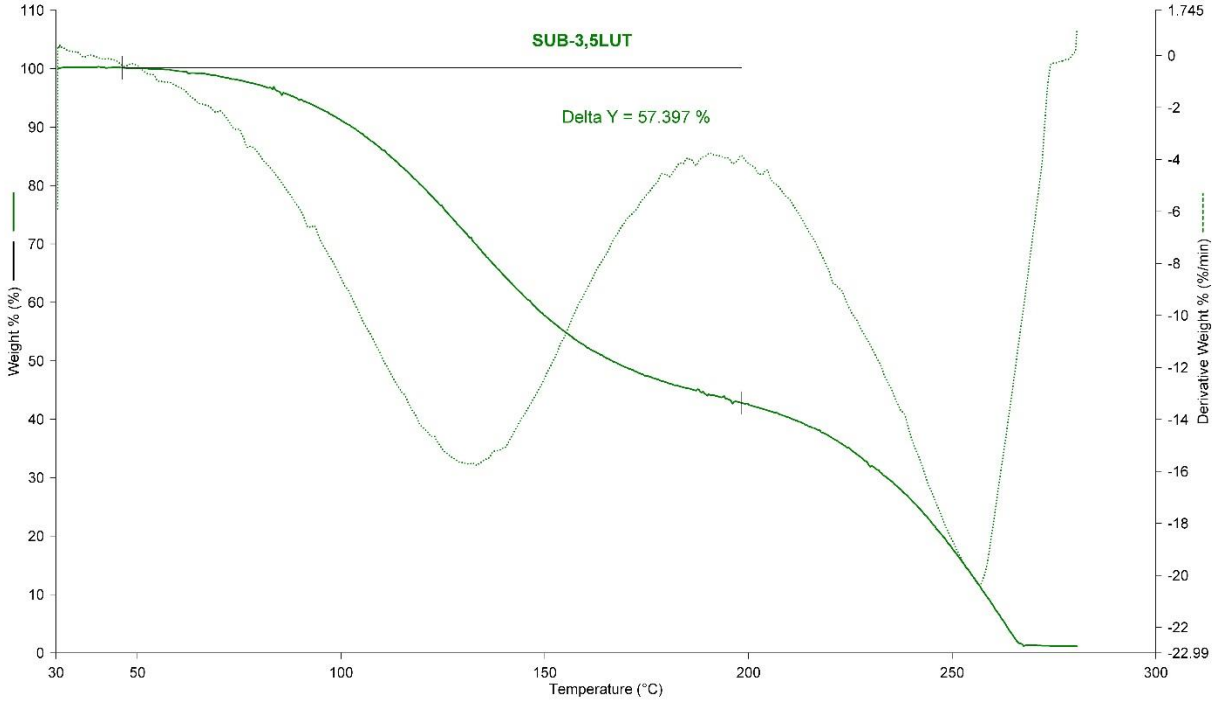

Figure A 13 TG curve of SUB•3,5LUT and the individual starting material, SUB.